NASA CR-72503
AEROJET 3661

9Cr-1Mo STEEL AS A MERCURY CONTAINMENT MATERIAL FOR THE SNAP-8 BOILER

by

B. E. Farwell, D. Yee, and S. Nakazato

AEROJET-GENERAL CORPORATION

prepared for

NATIONAL AERONAUTICS AND SPACE ADMINISTRATION

NASA Lewis Research Center
Contract NAS 5-417
Martin J. Saari, Project Manager

NOTICE

NASA CR-72503
AEROJET 3661

TOPICAL REPORT

9Cr-1Mo STEEL AS A MERCURY CONTAINMENT MATERIAL FOR THE SNAP-8 BOILER

by

B. E. Farwell, D. Yee, and S. Nakazato

AEROJET-GENERAL CORPORATION
Azusa, California

prepared for

NATIONAL AERONAUTICS AND SPACE ADMINISTRATION

January 1968

CONTRACT NAS 5-417

NASA Lewis Research Center
Cleveland, Ohio
Martin J. Saari, Project Manager
SNAP-8 Program Office

FOREWORD

The work described in this report was done primarily at Aerojet-General Corporation's Nuclear Division (formerly Aerojet-General Nucleonics) at San Ramon, California, as part of the SNAP-8 Electrical Generating System Contract being conducted within the Power Systems Department, Aerojet-General Corporation, Azusa, California. The work was performed under NASA Contract NAS 5-417, with Mr. Martin J. Saari as the NASA Project Manager.

CONTENTS

Figure

Figure

ABSTRACT

Various investigations were made to evaluate 9Cr-1Mo steel as a mercury containment material for use in the SNAP-8 boiler. Analysis and experimental data indicate that mercury corrosion of 9Cr-1Mo can be described as a mass transfer process of soluble constituents of the steel into mercury. Mercury corrosion rate is maximum under wetted condition and only such data should be used in evaluating the suitability of the 9Cr-1Mo steel. This report summarizes the corrosion studies made to evaluate 9Cr-1Mo steel.

I. INTRODUCTION

SNAP-8 is a 35 kwe turboelectric nuclear space power system using a mercury Rankine cycle, and powered by a NaK-cooled reactor. A simplified system schematic is shown in Figure 1. The operating life requirement for the system is a minimum of 10,000 hours. Inasmuch as the maximum temperature and liquid velocity of the mercury in the system occurs in the boiler, the operating condition of this component defines the requirement for a mercury containment material of this system.

Based on solubility of elements in mercury, refractory metals are most resistant to mercury corrosion (Figure 2). Of the conventional state-of-the-art alloy systems, however, the iron based alloys are preferred for minimal mercury corrosion potential. The 9Cr-1Mo steel was selected as a candidate SNAP-8 mercury containment material based on its high temperature strength, oxidation resistance, and resistance to corrosion by mercury. At the time of this selection there was insufficient data to reliabily establish its corrosion rate under SNAP-8 operating conditions. Since the selection of 9Cr-1Mo steel for the SNAP-8 system, a significant body of mercury corrosion test data has been generated by Aerojet, TRW, and Lewis Research Center, among others. These tests indicate a corrosion rate that apparently is strongly dependent on system design and operating conditions. The data are insufficient to accurately determine the life of 9Cr-1Mo steel in SNAP-8 use. The capability of the material to meet SNAP-8 system life requirements was evaluated by the application of mass transfer theory and experimental data obtained in subscale mercury loop tests. This report summarizes this evaluation.

A. HYPOTHESIS

To determine the suitability of 9Cr-1Mo steel for the SNAP-8 boiler, the hypothesis used is that corrosion is controlled by the diffusion of iron across liquid boundary layer adjacent to the surface of the 9Cr-1Mo steel. This hypothesis permits confining the study to the pre-heat region of the boiler where maximum liquid velocity and maximum temperature occurs. The superheat region of the boiler, although operating at higher temperature, will not have as much liquid phase in contact with the steel surface.

B. METHOD OF SOLUTION

Using the above hypothesis the method of solution was as follows:

1. Develop an analytical expression to describe the corrosion along the preheat section using the heat-mass transfer analogy.

2. Calculate the corrosion rate in the preheat region of test boilers using the above equation for comparison with experimental values.

3. Compare the experimental values of corrosion rate obtained in loop tests with predicted values to validate the analytical expression. Earlier work on capsule and loop tests designed to screen materials for SNAP-8 boiler is not suitable for the present purpose. The capsule does not have a geometry that defines liquid velocity well. Since the early loop tests were conducted, complete local wetting of the boiler surface was found to be necessary to ensure reproducibility of tests. Complete wetting is necessary to obtain the boiler heat-transfer performance, but under such a case the corrosion rate is also its maximum. A test series (designated 4A) was performed to test the hypothesis.

4. Using the established equation, predict the corrosion expected in a SNAP-8 boiler after 10,000 hours of operation.

C. 9Cr-1Mo STEEL

The 9Cr-1Mo alloy is a ferritic steel alloy that has been used mainly for its resistance to sulphide corrosion and oxidation resistance to 1300°F. The chemical composition of 9Cr-1Mo steel is given below in weight percent.

Carbon	0.015 Max.	Chromium	8 to 10
Molybdenum	0.90 to 1.10	Manganese	0.30 to 0.60
Phosphorus	0.03 Max.	Sulphur	0.03 Max.
Silicon	0.50 to 1.00	Iron	Balance

The 9Cr-1Mo alloy is used in the annealed condition for high-temperature service. The stability of 9Cr-1Mo is good for long-time exposure to elevated temperatures.

Typical values of elevated temperature tensile tests and effect of exposure to temperature are shown in Table 1. Figure 3 illustrates the creep and stress rupture properties of 9Cr-1Mo steel.

The ASME Boiler and Pressure Vessel Code, Section VIII, gives the following values for allowable stress at temperature:

Temperature, °F	Stress, psi
900	12,000
1000	8,500
1100	3,300
1200	1,500

As noted from the composition of 9Cr-1Mo steel, this alloy has no intentional nickel alloy addition as do most high temperature strength alloys. At the operating temperatures of the SNAP-8 boiler nickel is a hundred times more soluble in mercury than iron, and ten times more soluble than chromium (Figure 2). Therefore, 9Cr-1Mo steel, which is a commercially available material, appeared to represent the best balance between the strength and oxidation requirements and the mercury corrosion resistance requirements for the SNAP-8 boiler.

II. CONCLUSIONS

Analytical and controlled experimental studies conducted on the 9Cr-1Mo corrosion by mercury leads to several conclusions regarding the use of this alloy in the SNAP-8 system.

1. Corrosion of 9Cr-1Mo by flowing mercury is by dissolution of the alloy components by mercury.

2. Corrosion rate is velocity dependent which suggests that the controlling mechanism is the transport of solute molecules through the laminar sublayer by molecular diffusion.

3. Corrosion rate can be predicted by the mass-transfer equation.

4. Corrosion of 9Cr-1Mo in a high-temperature region of the SNAP-8 system results in a mass-transfer deposit in a cooler region of the system.

5. Corrosion of 9Cr-1Mo calculated by the mass-transfer equation in a SNAP-8 system indicates that, under a fully wetted condition desired for the boiler performance, 9Cr-1Mo is not suitable for 10,000-hr service.

6. Lower velocity boiler plug such as the multipassage plug results in a lower corrosion rate.

7. In the SNAP-8 boiler, a region of high temperature and high liquid velocity, materials insoluble in mercury, such as tantalum and columbium, are preferable to 9Cr-1Mo steel.

III. INITIAL EVALUATION OF 9Cr-1Mo STEEL MERCURY CORROSION RESISTANCE

There are three tests methods usually employed when evaluating the liquid metal corrosion resistance of engineering alloys such as 9Cr-1Mo. These are:

- Capsule tests
- Thermal convection loop tests
- Scaled dynamic loop tests

When capsule tests and thermal convection loop tests are used, it is not possible to simulate in one test the conditions found in the mercury Rankine cycle that is used in the SNAP-8 system. In addition to the above laboratory tests, full-scale prototype component operation also provides corrosion data. In the evaluation of 9Cr-1Mo steel for mercury corrosion resistance at SNAP-8 conditions all four types of tests mentioned above have been conducted and are summarized below.

A. CAPSULE TESTS

The capsules used in these tests were tubular, made of 9Cr-1Mo, and had a small quantity of mercury sealed inside under vacuum. The capsules were oriented vertically and the bottom part of the capsule was heated causing the mercury to boil and condense in the cooler top part of the capsule.

The corrosion found in these capsules showed a general solution attack on the top portion of the capsule where the mercury had condensed and run down the wall. The extent of corrosion was controlled by the temperature (1000 to 1250°F) of the capsule. At the higher temperatures of 1250°F, a roughening of the surface could be observed and some intergranular penetration. (Ref. 1, 2, 3, and 4)

The capsules tests indicated that 9Cr-1Mo steel was superior to other high-temperature alloys such as AISI Type 316 SS and Haynes 25, a cobalt base alloy. These alloys contain an appreciable nickel alloy addition that is readily dissolved by the mercury. Since the capsule test could not duplicate the expected conditions found in the SNAP-8 system, an estimate of corrosion penetration per unit time could not be calculated from these tests.

B. THERMAL CONVECTION LOOPS

Thermal convection loops of 9Cr-1Mo steel were operated and evaluated to further evaluate this material for mercury corrosion resistance and to evaluate mercury corrosion product separators. This study is reported in Reference 5.

These loops were operated with a boiling-condensing temperature of 1075°F, a superheat temperature of 1180°F and a subcooled temperature of 500°F. The operating time for each of the four loops was 1000 hr at an estimated mass flow of 7 lb/hr.

The evaluation of these loops revealed tube wall pitting to a depth of 0.0005 to 0.005 in. immediately above the condenser and no detectable wall recession.

As was the case for the capsule tests, no definite conclusion could be reached as to the rate of corrosion because of the extremely low mass flow in these loops (7 lb/hr vs 12,000 lb/hr in the full-scale system).

C. SCALED DYNAMIC LOOP TESTS

The data from the capsule and thermal convection test did not result in corrosion data that could be applied to the full-scale SNAP-8 system by any proven method. Therefore, three pumped corrosion test loops were operated that simulated the condition found in the SNAP-8 mercury system. The mass flow of these loops was scaled down from the full-scale system.

1. <u>TRW Loop</u>

This loop was fabricated from 9Cr-1Mo clad with Type 316 SS and was used to evaluate corrosion and corrosion product separator techniques. The mass flow of this loop was 100 lb/hr while all other conditions (temperatures and pressure) found in the SNAP-8 system were closely simulated. The results from this loop were reported in Reference 6.

Corrosion evaluation of this loop revealed even solution attack and penetration from 0.0003 in. to 0.0027 in. with the deepest penetration at the midpoint of the boiler. No appreciable attack was observed in the superheat section of the boiler.

2. Aerojet Loops

Two scaled corrosion loops (Corrosion Loop 3 and 4) were constructed to study corrosion and mass transfer in the SNAP-8 mercury system. These loops were identical and had a mass flow of 500 lb/hr of mercury. The loop is described in Section V, Experimental Study, of this report.

Corrosion Loop 3 (CL3) was operated for 4400 hr and was then completely dismantled and evaluated. During the operation of this loop the problem of boiler conditioning, or changing boiler performance, was encountered. Corrosion Loop 4 (CL4) was started with a boiler of the same design as CL3, but when the boiler performance was poor, design changes were made to the boiler inlet plug to overcome this problem. After the boiler in CL4 had operated for approximately 2500 hr, it was removed and replaced with another boiler. The experiments with the second boiler in CL4 are described in Section V of this report.

A summary of the evaluation of CL3 and the first boiler operated in CL4 is given below:

a. Corrosion Loop 3 (CL3)

The components from the loop (described in Ref. 7) were disassembled and all tubing in the loop was split longitudinally for examination. Component evaluation other than the boiler are included in this summary to support the conclusion that the SNAP-8 mercury corrosion problem is confined to the boiler.

The operating history of CL3 is given in Ref. 8 and 9.

(1). Mercury Boiler

The temperatures of the 9Cr-1Mo steel tubing along the mercury boiler are considered to be those given by NaK-temperature profiles. As for the NaK side of the boiler, the corrosion found on the mercury side (interior of the tubing) will be keyed in this discussion to the boiler profile after 2000 hr of operation.

The boiler-inlet-plug region is 5-ft long. Pitting was found on the 9Cr-1Mo steel plug in an area 7 to 21 in. from the boiler inlet.

The inner surface of the 9Cr-1Mo steel tubing in the plug area was lightly pitted. The NaK-temperature profile of the boiler indicates practically no heat transfer in the plug region after the liquid mercury was preheated in the first 2 ft of the boiler. This suggests that the corrosion in the first part of the plug was caused by solution attack until the mercury became saturated. After saturation, no attack on the 9Cr-1Mo steel occurred until higher wall temperatures were encountered farther downstream.

Visual examination of the interior of the 9Cr-1Mo steel tubing following the plug region indicated heavy pitting in some sections. The maximum pitting depths are plotted in Figure 4, and Figure 5 reproduces photographs of boiler-tube sections where pitting was found. The heaviest pitting is associated with the boiler area where the heat transfer from the NaK to the mercury was the greatest, as indicated by the boiler-temperature profile.

The microstructure of the interior of typical sections of the tubing is shown in Figure 6. Tube cracking can again be seen in the boiler area where the maximum heat transfer occurred. Corrosion-product deposition is also shown.

The pattern of corrosion and corrosion-product deposition in the boiler suggests a relationship to the mercury flow pattern or hydrodynamics during the boiling process. It is postulated that the flow consisted of large drops or globules of mercury from the plug. These drops were forced along at a low velocity and pitted the tubing by solution attack. As drop velocity was increased and drop size was reduced by the increase in quality, the swirl wires in the boiler tube became effective in breaking up the drops and increasing the heat transfer. As shown in Figure 5, at the beginning of the boiler (5 to 15 ft) the pitting was independent of the swirl wire but was predominant in the swirl-wire areas (15 to 28 ft) as droplet velocity increased. It may have been possible for the swirl wires to trap several mercury droplets in the higher-velocity regions, thereby increasing their residence time. In the first 5 to 15 ft of the boiler, the pitting was predominantly in the bottom of the tubing (with respect to gravity), indicating low droplet velocities and swirl-wire ineffectiveness.

Most of the corrosion-product deposition was found 25 to 30 ft from the boiler inlet. As shown in Figure 4 this is the area where pitting depth decreases sharply. The corrosion products are deposited as the quality approaches 100% and the liquid mercury in the stream becomes supersaturated with the corrosion products.

The change in the NaK-temperature profile with operating time indicates that the mercury-flow pattern was changing constantly up to 2000 hr of operation. This would account for the pitting and corrosion-product deposition observed 30 to 50 ft from the mercury inlet.

(2). Choked Nozzle

The adjustable choke nozzle, which could not be adjusted during the last portion of CL3 operation, was disassembled (Figure 7) and examined visually. A sheared pin was found in this operating mechanism. The Stellite 6B nozzle and pintle tip were not eroded by the mercury vapor; there was a slight amount of corrosion-product buildup in the nozzle, and the pintle tip and nozzle were wetted by the mercury.

(3). Turbine-Simulator Heat Exchanger

No significant evidence of corrosion or mass transfer was found in the turbine-simulator heat exchanger. The tubing appeared to be wetted in some areas.

(4). Turbine Blade Section.

The blade-section assembly was disassembled and the blade section was removed for inspection. Figure 8 compares the blade section before and after exposure. The vapor velocity through the blade section was estimated at 206 ft/sec, and the vapor quality was 75% at 715°F. Exposure to these conditions produced no corrosion, mass transfer, or erosion in the blade section.

(5). Condenser

Examination of the tapered tubes on the mercury side of the condenser indicated very little corrosion of tube walls. No mass-transfer deposits were found in the condenser tubes.

(6). Mercury Pumps

(a) 9Cr-1Mo Steel Pump

This pump was operated for a total of 3971 hr in CL3. It was then disassembled and inspected for wear, mass transfer deposits, and erosion. The inspection indicated some Teflon-journal wear (Figure 9, Parts 6 and 12), a crack in the flange area of the front bearing housing (Figure 9, Part 4), and wear marks on the lower side of the hydraulic equalizing grooves. The journal wear amounted to approximately 0.025 in. The crack in the front bearing housing appears to have been caused by thermal stress in a weld area. Considerable weld metal was machined off during the finishing operation, and the indications are that the heat buildup in this area was caused by rubbing of the impeller's hydraulic balancing vanes against the housing.

There were also indications that the shaft was rubbing on the bottom of the shaft hole. The rub marks were all on the lower side of the case, indicating that the Teflon-journal wear was excessive and allowed the impeller shaft to drop and rub, thereby causing abnormal heat buildup. No mass-transfer deposits or erosion were found inside the impeller case or on the impeller (Figure 9, Parts 1 and 2).

The Type 405 SS pump was operated for 421 hr in CL3 as a standby pump. Its total operating time was 1494 hr, including operation in a pump-test loop and in CL3, before disassembly. On visual inspection, the pump was found to be in satisfactory condition and reusable after the installation of new Teflon journals. No mass-transfer deposits were found on the impeller or impeller case.

(7). Valves and Tubing

Three valves and a check valve in the all-liquid section of the mercury system was disassembled. The valve seats, valve parts, and tubing showed no indications of corrosion or mass-transfer buildup.

(8). Discussion

Evaluation of CL3 indicates that the main corrosion and materials problem with the SNAP-8 system is likely to arise in the mercury side of the boiler. The 9Cr-1Mo steel has limited solubility in mercury at the expected boiler temperatures, and corrosion will occur. The mercury-flow pattern during boiling appears to control the location of boiler-tubing corrosion. Exterior and interior cracking of the 9Cr-1Mo steel boiler tubing should also be of concern. The mechanism of this cracking has not been determined; because most of it occurs in the area of greatest heat transfer, however, it is probably associated with thermal stress or thermal fatigue.

Other areas of the mercury system appear to be free of serious corrosion and mass-transfer problems when 9Cr-1Mo steel is used. Essentially no mass-transfer deposits were found in the condenser and the liquid lines in the loop. The corrosion products generated in these areas apparently remained suspended in the mercury and/or floated at the mercury interface, eliminating the problem of tube restriction found in many liquid-metal systems.

b. Corrosion Loop 4 (First Boiler)

The CL-4 boiler was used for a variety of corrosion tests and boiler performance tests. During the boiler performance tests, the boiler inlet plug was changed frequently so the corrosion pattern in the boiler cannot be related to the operating time with a specific boiler inlet plug.

In general, the pitting at the end of the mercury tubing (50 ft from the mercury inlet) in the boiler is considered to be associated with the first 600 hours of operation when the boiler was deconditioned and the mercury boiling was taking place at the end of the boiler. The deep grooves in the boiler inlet plug section 17 to 26 in. from the mercury inlet are considered to be the result of the last 1900 hours of operation when multipitch boiler inlet plugs were used. This boiler does illustrate the influence of heat-transfer performance on the corrosion pattern of the SNAP-8 type of mercury boiler constructed of 9Cr-1Mo.

Various NaK temperature profiles were generated during the testing of this CL4 boiler. Most of these can be represented by the temperature profiles shown in Figure 10. Mercury boiling during the operation represented by Curve 1 occurred 50 to 60 ft from the mercury inlet. Curve 2 indicates mercury boiling took place 2 to 8 ft from the mercury inlet. The shift in profile was caused by the design changes to the boiler inlet plug. A detailed description of these tests is given in Ref. 10 and 11.

After the boiler was removed from the loop, the tubing was split longitudinally for evaluation.

(1). Coil Section

One area of pronounced pitting occurred in the coiled section of the mercury boiler. This area was approximately 50 to 60 ft from the mercury inlet. The location of this pitting area coincides with the maximum heat flux area for the 600-hr corrosion run (Figure 10). The deepest pit in this area was 0.0065 in. The pits assumed one of three different configurations: isolated single pits, pits combined into straight line segments, and pits combined in the form of circular dished out areas. The link segments were about 1-1/2 in. apart, with the circular dished-out areas between them.

Corrosion product deposition (Figure 11) was found immediately after the boiler inlet plug region (5 to 12 ft from the mercury inlet) with a maximum thickness of 0.004 in. There were minor deposits at the end of the boiler (50 ft from the mercury inlet) that were approximately 0.001 in. thick.

Examination of the microstructure of the inside diameter of the tubing indicated a white layer approximately 0.0001-in. thick along the coiled section of the tubing. Other than this layer, there were no other changes in the microstructure of the 9Cr-1Mo. No cracks were observed in the tube wall originating from the inside diameter.

(2). Boiler Inlet Plug Section

In the CL4 boiler, the area of major pitting was 17 to 26 in. from the mercury inlet or in the preheat section of the boiler (Figure 12). In this area, a large percentage of the pits had united to form transverse grooves (0.0265-in. deep maximum) and shallower grooves at 20° from the transverse position. The groove configuration indicates the effect of the tight-pitch region of the various multipitch plugs operated in this boiler. The probability that some form of tube wall corrosion would appear in this area was high since corrosion was noted in the tight-pitch region of the multipitch plugs when they were removed after the boiler performance tests.

Examination of the microstructure of the tubing in this section showed no white layer on the surface. The microstructures are typical of 9Cr-1Mo exposed to general solution attack by mercury. No cracking was observed in any of the tube sections examined.

c. Corrosion Mechanism Loop 1 (CML-1)

The CML-1 was designed to define the relationship of flow velocity to corrosion when 9Cr-1Mo steel was used. A complete description of this test is given in Ref. 12; the results are summarized below.

The test was operated for 200 hr at a temperature of 1100°F with some difficulty in maintaining wetted conditions in the 9Cr-1Mo test section. The measured rate of wall recession vs flow velocity was

Flow Vel., ft/sec	Wall Recession Rate in./100 hr
2.25	0.00044
4.5	0.00075
9.0	0.00225

d. Seventh-Scale Loop (SSL)

The SSL was operated to investigate SNAP-8 boiler problems using a facility that would simulate one full-size tube of the seven-tube full-size

SNAP-8 boiler. The areas of investigation include boiler conditioning, boiler lifetime, and boiler stability.

The first test section (designated SA-1) operated in the SSL was fabricated from 9Cr-1Mo steel. A complete description of the test section is given in Ref. 13 and the operation and evaluation is summarized below.

(1). Operation

The SA-1 test section was operated intermittently at elevated temperatures for 473 hours over the period of 19 April 1967 through 18 July 1967. This period represented the startup and checkout of the new SSL facility as well as the operation of a full-size single-tube model of the SNAP-8 tube-in-tube boiler. The test section operating history was as follows:

Run	Operating Time, hr	Remarks
1	58	1st SSL startup. Loop shakedown and check-out. Data point at design flow and low NaK schedule.
1	115	Loop shakedown and checkout.
1	5	Loop shakedown and checkout.
	-	Hg tube soaked with lithium-mercury mixture at 950°F to improve performance.
	-	Mercury pump replaced.
1A	27	Startup after 1st Li-Hg treatment. Boiler performance still degraded.
1	-	2nd Li-Hg mixture treatment. @ 950°F
1B	166	Startup after 2nd Li-Hg treatment. Improvement in boiler performance was noted. Heat-transfer survey at various mercury flows and NaK schedules.
1C	102	Additional heat transfer survey taken following installation of expanded range scales on test section temperature recorders.
Total	473 hr	

(2). Evaluation

Post-test disassembly and examination of the SA-1 test section showed essentially no corrosion of the tight-pitch region. A heavy black deposit (55% carbon) and a black film was found in the tight-pitch region. The black film was found in the loose pitch and unplugged regions. The origin of the deposit and film was thought to be the mercury pump silicone oil released into the mercury stream during pump failure. It is postulated that decomposition of the pump oil prevented mercury wetting and resulted in poor test-section performance. Two lithium-mercury treatments could not remove the heavy surface contamination.

Samples of the 9Cr-1Mo containment tube were mounted, polished, etched and examined. The microstructures were typical of those observed in other 9Cr-1Mo test sections operated in Corrosion Loop 3 and 4.

D. FULL-SCALE BOILER TESTS

1. Objectives and Conclusions

The primary objectives of the tests summarized in this section was to determine the lifetime of a SNAP-8 system based on the mercury corrosion rate of 9Cr-1Mo steel at SNAP-8 operating conditions. It was recognized that 9Cr-1Mo steel would corrode and mass-transfer products would collect in the system.

The erratic heat-transfer performance of the mercury boilers in the corrosion loops that closely simulated the actual SNAP-8 conditions made the results obtained from scaled loop difficult or impossible to apply to the full-size system.

The key to both heat-transfer performance and consistent corrosion results is considered to be the wetting of the containment material by the mercury. Wetting implies that there is no surface film to prevent the mercury from dissolving the containment material according to the solubility relationships. The pitting found in many of the 9Cr-1Mo steel subscale mercury boilers is believed to have been caused by uneven wetting of the boiler tubing inside surface. If an area of the boiler tubing was wetted by mercury while an adjacent area was not, corrosion would take place in the wetted area forming a pit.

During full-scale boiler test section operation it was evident that satisfactory heat-transfer rates or conditioned performance was obtained when the mercury wet the inside surfaces of the boiler tubes. Wetting by the mercury could be induced by additives such as rubidium that lowered the surface tension of the mercury. The other mechanism for mercury wetting was the removal of all surface films on a metallic surface.

If mercury could be made to wet a 9Cr-1Mo boiler tube surface without the use of mercury additives, then satisfactory heat transfer should be achieved as well as consistent corrosion results. Data of this type would provide a firm base for assessing the potential of 9Cr-1Mo steel as a containment material for the SNAP-8 system.

2. Description of Testing

A full-scale 9Cr-1Mo steel boiler used in a breadboard system was evaluated after approximately 1400 hr of operation. This boiler was a tube-in-shell design rather than the tube-in-tube boilers discussed in the subscale loop tests. The boiler was a combination cross-counter flow, tube-in-shell heat exchanger. The mercury flowed in four 60-ft-long tubes which were coiled on two double-lead helices. A plug to restrict the flow as placed in the inlet to each of the four parallel flow passages, giving a liquid velocity of 0.8 ft/sec. The plug in this restricted flow section was a solid rod spaced from the inside of the tube by a wire spring forming a spiral flow path for the mercury. This insert continued through the boiler for 10 ft. Downstream of the plug, the spiral flow was maintained by a twisted ribbon insert which continued for the remainder of the boiler length. Thw swirl flow served to separate the high-density liquid from the vapor, making the boiler operation insensitive to gravity and increasing heat-transfer rates. The mercury coils were surrounded by two concentric cylindrical shells which formed an annular flow passage for the reactor coolant, NaK-78 (the eutectic mixture of sodium and potassium). The Hg tubes were 0.902-in. ID by 0.125-in. wall 9Cr-1Mo steel, and the shells were 316 SS. The plug consisted of a 0.600-in. OD low-carbon steel rod and 0.135-in. dia. low carbon steel wire. The ribbon was also of low-carbon steel, 0.016 in. thick.

a. Operating History

The rated design parameters of the Hg side of the boiler, and typical performance characteristics during the test period, are shown in Table 2. The boiler started the test series with a less than satisfactory heat-transfer capability (unconditioned state), and saturated vapor was not produced (Ref. 14). The boiler was operated intermittently for approximately 300 hr with a Rb additive in the Hg to promote full conditioning and attainment of rated boiler outlet conditions. Testing continued thereafter until a total 1415 hr of operating time was logged. During the last half of the total test period (approximately 700 hr), boiler characterization tests were conducted under varying operating conditions.

b. Evaluation

One of the four tubes contained mass-transfer deposits directly at the Hg outlet manifold (Figure 13). Such a deposit would be expected at the manifold only if the tube operated with no superheat length for a major portion of the test period. It is not clear why only one of four tubes should exhibit mass-transfer deposits at the Hg outlet.

The 0-4 tube, one of the two tubes coiled in the outer layer of the two-layer tube bundle, was completely dissected. The coil was cut transversely into sections comprising 180° of a single turn. Each section was then cut longitudinally. The surfaces of the tube, twisted tape, and the Hg inlet plug and associated wire were examined for surface effects. Significant findings are summarized below and in Figures 13 and 14.

(1). Macrographic Examination of Tube 0-4

Surface effects found at the Hg inlet region (including the tube, plug, and wire) up to the 23-ft point are presumed to be liquid Hg corrosion effects. There appeared to be no orientation of the attack with respect to gravity. The surface deposits resulted from the precipitation of soluble corrosion products from the liquid Hg as it vaporized.

(2). Microscopic Examination of Tube O-4

(a). Pitting

Pitting was found in the first 23 ft of tube O-4 (measured from the Hg inlet). Figures 13 and 14 show photomicrographs of a section of the tube 11 ft from the inlet. The pits were approximately circular, with a diameter-to-depth ratio between 1 and 10 and a maximum depth of 5.5 mils. Figure 15 describes the maximum pit depth distribution along the tube length. There was no apparent orientation of pitting or maximum pit depth with respect to either gravity or centrifugal forces on the flowing Hg.

(b). Mass Transfer

Microscopic mass-transfer surface deposits were found in the area 13 to 57 ft from the Hg inlet end. The maximum depth at the 47-ft point was 4 mils. It is postulated, confirmed by the operating history (Table 2) that the boiler operated for significant time periods with a very short superheat length. This would explain the presence of deposits only 3 to 4 ft from the Hg outlet in this tube coil.

IV. FINAL EXPERIMENTAL STUDY

A. LOOP DESCRIPTION

Corrosion Loop 4 (CL4) was designed to simulate the SNAP-8 dynamic cycle conditions for corrosion study. This three-loop system consisted of (1) a heated primary NaK loop coupled through (2) a boiler-simulated mercury Rankine-cycle loop which rejects its heat through the condenser to (3) an air-cooled circulating NaK loop. Figure 16 is a flow diagram of the loop and Figure 17 shows the arrangement. The three-loop system was constructed to high-vacuum standards.

The NaK primary loop employed a direct resistance heater in which low-voltage electrical current was passed through a NaK-carrying tube and the NaK. The heater was in a coiled configuration with the two grounded leads on the loop side and an insulated low-voltage lead at the midpoint of the coil. Since the resistance of each leg was fixed, the power input was varied by controlling the voltage across the terminals. The voltage was regulated with a saturable core reactor transformer. An electromagnetic pump maintained the NaK flow which was measured by a magnetic flowmeter.

The mercury loop used two Chempump* Model CFRT-7 1/2-65 (one on a stand-by basis) for pumping the liquid mercury. A venturi flowmeter was used to measure mercury flow. Two semistandard valves were used for control and for imposing a resistance between the pump and boiler. An adjustable choked nozzle was located downstream of the boiler outlet to regulate boiler outlet pressure. The adjustable choked nozzle was a convergent-divergent nozzle in which the throat area could be varied with a movable pintle. The mercury vapor was then passed through a desuperheater and a turbine-blade test section before entering the condenser. The desuperheater and the blade section were not necessary for the boiler experiment, but were originally designed for corrosion study. The NaK-cooled mercury condenser was a counter-flow heat exchanger consisting of three tapered condensing tubes with a straight length for subcooling.

---

*Manufactured by Chempump Division of Fostoria Corp., Huntington Valley, Penn.

The rest of the mercury loop consisted of semiconventional liquid metal components such as bellows sealed valves, electrical resistance level probes, and a cover-gas system.

B. TEST SECTION DESIGN

Using the approach that decreasing the mercury mass velocity in the preheat region reduces its corrosion rate, three test sections were specified for testing in CL4.

A test section (identified as 4A-3) simulating the base case of the full-scale boiler was designed. A schematic of this test section is shown in Figure 18. The calculated corrosion performance of this test section is given in Figure 19.

A constraint imposed upon the design effort was that the presently available 9Cr-1Mo tubing be utilized. Therefore, the lower limit upon the mercury mass velocity would be an empty (no plug) tube. A test section (identified as 4A-4) was designed utilizing an empty tube for the preheat region. A schematic of the 4A-4 is given in Figure 20. The calculated corrosion performance of this test section is given in Figure 21.

During this phase of the analytical effort, other boiler design criteria (i.e., control of slug flow boiling length) dictated the use of a multi-passage plug insert in the SNAP-8 boiler. A test section (designated 4A-1) was adapted to the CL4 requirements. It was fortuitous as this particular design has a mass velocity between that of the base case and the empty tube. The 4A-1 test section is shown schematically in Figure 22. The calculated corrosion performance of this test section is given in Figure 23.

C. 4A SERIES TESTS

The procedures used in the 4A tests were to install the test sections described above in the CL4 loop in series with the coiled boiler section. The test procedure included several short-term tests. Prior to a long corrosion run, the test section was wetted by the method described in the Appendix of this report.

The test sequence was:

- Loop startup
- Boiler heat-transfer survey
- Loop shutdown
- Pre-wet the test section with Hg-Li solution
- Restart loop
- Boiler heat-transfer survey
- Corrosion run
- Boiler heat-transfer survey
- Pressure drop test

1. <u>4A-3 Test</u>

The 4A-3 test section was installed in CL4. Three boiler data points were taken to define the performance of the boiler before the Hg-Li pre-wetting solution was used. The boiler was "conditioned" in that the boiling was completed in 6 to 8 ft, but the local NaK temperature profile across the inlet plug was relatively flat.

The loop was shut down and the test section was pre-wetted using a Hg-Li solution containing 351 ppm of Li using the procedure given in the Appendix. This solution was held in the boiler for 4 hr at 950°F with an argon cover gas to suppress the boiling. After the 4-hr soak, the boiler was allowed to cool to approximately 350°F and the Hg-Li solution was drained from the boiler. The Li content in the solution drained from the boiler was 216 ppm.

Mercury boiling was re-started and three boiler data points were taken to define the boiler performance. There was no improvement in the performance of the boiler, especially in the inlet plug region and it was concluded the Hg-Li solution had not caused the 9Cr-1Mo surfaces to be wetted by the mercury.

The loop was shut down and the pre-wetting procedure was repeated using a high Li content in the Hg-Li solution and an increase the soak time at 950°F from 4 to 16 hour.

The test section was retreated with Hg-Li solution containing 574 ppm Li before the solution was introduced into the boiler. After a soak at 950°F for 16 hr, the boiler was allowed to cool to 500°F and the Hg-Li solution was drained from the boiler. The Li content was 271 ppm.

Mercury boiling was started and the NaK temperature profile (Figure 24) showed an improvement in the performance of the boiler inlet plug section. The corrosion run was started at this point since the pre-wetting treatment had apparently promoted mercury wetting of the 9Cr-1Mo boiler tube surfaces.

After 30 hr of operation, the ΔP across the boiler inlet section began to increase gradually; the boiler inlet pressure increased from 442 psia to over 500 psi at 70 hr of operation. This was above the range of the boiler inlet pressure transducer readout so that NaK flow was reduced to decrease the mercury boiler inlet pressure.

After 90 hr running time, three boiler data points were taken; it was found that the increased ΔP across the boiler plug insert suppressed the boiling and forced the liquid vapor interface almost to the end of the loose-pitch section of the inlet plug. Normally, the boiler interface is near the end of the tight-pitch section. The loop was operated for 120 hr after wetting was established then shut down intentionally so the cause of the high ΔP in the inlet plug region could be determined. The total operating time on 4A-3 test section was 133 hr.

After the loop had cooled, ΔP tests with mercury were made on the inlet section. The pressure drop of the inlet section had increased from 37 to 52 psi at 550 lb/hr mercury flow, indicating flow blockage.

The test section was removed from CL4, decontaminated, and the NaK jacket removed. X-rays of the mercury containment tubing with the inlet plug in place showed a deposit immediately after the tight-pitch section where the pitch flares from 0.200 to 1-1/2 in. The tubing was removed from the plug without disturbing the area where the blockage was observed. Figure 25 shows the location of the deposit (lower left and lower center photos) and its formation in one quadrant of the tubing.

The wall thickness of the 9Cr-1Mo mercury containment tubing was measured and compared to the original measurements. Figure 26 illustrates the wall loss along the tube for the mercury inlet. In the area where the mass-transfer deposit was formed (24 in. from the Hg inlet), wall loss was found in areas where deposits had not built up.

Measurements of the inlet plug revealed no dimensional change within the accuracy of the measurements and, therefore, no apparent corrosion of the inlet plug occurred.

A spectrographic analysis was made of a sample of the mass-transfer deposits that cause the blockage in the section. The results showed the following:

Hg	=	> 10%
Fe	=	0.1 to 1.0%
Cr	=	0.001 to 0.01%
Li	=	Not detected

A wet-chemical analysis was made of another sample of the mass-transfer deposit for Li; this analysis indicated 80 ppm Li. A microstructure of the deposit is shown in Figure 27.

2. 4A-1 Test

Mercury boiling was started and boiler data points were taken to define the performance of the boiler before the Hg-Li pre-wetting solution was used. The mercury vapor quality was approximately 25% at the test section outlet and this was in agreement with the predicted results.

The loop was then shut down and the test section was pre-wetted using a Hg-Li solution containing 538 ppm of Li. This solution was held in the boiler for 16 hr at a temperature of 950°F, with an argon cover gas to suppress the boiling. After the 16-hr soak, the boiler was allowed to cool to approximately 350°F and the Hg-Li solution was drained from the boiler. The Li content of the solution was 451 ppm. Mercury boiling was restarted and no improvement in boiler performance was noted. The corrosion run was started at this point since the test section was considered to be wetted by the Hg-Li solution treatment based on the experience with the 4A-3 test section. The loop was shutdown after a corrosion run of 304 hr. The total time on the 4A-1 test section was 334 hr including the operating time prior to the pre-wetting treatment.

The test section was removed from CL4, decontaminated, and the NaK jacket removed. Since the tube was swaged over the plug the tube was split by milling two grooves through the wall 180° apart. Figure 28 shows the 4A-1 test section disassembled, several photos of the multipassage plug, and the inside diameter of the 9Cr-1Mo mercury containment tubing. Figure 29 and Figure 30 are photomicrographs of the tube and plug surfaces that were in contact with mercury.

Tubing wall thickness measurements were made at the areas where the grooves and tube wall formed the mercury channels. Adjacent areas of the tube wall not contacted by the flowing mercury were also measured. The inlet plug was measured for OD and the depth and width of the grooves. Figure 31 shows a plot of the average change in wall thickness of the five grooves along the 9Cr-1Mo containment tubing.

3. 4A-4 Test

Mercury boiling was started and boiler data points were taken to define the performance of the boiler before the Hg-Li pre-wetting solution was used. The loop was shut down after 54 hr of operation.

The test section was pre-wet using a Hg-Li solution containing 617 ppm Li. The solution was held in the boiler for 16 hr at 950°F with an argon cover gas to suppress the boiling. After the 16-hr soak the boiler was cooled to approximately 350°F and the Hg-Li solution was drained from the boiler. The Li content was 435 ppm. Mercury boiling was restarted and the loop was operated for 304 hr for the corrosion run. The total operating time on the test section was 358 hr.

The test section was removed from CL4, decontaminated, and the NaK jacket removed. The orifice carrier was cut from the mercury containment tubing by making transverse cuts in each side of the carrier. The tubing downstream of the orifice that contained the swaged-in plug was split longitudinally by milling two grooves in the tube 180° apart. Figure 32 shows the 4A-4 test section and photos of the various parts of the section. Visual inspection revealed that the tungsten orifice had become loose in the 9Cr-1Mo orifice carrier because of corrosion of the 9Cr-1Mo. This allowed the mercury to bypass the orifice and caused the decrease in pressure drop through the test section. There was no visible change in the tungsten orifice. Figure 33 shows photomicrographs of the 9Cr-1Mo tube and plug surface that were in contact with mercury.

Wall thickness measurements were made on the tubing upstream of the orifice (preheat region) and the tubing downstream of the orifice to determine the corrosion rate and pattern. The change in wall thickness is shown on Figures 34 and 35.

D. DISCUSSION OF 4A TEST RESULTS

The corrosion measured in the 4A tests is compared with the values calculated by the SNAP-Eight Corrosion and Thermal (SECAT) analyses (described in Section V) in a composite of curves shown in Figure 36. Examination of these curves indicates that the experimental data supports the corrosion model of dissolution of the 9Cr-1Mo by mercury with the rate determined by a diffusion through the stagnant liquid boundary layer.

The calculation utilized the available transport and solubility properties and also ignored the entrance effect. The latter would tend to give higher mass transfer rates at the entrance such as were obtained in the 4.5 ft/sec case.

Metallurgical analyses also support the corrosion model potential. Photomicrographs of the 9Cr-1Mo surfaces corroded by mercury shows a dissolution pattern. Analysis of the mass-transfer deposits also shows the presence of iron and chromium.

The model predicts the worst case i.e. the case in which the 9Cr-1Mo is fully wetted. As was stated previously, corrosion runs with the 4A test sections were made after a wetted condition was obtained with the Hg-Li treatment.

A comparison of the 4A test data, in which wetting was obtained, with the data from nonwetted cases (Ref. 12, 13 and 15) shows that the corrosion in the nonwetted cases is much less than that measured corrosion in the 4A tests. Consequently, extrapolation of the nonwetted-testing data to 10,000 hours can lead to optimistic conclusions. In general, the heat-transfer performance in a nonwetted case is not acceptable.

V. ANALYTICAL TREATMENT OF CORROSION

An analytical expression was developed to describe corrosion in the preheat region of the SNAP-8 boiler. Further, an analysis was conducted to determine the SNAP-8 tube-in-tube boiler design parameters that could be modified to minimize the corrosion potential of 9Cr-1Mo steel in the preheat region, and to design tests to evaluate the analytical procedures. The analytical program was divided into the three phases:

- Develop a method to predict corrosion performance in the preheat region of SNAP-8 type of boiler.
- Perform analyses to determine which boiler design parameters could be modified to minimize corrosion.
- Design and/or analyze several test sections to evaluate the corrosion prediction method.

Each phase will be described in the following three sections.

A. ANALYSIS - COMPUTER CODE SECAT

As the mercury traverses the preheat region of the boiler, iron, 9Cr-1Mo steel's main constituent, is dissolved by the mercury. The driving potential for this dissolution process is the difference between the solubility of the iron evaluated at the wall temperature and the bulk mercury iron concentration. If it is postulated that the rate of dissolution of the 9Cr-1Mo steel is controlled by diffusion rate of iron across the laminar boundary layer, it can be seen that what has been described and postulated is a mass transfer process. Apply the techniques used to analyze a mass transfer process to a differential length of the preheat region shown in Figure 37. Note that although Figure 37 depicts an annular geometry for both the NaK and mercury side, any geometry may be analyzed by using appropriate geometric factors and heat-transfer correlations in the following analysis.

To predict corrosion rates, the heat-transfer performance of the preheat region must be known. Applying a heat balance to each of the fluids we obtain

$$q = W_N C_{P_N} dT_N \quad (1)$$

$$q = W_H C_{P_H} dT_H \quad (2)$$

Ignoring the Nak side heat loss to environment, the rate-potential equation for the heat exchange process is

$$q = U_o P (T_N - T_H) d\ell \quad (3)$$

Substituting Eq. (3) into both Eq. (1) and Eq. (2) yields the following:

$$\frac{dT_N}{d\ell} = \frac{U_o P}{W_H C_{P_H}} (T_N - T_H) \quad (4)$$

$$\frac{dT_H}{d\ell} = \frac{U_o P}{W_H C_{P_H}} (T_N - T_H) \quad (5)$$

The mass flux of iron from the surface in contact with mercury (the mercury tube and the plug) may be expressed as:

tube side:

$$N_t = K (C_t^s - C_b) \rho_H \quad (6)$$

plug insert side:

$$N_P = K (C_p^a - C_b) \rho_H \quad (7)$$

The saturation concentration of the iron in mercury of the plug surface is evaluated at the bulk mercury temperature. The saturation concentration of iron in mercury of the tube wall is evaluated at the tube wall surface temperature (the mercury contact side).

The mass-transfer coefficient, K, was calculated using the following equation:

$$\frac{K}{V} = \frac{0.023}{Re^{0.2} Sc^{0.67}} \qquad (8)$$

The above is derived using a Reynolds analogy on the Colburn equation for heat transfer.

The solubility of iron in mercury, as a function of temperature, was evaluated from the following equation obtained from Ref. 16.

$$C^s = \exp\ (1.217 - 2113./\text{Temperature, } ^\circ R) \qquad (9)$$

Using the expressions for the mass flux given above, a mass balance for the bulk mercury iron concentration may be written.

$$\frac{dC_b}{d\ell} = \frac{K}{W_H} \left[P_t\ (C_t^s - C_b) + P_p\ (C_p^s - C_b)\right]\ \rho_H \qquad (10)$$

Integration of the above equation yields the axial distribution of the bulk iron concentration in the mercury. Knowing this distribution, the wall recession rates is found by dividing the mass flux (given by eq. (6) and (7)) by the iron density. The temperatures required to evaluate the transport and solubility properties are obtained by integrating Eq. (4) and (5).

SECAT is given an IBM 7094 computer code, written in FORTRAN to predict the corrosion and thermal performance of the preheat region of the SNAP-8 tube-in-tube boiler using the above equations. For a given set of operating conditions and NaK and mercury flow channel geometries, SECAT will calculate the required heat-transfer length and corrosion performance of the preheat region of the boiler. The method employed by the code is to numerically integrate, by a Range-Kutta scheme, the differential equations defining the spatial behavior of the heat transfer and corrosion processes. The code output is a tabulation of the calculated axial variation of the significant performance parameters in the preheat region. A sample output is given in Figure 38.

B. PARAMETRIC ANALYSIS OF 9Cr-1Mo CORROSION

The manner in which the parametric analysis was conducted was as follows:

- The basic SNAP-8 tube-in-tube boiler design was examined to determine which parameters could be easily modified.
- Each of these parameters was varied, one at a time, over a small range to determine which yield the most significant reduction of corrosion.
- Combinations of the above parameters were varied over a large but reasonable range to determine their effect on corrosion.
- The results are examined for significant trends.

The parameters selected to be varied were as follows:

1 NaK jacket inside diameter,

2 Mercury tube inside diameter,

For the plug insert, the parameters varied were:

3 Thread height

4 Thread pitch

5 Thread width

6 The number of mercury passages per tube

To facilitate interpretation of the results, all results of the parametric analyses were presented as a percentage change from the base geometry. The base geometry is that described in Ref. 17. A summary of the base geometry performance is given in Figure 39. The above listed parameters were varied by ±5% (from the base geometry) and their effect on corrosion behavior calculated. The results are given in Tables 3 and 4. Since the heat-transfer performance will change with the above parameters, the effect on heat-transfer performance (of these parameters) is also noted on the tables. Examination of the results indicate that increasing thread pitch, thread height, and number of mercury flow channels per tube yields the most significant reduction in the maximum penetration rate. However, the exit (preheat) mercury iron concentration increases with increasing number of channels. This is due to a longer preheat length being required, thereby distributing the corrosion over a larger area. The exit iron concentration is important from two aspects. First, the exit value represents the amount of material removed from the mercury tube and plug insert. Second, the same amount of material is later deposited somewhere in the system. The base case exit concentration is equivalent to 0.3 lb of iron removed and deposited per 100 hr. Therefore, the only parameters that were considered further, in this phase, were the thread pitch and thread height.

A series of cases was set up for SECAT which varied the thread pitch from 3/8 to 2 1/4 in. and the thread height from 0.062 to 0.122 in. The results are given in Table 5.

Examination of Eq. (6) and (7) reveals that the wall recession rates are functions of K, C^S and C_b. Now interpret the results of the parametric analysis in terms of the effect of boiler geometry changes upon corrosion performance by using the above mentioned variables.

The value of C^S is evaluated at either the plug or wall temperature. Although the plug wall temperature is at the fluid temperature, and therefore defined by the preheat requirements, the tube wall temperature is a function of the ratio between the mercury side resistance to the overall resistance. If the overall resistance is increased while maintaining the same mercury side resistance, the tube wall temperature, the C^S term, and the wall penetration should decrease. Increasing the NaK jacket diameter accomplishes this as shown by the results given in Table 3. The increase in exit iron concentration is due to the longer preheat length required.

If the preheat length is increased by appropriate modification of the boiler geometry, corrosion will occur over a larger area which should result in (1) an increase in the total amount of iron dissolved in the mercury (C_b), and

(2) a decrease in the maximum wall recession rate due to the lowered driving potential for the dissolution of iron. (The term $C^s - C_b$ at Eq. (6) and (7) decreases.)

Examine this supposition by applying it to the results of Table 4, the effect of increasing the number of Hg passages per tube. The model used by SECAT assumes that the heat-transfer area is that portion of the tube in contact with mercury. Since the thread pitch and width are held constant, doubling the number of channels per tube should increase the required preheat length by 24.7%. The results in Table 4 show a length increase of 24%. The lesser increase is due to the increased Hg side heat-transfer coefficient. The combination of increased length and doubling the number of channels results in a net increase in the area exposed to Hg by 34.7%. If the differential equation defining the C_b term is examined, Eq. (4), an approximate solution to it will be the following form:

$$C_b \cong C^s - \left[C^s - C_i\right] e^{-\alpha A} \qquad (11)$$

If the base case results are used, the term αA may be calculated and found to be ~ 0.718. If it is assumed that the α term is essentially invariant with the number of channels, the value of C_b for an increased (by 34.7%) corrosion area may be calculated. The increase in C_b is found to be 20.4% using Eq. (11) compared to 19.7% calculated by SECAT. This increase in the bulk iron concentration due to increase in the corrosion area should decrease the maximum wall recession rate (due to a lowering of the driving potential for dissolution). This effect is found in the results of Table 4.

The mass transfer coefficient (K) is calculated from Eq. (8). Algebraic manipulation of this equation will reveal that K is proportional to the mass velocity (G) raised to the 0.8 power. Therefore, it would appear that, if the mass velocity is decreased, a proportionate decrease in the wall recession should result. Examine the effect of increasing in the thread height by 5%. This 5% increase corresponds to a 4.45% increase in flow area. This in turn results in a 3.4% decrease in K. The results in Table 5 show that a 5% increase in thread height yields a 2.9% decrease in maximum wall recession rate.

Further examination of the results revealed that decreases in both wall penetration and exit iron concentration were effected by changes in the boiler geometry that decrease the mass velocity of the mercury. To illustrate this point, the results of Table III-3 were plotted in Figures 40 and 41 (corrosion performance versus mass velocity). It can be seen that both the maximum wall recession rate and preheat exit iron concentration decreases with decreasing mass velocity (or its equivalent liquid velocity).

REFERENCES

1. A. R. Herdt, Mercury Corrosion Resistance of Welded Joints, AN-TM-214, 18 February 1965.

2. SNAP 8 Mercury Corrosion and Materials Research, Topical Report for the Period June 1960 to December 1962, Aerojet Report 2517, Vol. III, 1963.

3. SNAP 8 Materials Programs, Quarterly Progress Report for Period 23 February to 24 May 1963, AN-976, October 1963.

4. L. Rosenblum, et al, Mechanism and Kinetics of Corrosion of Selected Iron and Cobalt Alloys in Refluxing Mercury, NASA-TN-D-4450, April 1968.

5. Mercury Corrosion and Evaluation of Corrosion Product Separators in 9Cr-1Mo Boiling Thermal Convection Loops, Aerojet TM-390:64-4-205, 18 February 1964.

6. Operation of a Forced Circulation Croloy 9M Mercury Loop to Study Corrosion Product Separation Techniques, ER-6123, 2 November 1964.

7. Dynamic Corrosion Loop Design Report, Aerojet Report 2596, July 1963.

8. SNAP-8 Materials Report for January to June 1964, Aerojet Report 2880, July 1964.

9. SNAP-8 Materials Report for July to December 1964, Aerojet Report 2989, January 1965.

10. SNAP-8 Materials Report for January-June 1965, Aerojet Report 3038, July 1965.

11. SNAP-8 Materials Report for July to December 1965, Aerojet 3134, January 1966.

12. SNAP-8 Electrical Generating System Development Program, Progress Report for January-March 1967, Aerojet Report 3379, May 1967.

13. S. Nakazato, SNAP-8 Program Work Performed by Nuclear Division, Aerojet-General Corporation July-September 1967, Aerojet TM 4923:68-496, 22 January 1968.

14. J. N. Hodgan, L. B. Kelly and A. H. Kreeger, Performance Analysis on the -1 Boiler Conditioning (RPL-2), Aerojet TM 4833:64-8-259, 18 December 1964.

15. SNAP-8 Materials Report for January-June 1966, Aerojet Report 3232, July 1966.

16. M. F. Parkman, D. K. Whaley, The Solubility of Iron, Chromium, Nickel, Cobalt and Vanadium in Mercury and Concentrations of Those Elements Found in Mercury After Contact with Iron-Cobalt, and Vanadium - Base Alloys, AN-957, Aerojet-General Nucleonics, July 1963.

17. A. J. Sellers, SNAP-8 Tube-in-Tube Boiler Design Analysis, Aerojet TM:4803-2-223, February 1965.

TABLE 1

TYPICAL MECHANICAL PROPERTIES OF 9Cr-1Mo STEEL

Typical Tensile Properties

Temp (°F)	UTS* (ksi)	.2% Offset YS** (ksi)	Elong. in 2 in. (%)	Reduction of Area (%)
70	82.0	45.0	35	72
300	76.0	39.5	33	71
700	65.5	36.0	31	68
900	59.0	34.5	35	74
1100	41.0	27.5	45	86
1300	18.5	10.5	62	94

EFFECT OF PROLONGED EXPOSURE OF 9Cr-1Mo STEEL
AT ELEVATED TEMPERATURES

Impact Strength and Hardness

At Room Temperature	Unexposed	Exposed 10,000 hr at 900°F	1050°F	1200°F
Impact Values (ft-lb)	63	50	32	37
Brinnell Hardness	161	172	119	140
Transition Temperature (°F) (15 ft-lb level)	-100	- 80	- 65	- 80

Stress Rupture

Exposure & Testing Temp. (°F)	Stress for Rupture in 1000 hr before exposure (ksi)	Stress for Rupture in 1000 hrs after exposure for 10,000 hrs without stress (ksi)
900	42.5	39.0
1050	16.3	13.8
1200	5.8	5.5

*UTS: Ultimate Tensile Strength
**YS: Yield Strength

TABLE 1

TABLE 2

SNAP-8 TUBE-IN-SHELL BOILER PERFORMANCE HISTORY

NaK Side	
Total operation	2350 hr*
Nominal boiler design conditions	
Flow (lb/hr)	32,000
Temperature (°F)	
Inlet	1300
Outlet	1100
Hg Side	
Total operation	1415 hr
With rubidium	320 hr (Nov. 1964 to Mar. 1965)
Nominal boiler design conditions	
Flow (lb/hr)	11,400
Temperature (°F)	
Inlet	513
Outlet	1265
Pressure (psia)	
Inlet	340
Outlet	270
Vapor outlet conditions (typical of various test periods)	
90% quality	470 hr**
Saturated vapor	240 hr
9 ft superheat length	125 hr
27 ft superheat length	460 hr
42 ft superheat length	120 hr

*Approximately the last 300 hr included a NaK purification system.
**Flow was 50% of nominal to enhance conditioning.

TABLE 3

EFFECT OF GEOMETRY ON THE PERFORMANCE CHARACTERISTICS OF THE PREHEAT REGION OF THE SNAP-8 BOILER

Percent Change* in Performance Characteristics for

Variable	5% Increase in Variable: Maximum Penetration	Exit Concentration**	Preheat Length	Hg Side ΔP	5% Decrease in Variable: Maximum Penetration	Exit Concentration**	Preheat Length	Hg ΔP
NaK Jacket ID	-1.4	+1.6	+2.8	+2.8	+1.6	-1.7	-3.0	-3.1
Hg Tube ID***	- .11	+ .04	-5.0	~0	+ .27	- .16	+5.2	~0
Thread Height	-2.9	-2.0	+ .69	-12	+3.1	+2.1	- .71	+15
Thread Pitch	-2.2	-3.0	- .49	-15	+2.3	+3.3	+ .58	+19
Thread Width	+ .40	+ .54	+ .92	+2.9	- .36	- .54	- .91	- 3.3

TABLE 3

NOTE:

*The change in the performance characteristics is that compared to the values calculated for the base geometry. The base geometry is that described in Reference

**Preheat exit concentration of iron in the mercury.

***The corresponding OD is changed to maintain a tube wall thickness of 0.09 inches.

TABLE 4

EFFECT OF THE NUMBER OF CHANNELS PER TUBE ON THE PERFORMANCE CHARACTERISTICS OF THE PREHEAT REGION OF THE SNAP-8 BOILER AT A CONSTANT MASS VELOCITY

No. of Channels per tube	Maximum Penetration	Exit[2] Concentration	Preheat Length	Hg Side ΔP	
	Percent Change in Performance[1] Characteristics				
2	-12	+18	+ 24	+ 34	(3)
3	-31	+45	+ 61	+116	(3)
4	-58	+72	+133	+370	(3)
5	-84	+82	+338	~15X	(3)
2	- 5.4	+10	+ 15	+ 19	(4)
3	-10	+19	+ 29	+ 40	(4)
4	-15	+27	+ 43	+ 61	(4)
5	-19	+33	+ 57	+ 83	(4)

(1) The change in the performance characteristics is that compared to the values calculated for the base geometry. The base geometry is that described in Reference 18

(2) Preheat exit concentration of iron in mercury.

(3) Constant mass velocity (G) maintained by increasing thread height.

(4) Constant mass velocity (G) maintained by increasing thread pitch.

TABLE 5

EFFECT OF THREAD HEIGHT AND PITCH ON THE PERFORMANCE CHARACTERISTICS OF THE PREHEAT REGION OF THE SNAP-8 BOILER

Thread Height, in.	Performance Characteristic	Percent Change(1) in Performance Characteristics Thread Pitch, inches .375	.75	1.125	1.5	1.875	2.25
.062	Maximum Corrosion Rate	(3)	-29	-42	-49	-54	-57
.082		-16	-42	-53	-60	-63	-66
.102		-27	-51	-61	-66	-69	-71
.122		-36	-57	-66	-71	-64	-76
.062	Exit(2) Concentration	(3)	-34	-47	-53	-57	-59
.082		-11	-44	-55	-60	-63	-65
.102		-18	-49	-60	-64	-67	-68
.122		-24	-54	-63	-67	-70	-74
.062	Preheat Length	(3)	- 2.9	- 2.1	- 1.0	- 1.0	+ .60
.082		+ 4.4	+ 3.3	+ 5.3	+ 7.2	+ 8.7	+ 9.9
.102		+ 8.6	+ 9.3	+13	+16	-18	+19
.122		+12	+15	+18	+24	+27	+29
.062	Hg Side ΔP	(3)	-88	-96	-98	-98	-99
.082		-54	-94	-98	-99	-99	-99
.102		-74	-99	-99	(4)	(4)	(4)
.122		-84	-98	-99	(4)	(4)	(4)

NOTES:

(1) The change in the performance characteristics is that compared to the values calculated for the base geometry. The base geometry is that described in Reference 18

(2) Preheat exit concentration of iron in mercury.

(3) Base case.

(4) Greater than 99.5% increase.

566-216

SNAP-8 SYSTEM SCHEMATIC

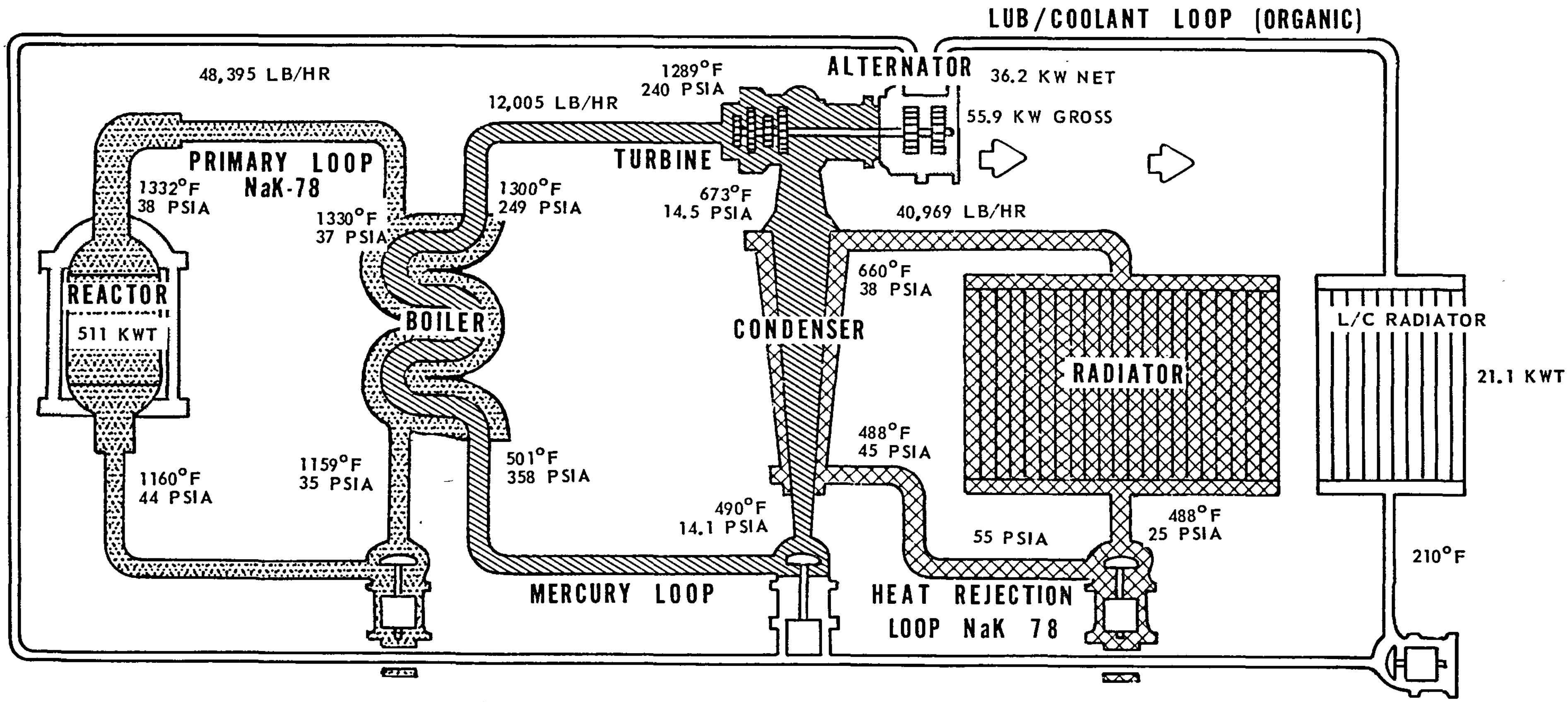

Figure 1

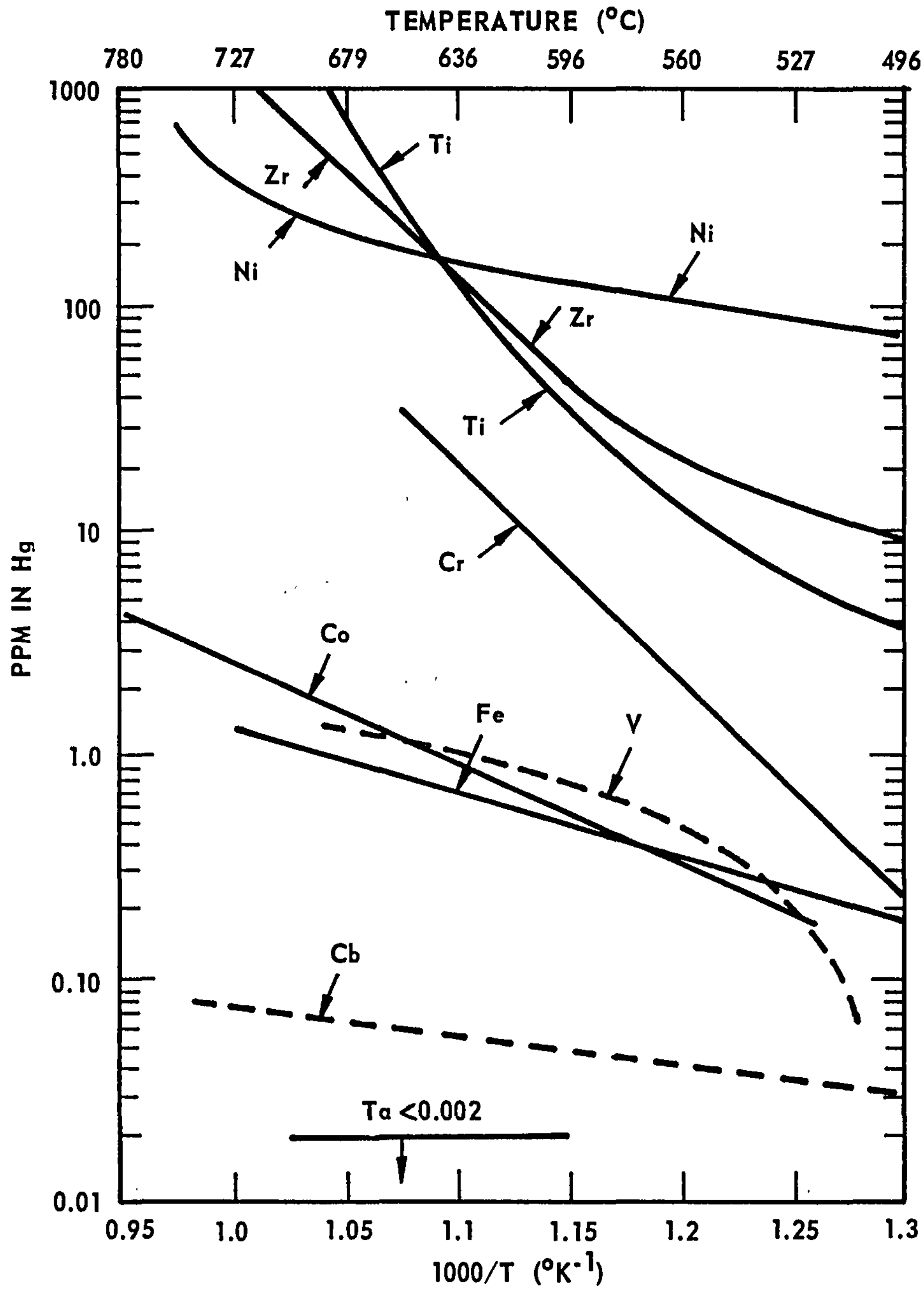

Solubility of Elements in Mercury

Figure 2

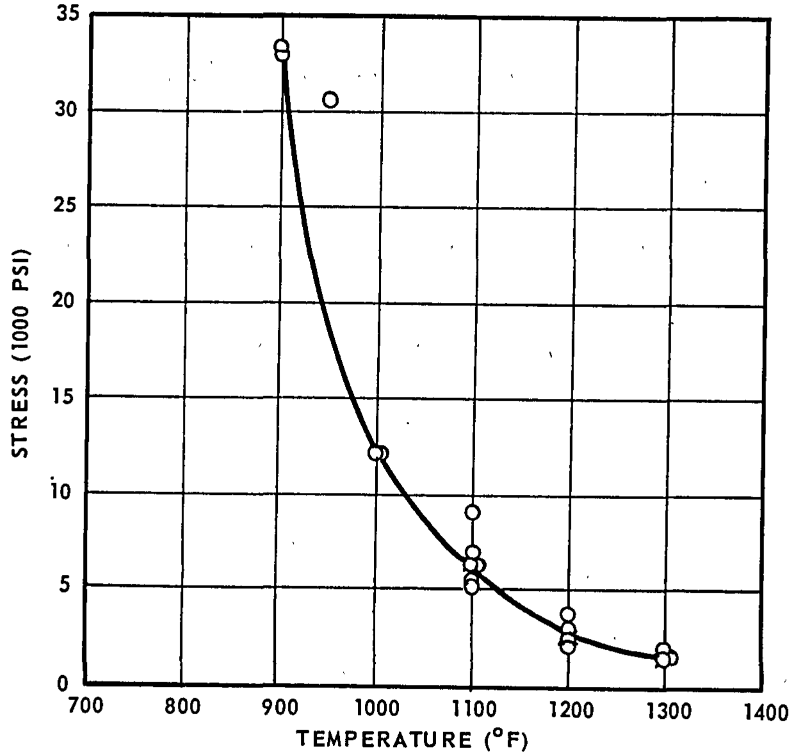

CREEP RATE 0.0001 PERCENT PER HOUR
(1 PERCENT IN 10,000 HOURS)
9.0 Cr, 1.0 Mo STEEL

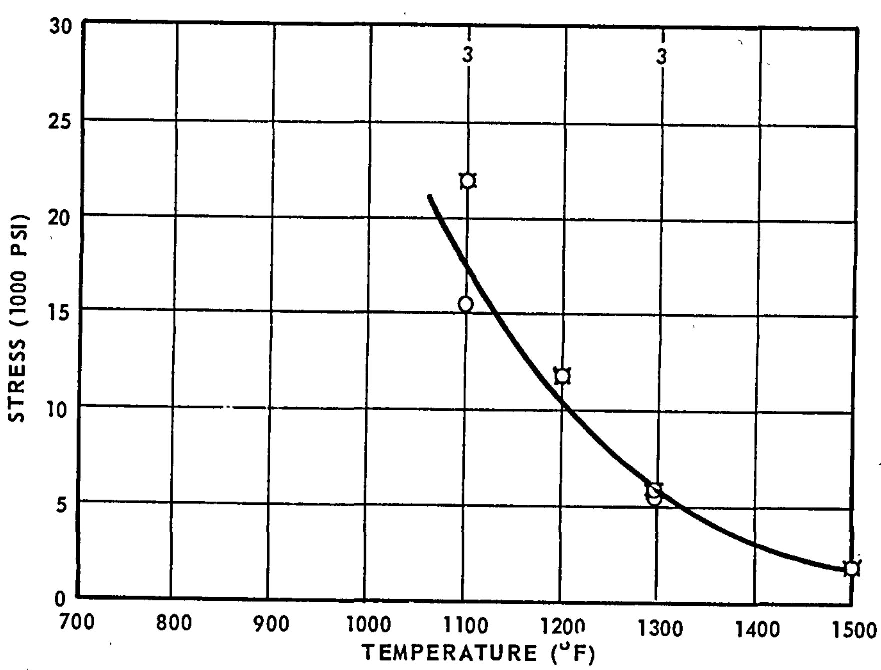

RUPTURE IN 100 HOURS
9.0 Cr, 1.0 Mo STEEL

Typical Creep and Stress-Rupture Properties of 9Cr-1Mo Steel

Figure 3

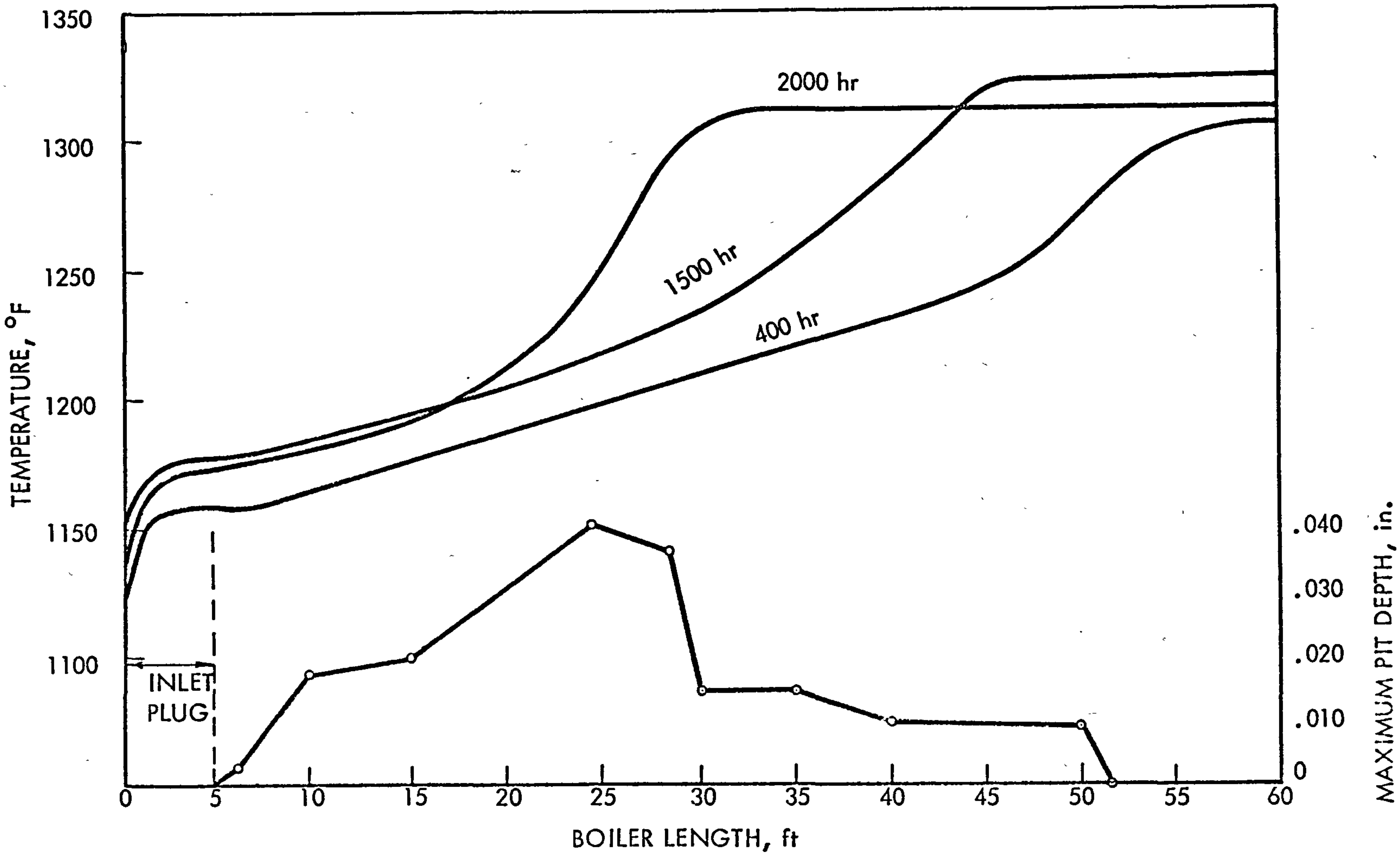
2000 hr
1500 hr
400 hr
TEMPERATURE, °F
1350
1300
1250
1200
1150
1100
INLET
PLUG
0
5
10
15
20
25
30
35
40
45
50
55
60
BOILER LENGTH, ft
.040
.030
.020
.010
0
MAXIMUM PIT DEPTH, in.

Figure 4

1268-NF-1185

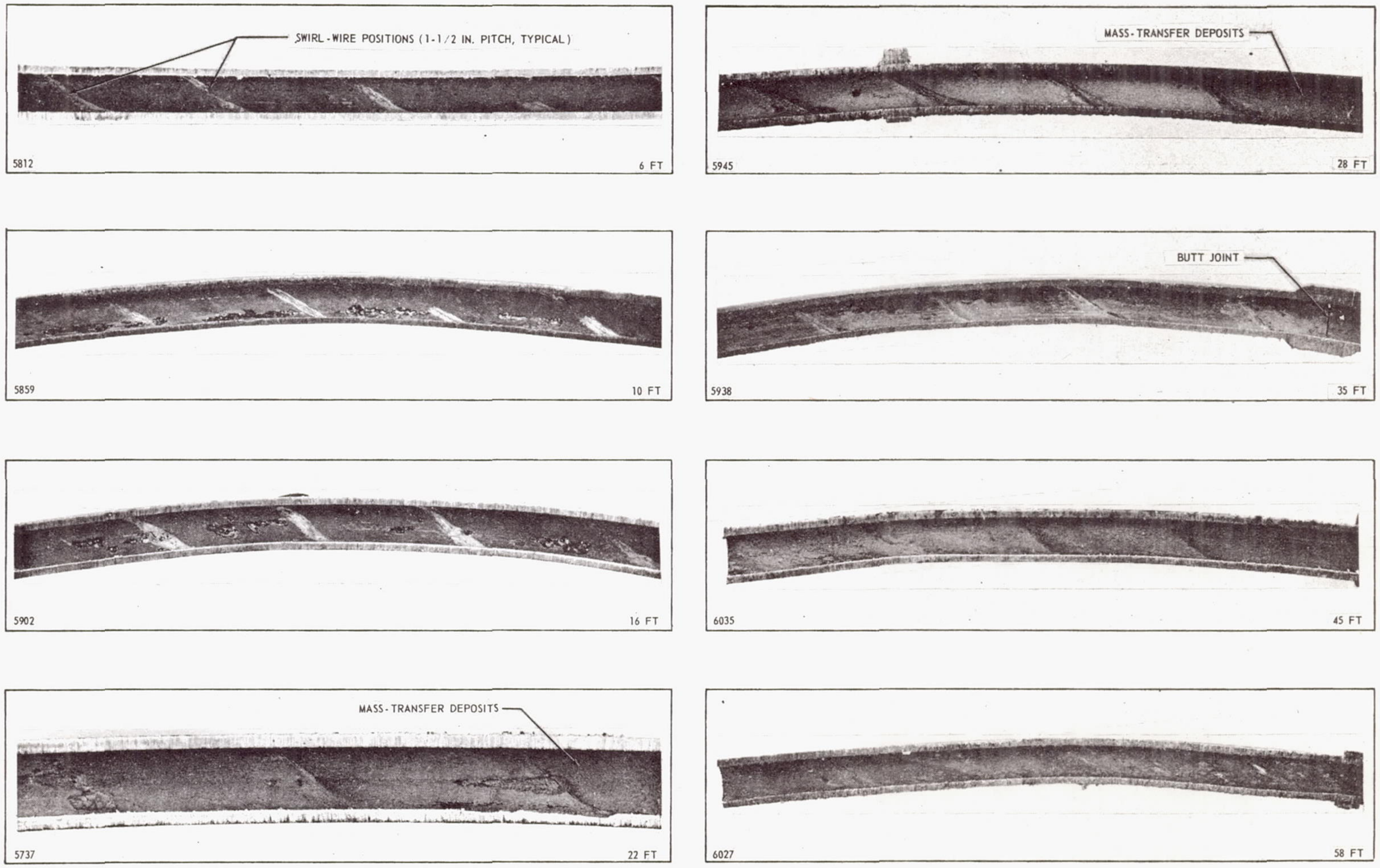

ALL VIEWS: THE MERCURY FLOW IS FROM LEFT TO RIGHT. THE INDICATED LOCATIONS ARE AS MEASURED FROM THE MERCURY INLET.

Figure 5

Views of Pitting in 9Cr-1Mo Steel Tubing, CL-3 Boiler

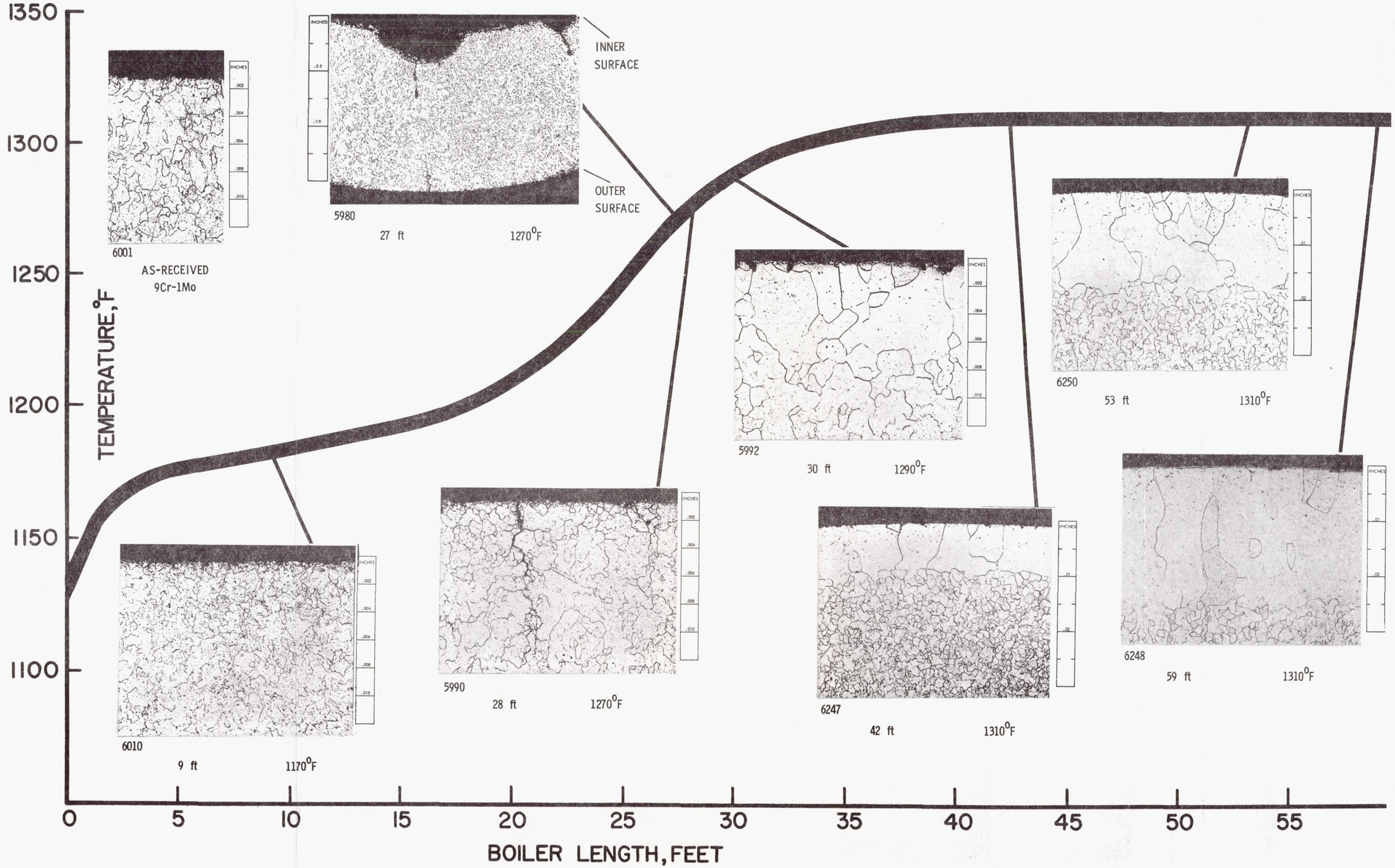

Microstructure at Exterior of 9Cr-1Mo Steel Tubing, CL-3 Boiler

Figure 6

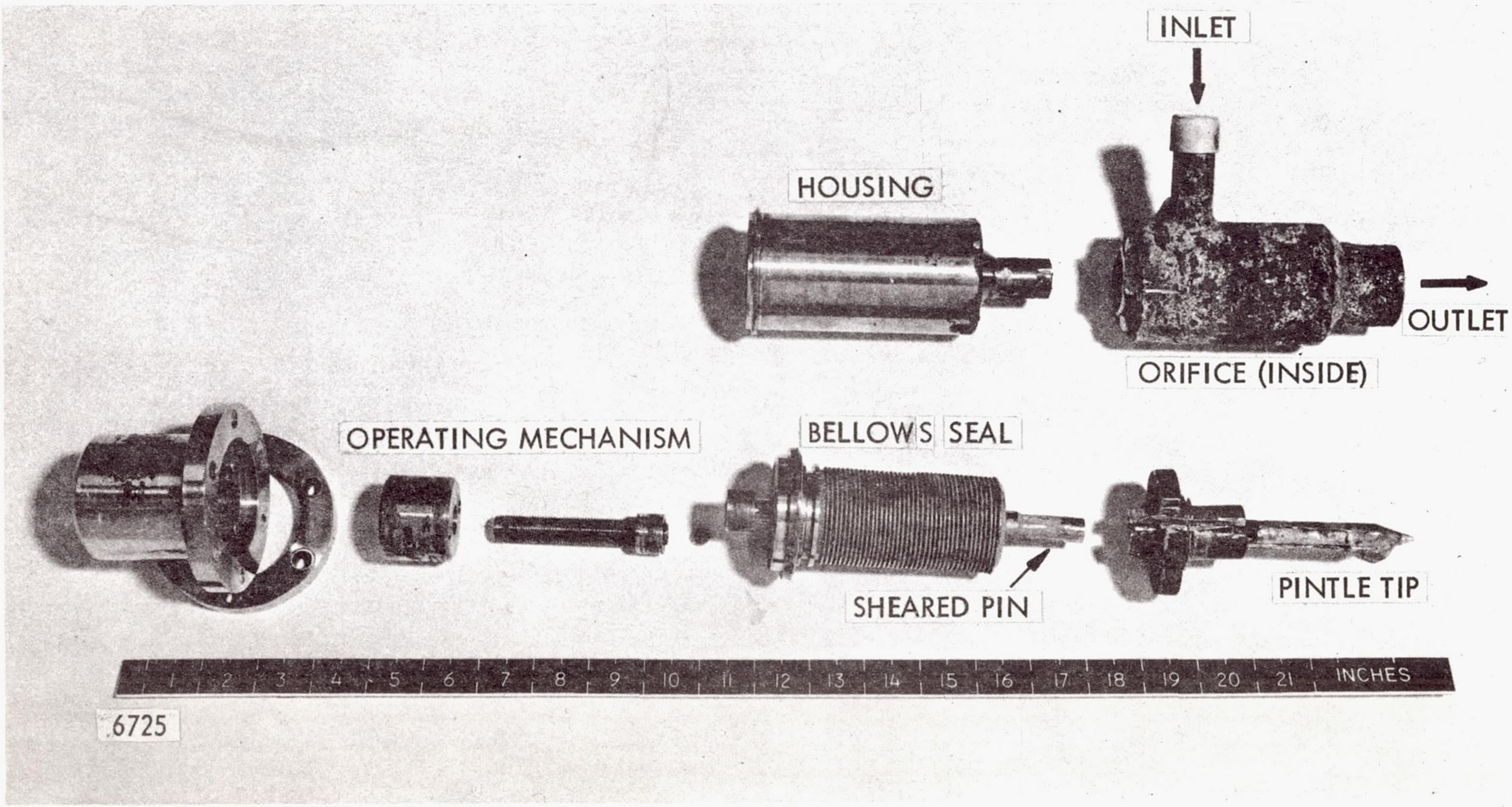

Adjustable Choked Nozzle, CL-3

Figure 8

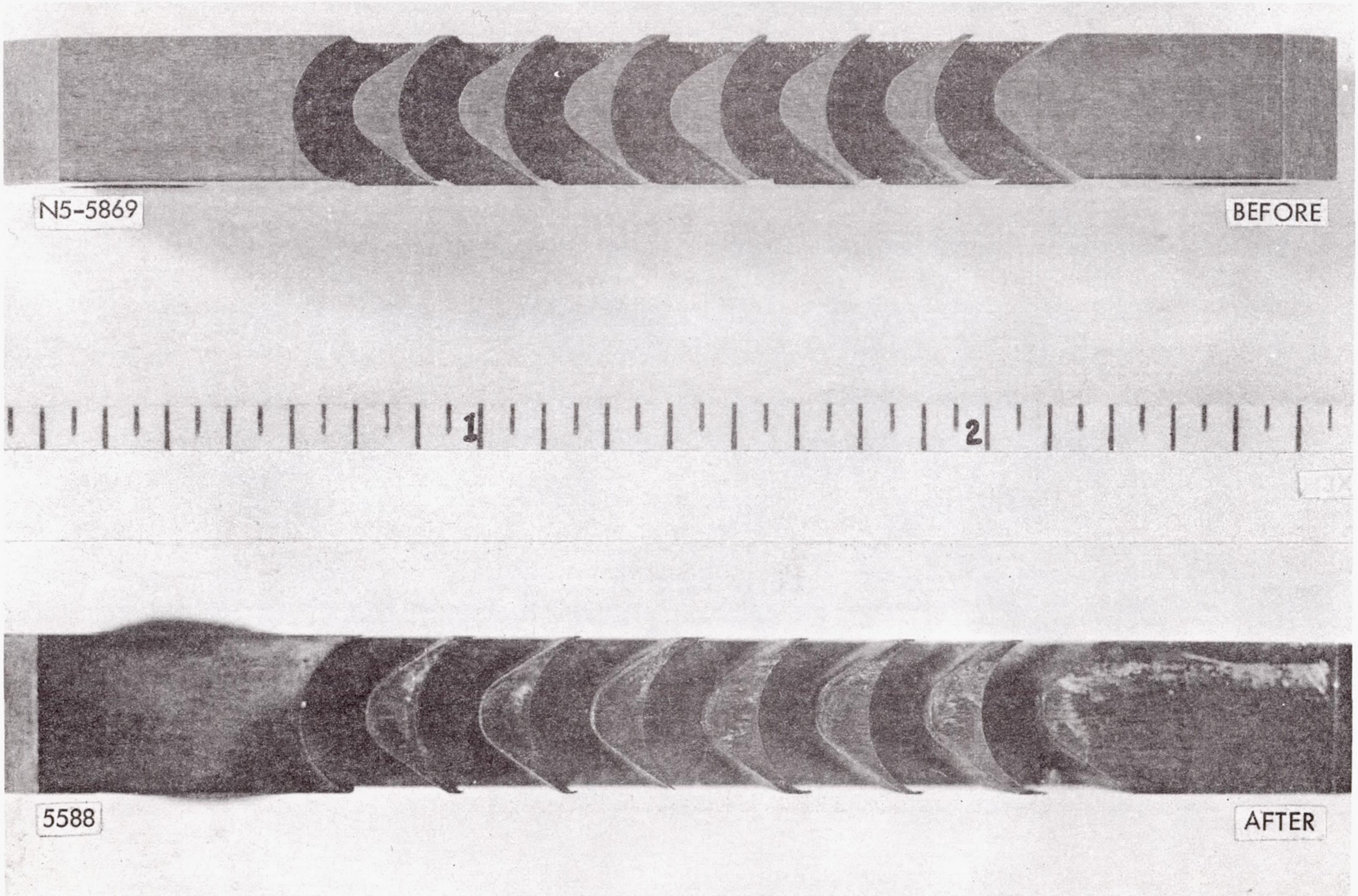

Blade Section Before and After Exposure, CL-3

1268-NF-1189

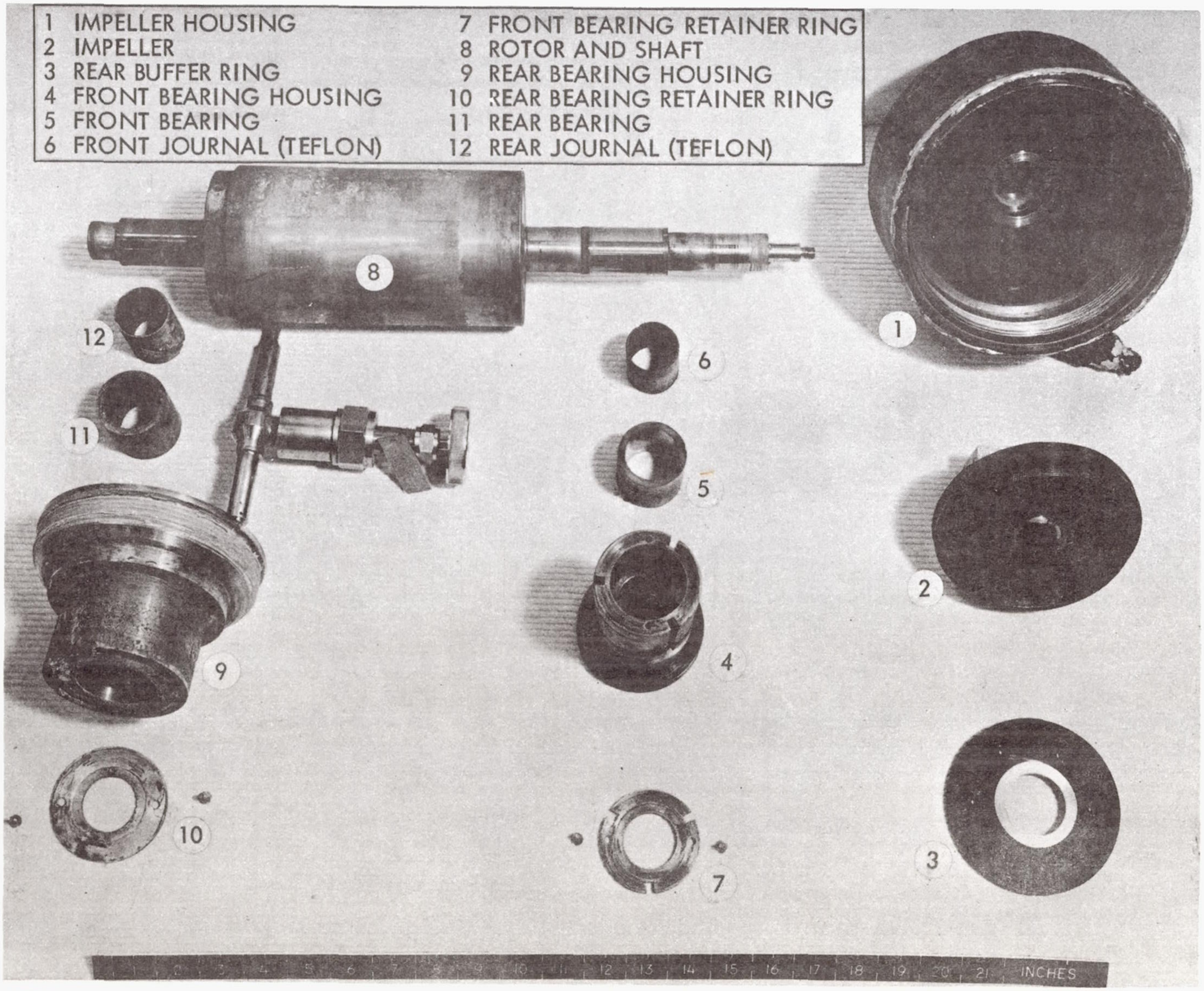

6770

Figure 9

Internal Parts of Mercury Pump (9Cr-1Mo Steel), CL-3

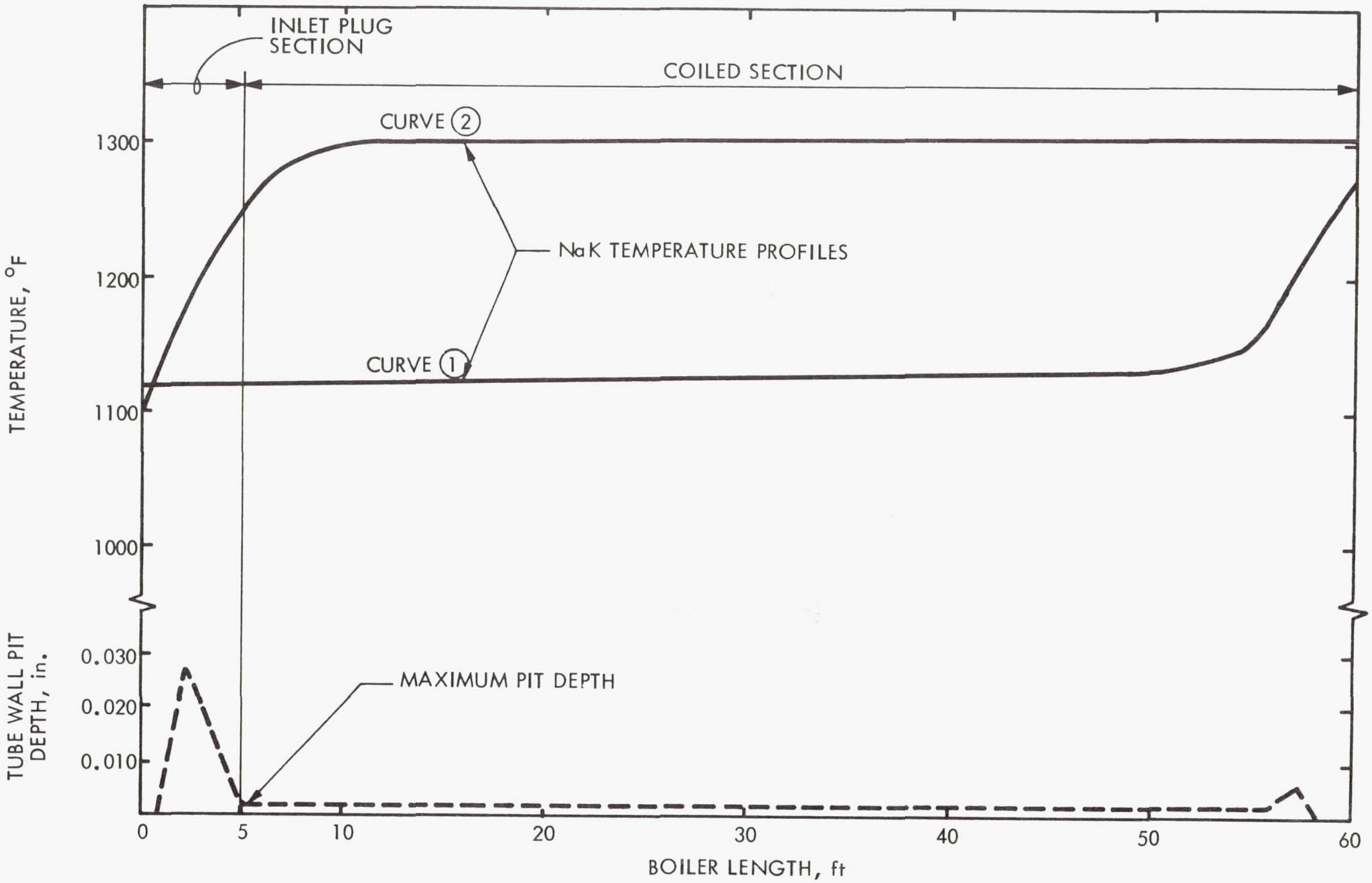

Figure 10

Typical NaK Temperature Profiles and Pit Depths, CL4 Boiler

*Distance from Mercury Inlet

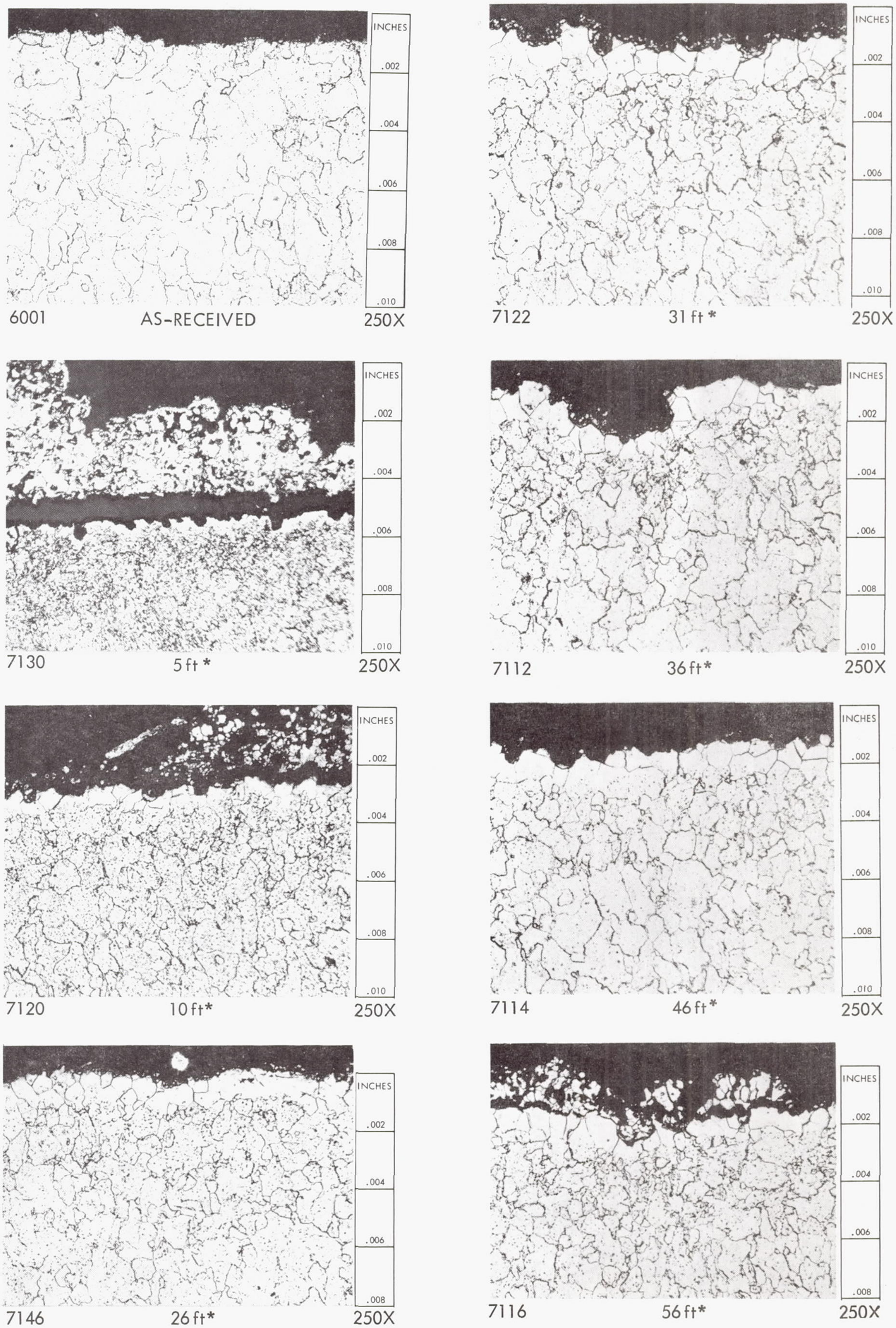

MICROSTRUCTURE OF THE MERCURY SIDE OF THE 9Cr-1Mo
TUBING - CL 4 BOILER COILED SECTION

Figure 11

866-NF-1125

.30 .50 .70 1.00 1.30 1.60 1.90

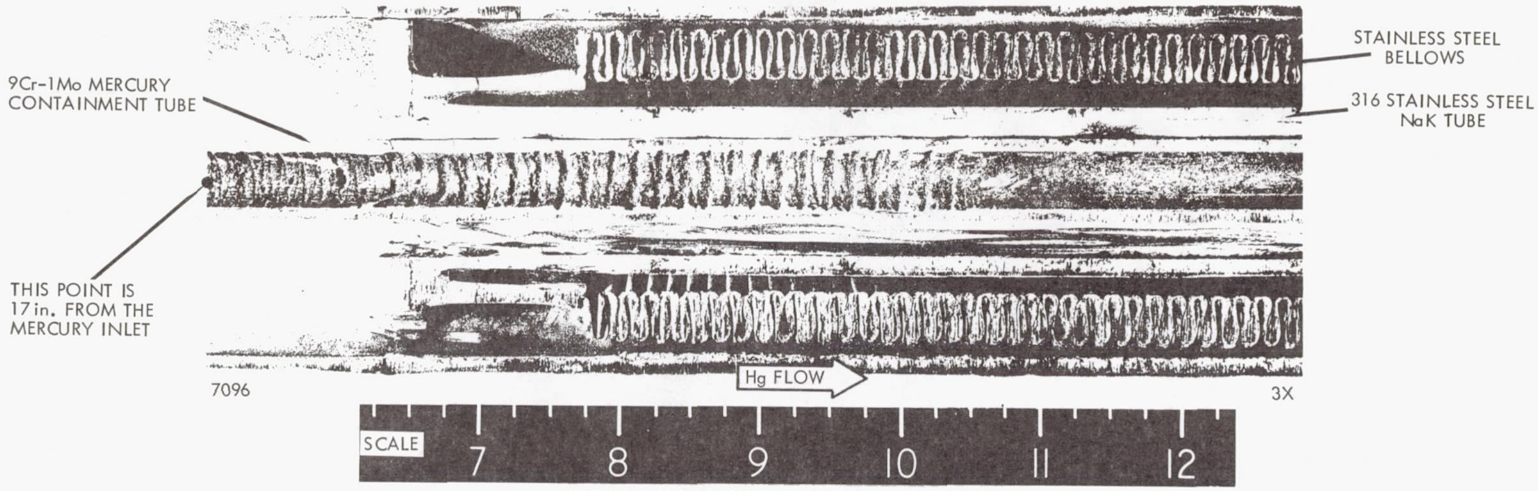

PHOTO MACROGRAPH - CL 4 BOILER INLET SECTION

6001 AS-RECEIVED 250X

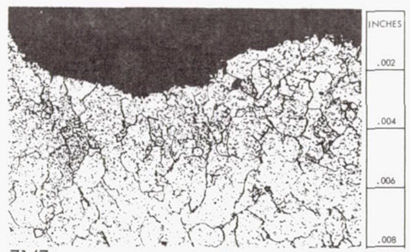

7147 18 in.* 250X

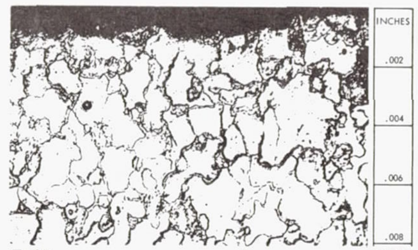

7165 22 in.* 250X

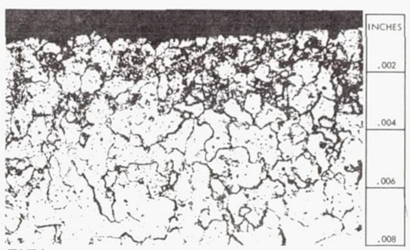

7174 24 in.* 250X

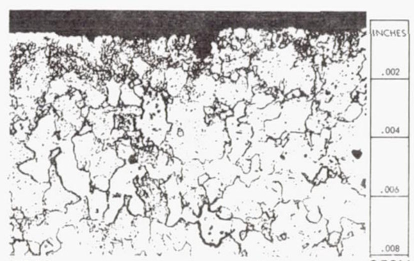

7159 29 in.* 250X

*Distance from Mercury Inlet

PHOTO MICROGRAPHS - INSIDE DIAMETER OF 9Cr-1Mo TUBING

CL 4 BOILER INLET SECTION

Figure 12

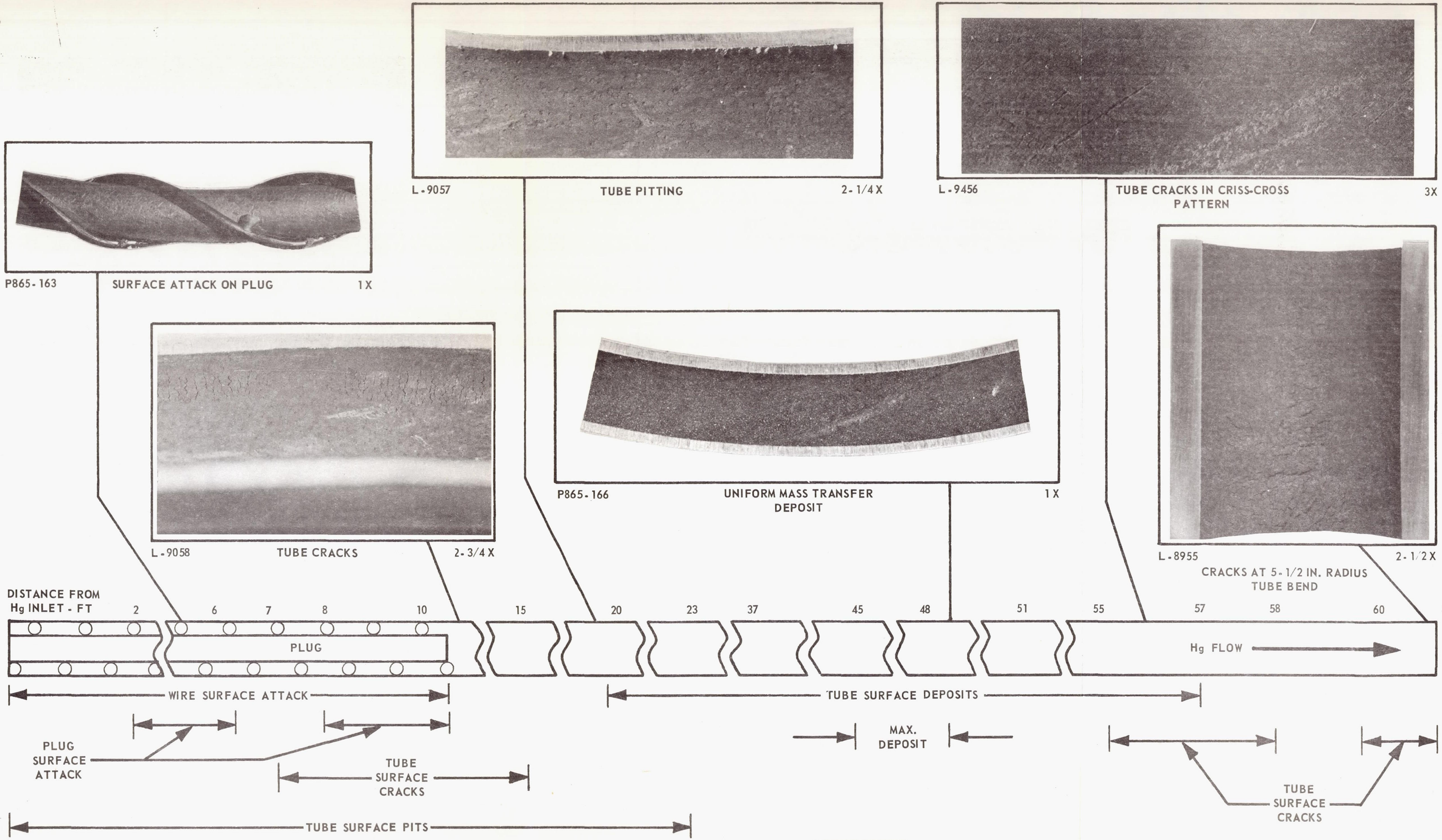

Mercury Side of Tube Coil No. 0-4 of -1 Boiler Removed From RPL-2
After 1415 hr of Mercury Operation

Figure 13

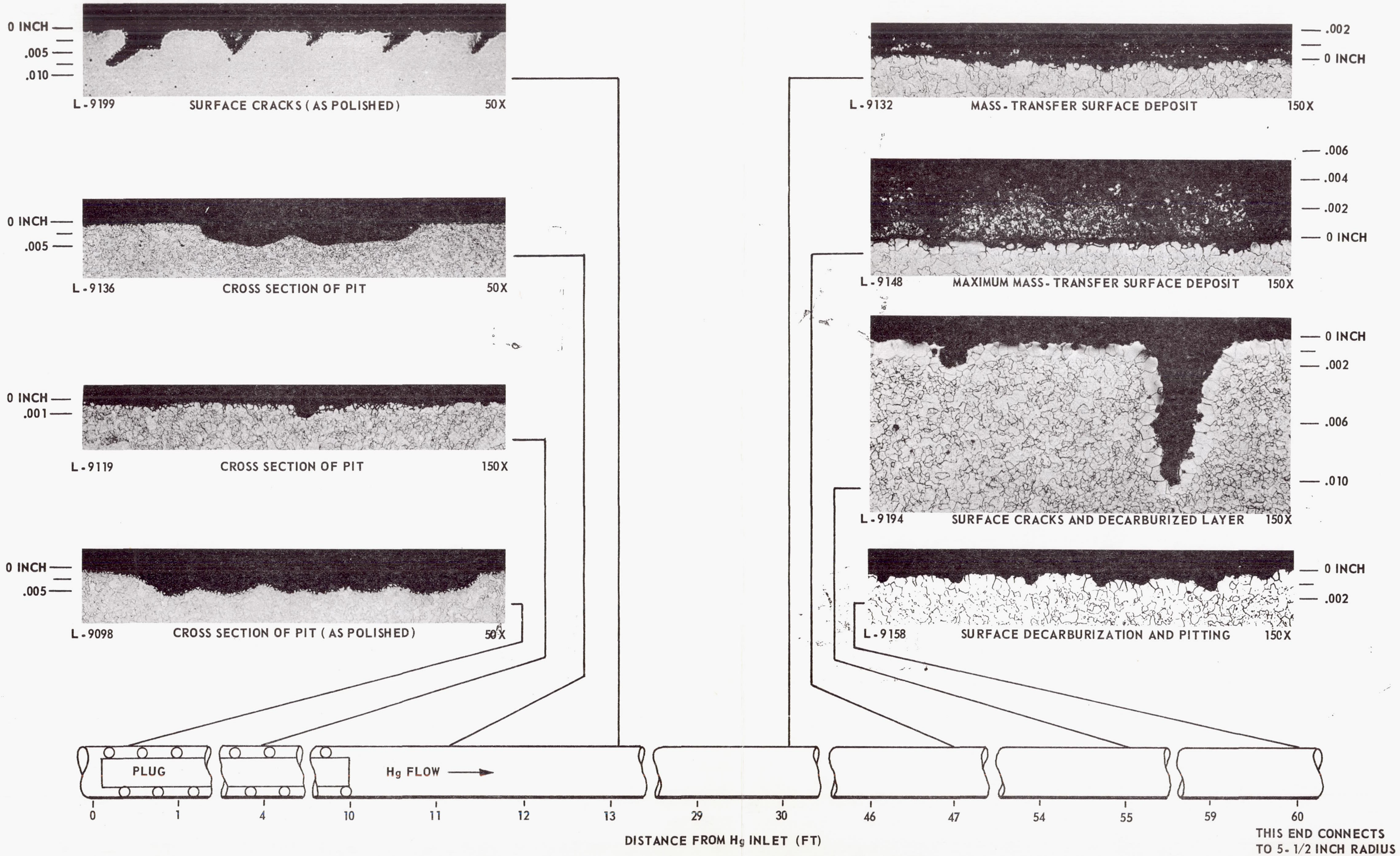

Mercury Exposed Surfaces of Tube Coil No. O-4 Removed from -1 Boiler After 1415 hr of Operation in RPL-2 (Vilella's Etch)

Figure 14

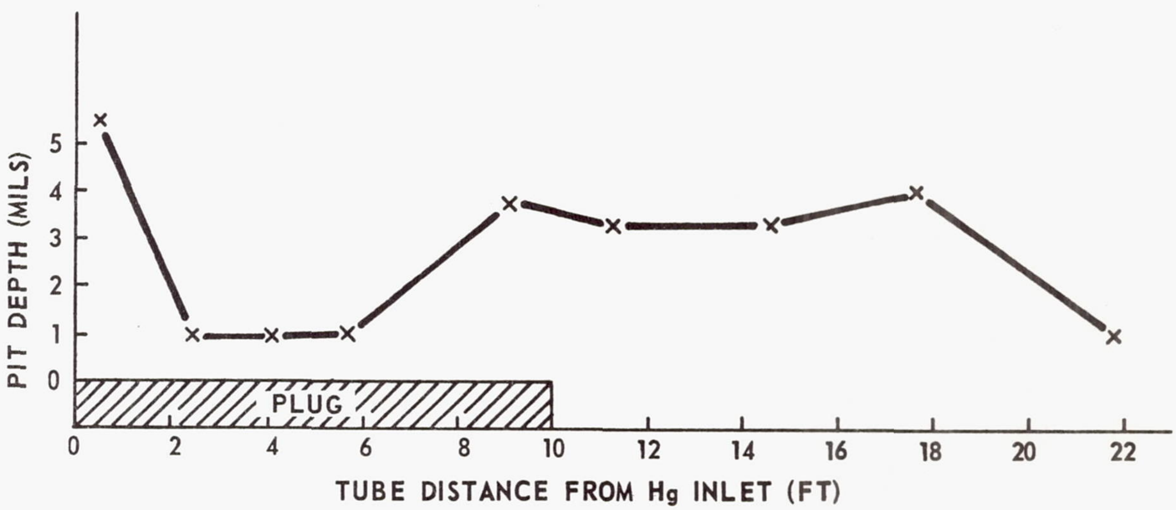

Pit Depth Distribution on Mercury-Exposed Surface of Tube 0-4 from Tube-in-Shell Boiler After 1415 Hr of Mercury Operation

Figure 16

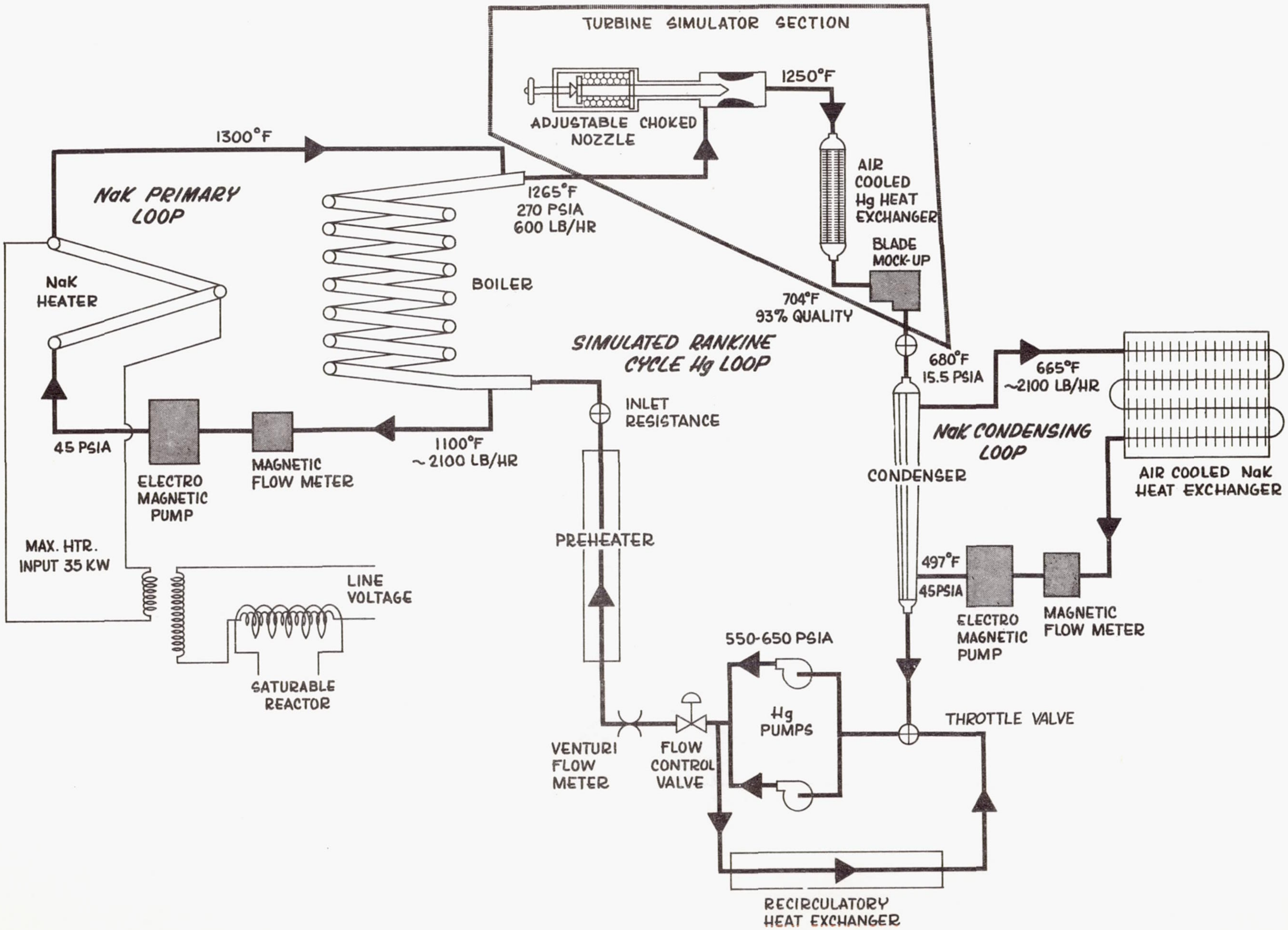

Corrosion Loop 4 Schematic

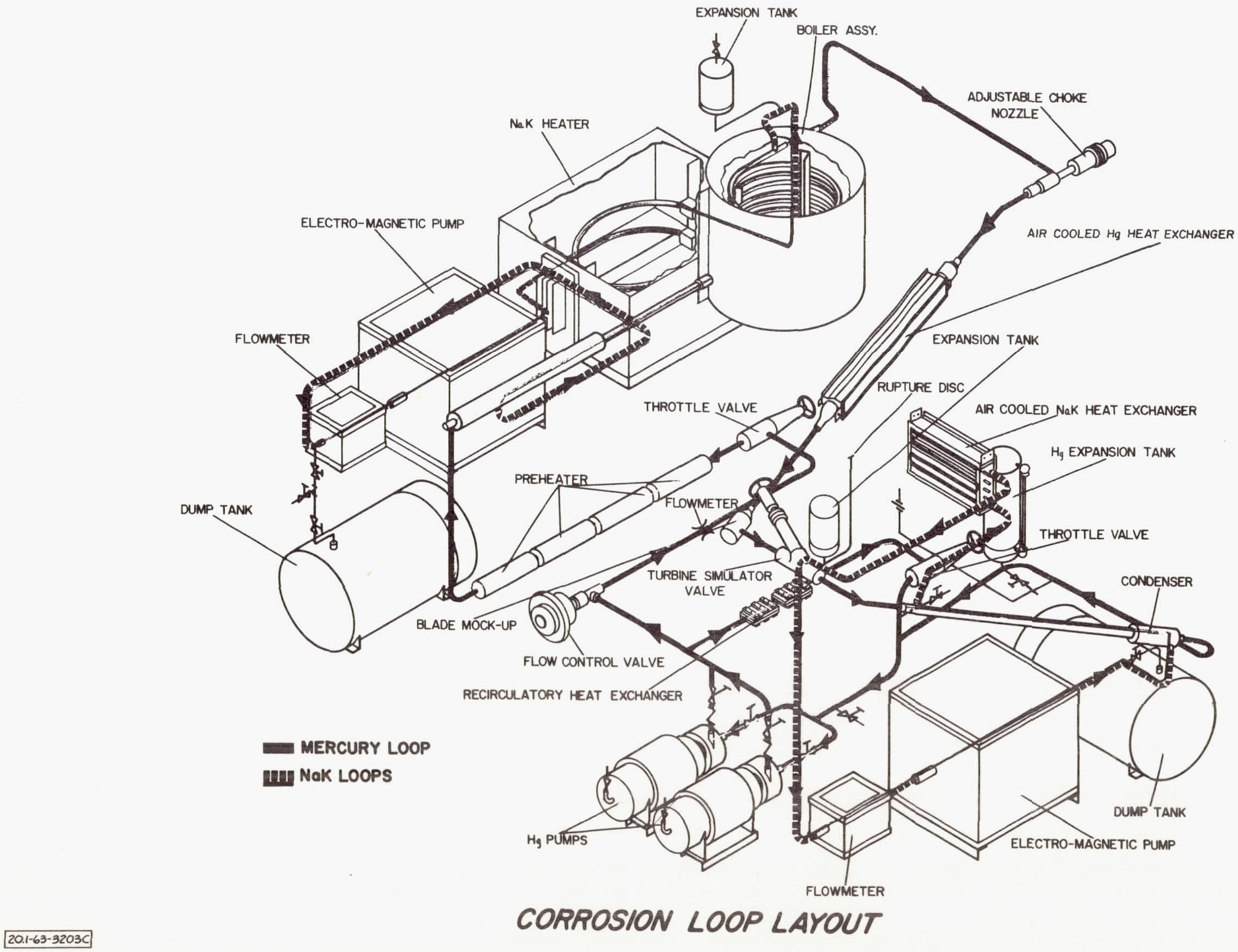

Corrosion Loop 4 Arrangement

Figure 17

866-NF-1134

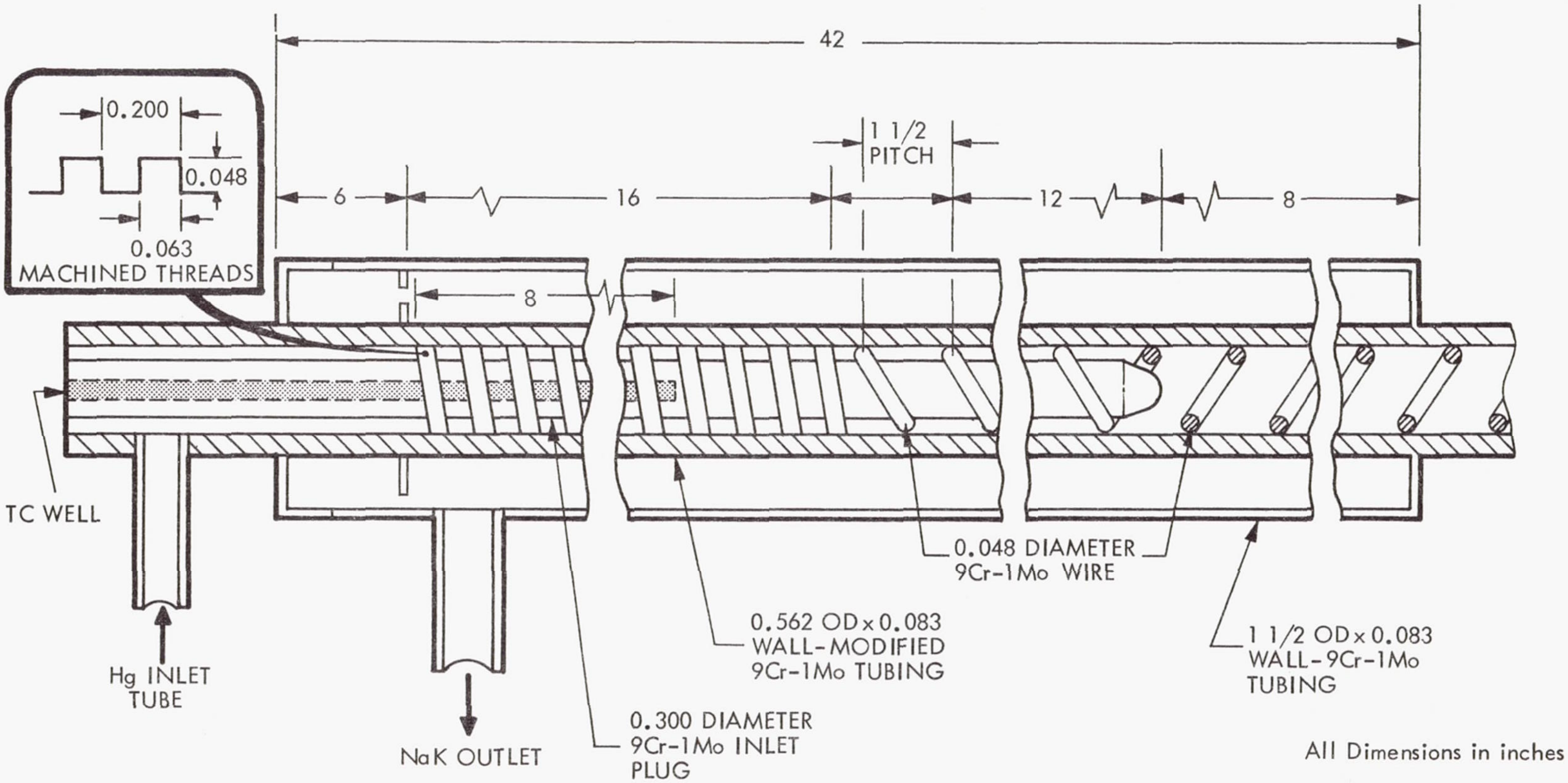

Test Section 4A-3 Schematic

Figure 18

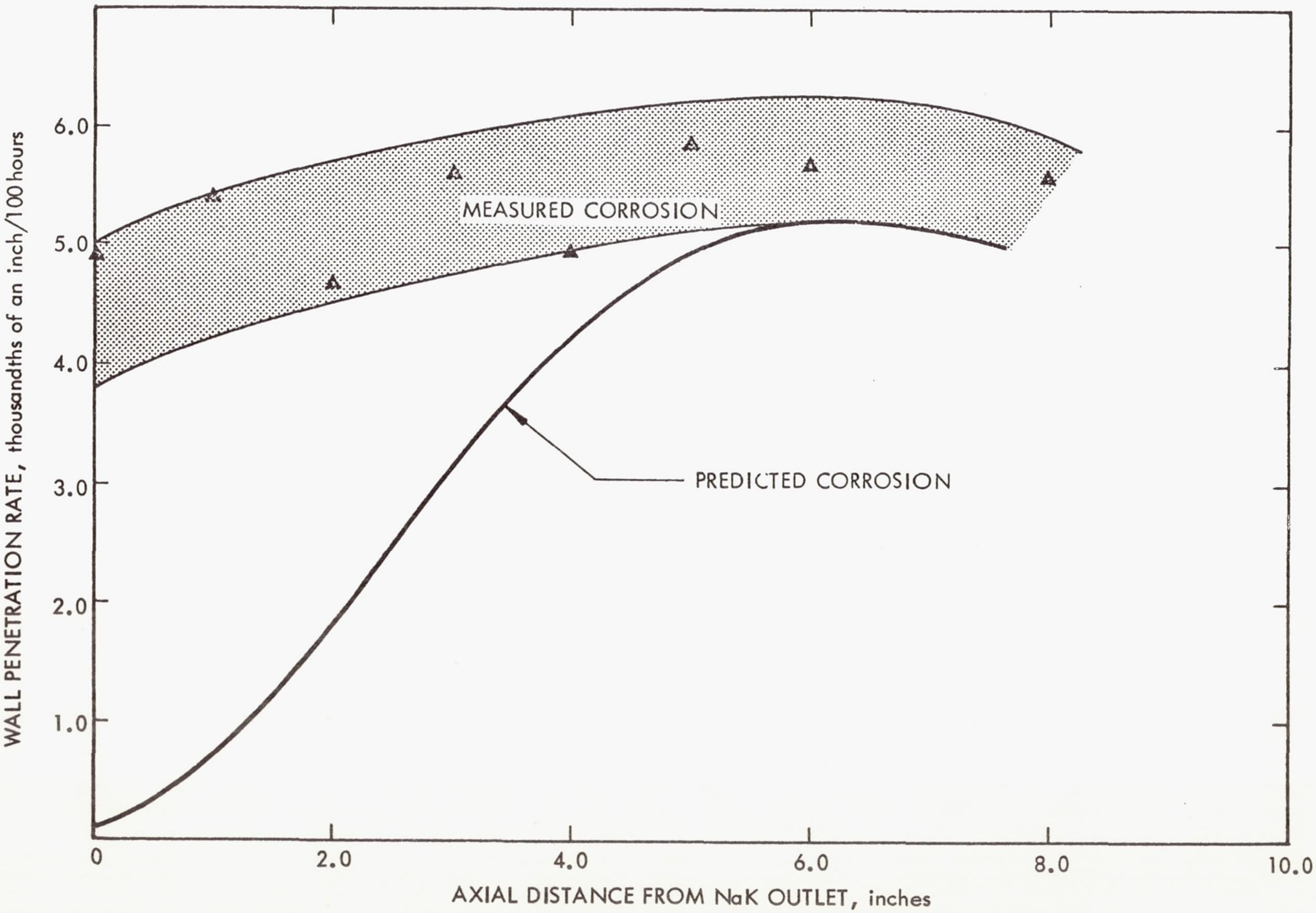

Figure 19

Predicted Preheat-Region Corrosion Rate for Test Section 4A-3

Figure 20

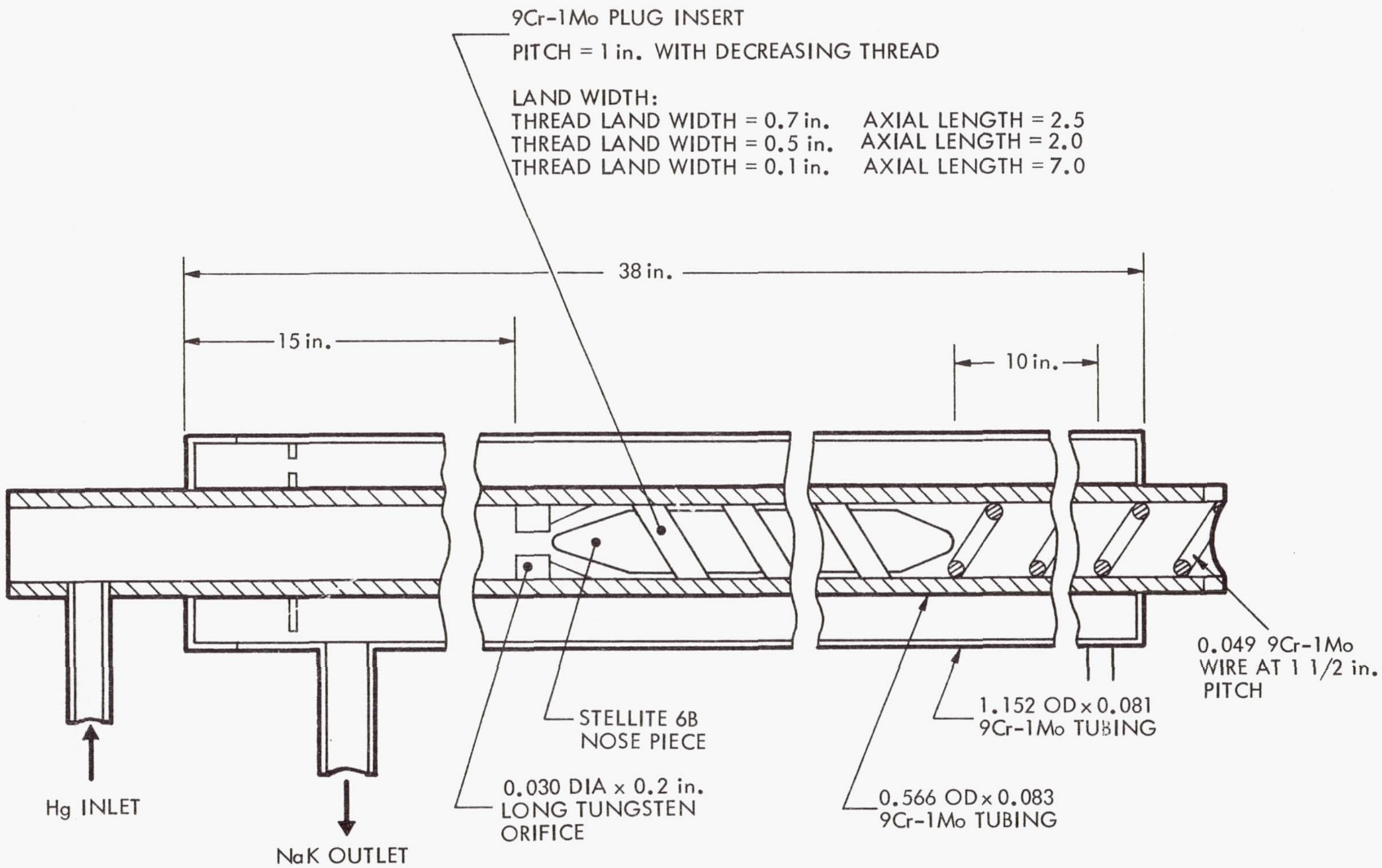

Test Section 4A-4 Schematic

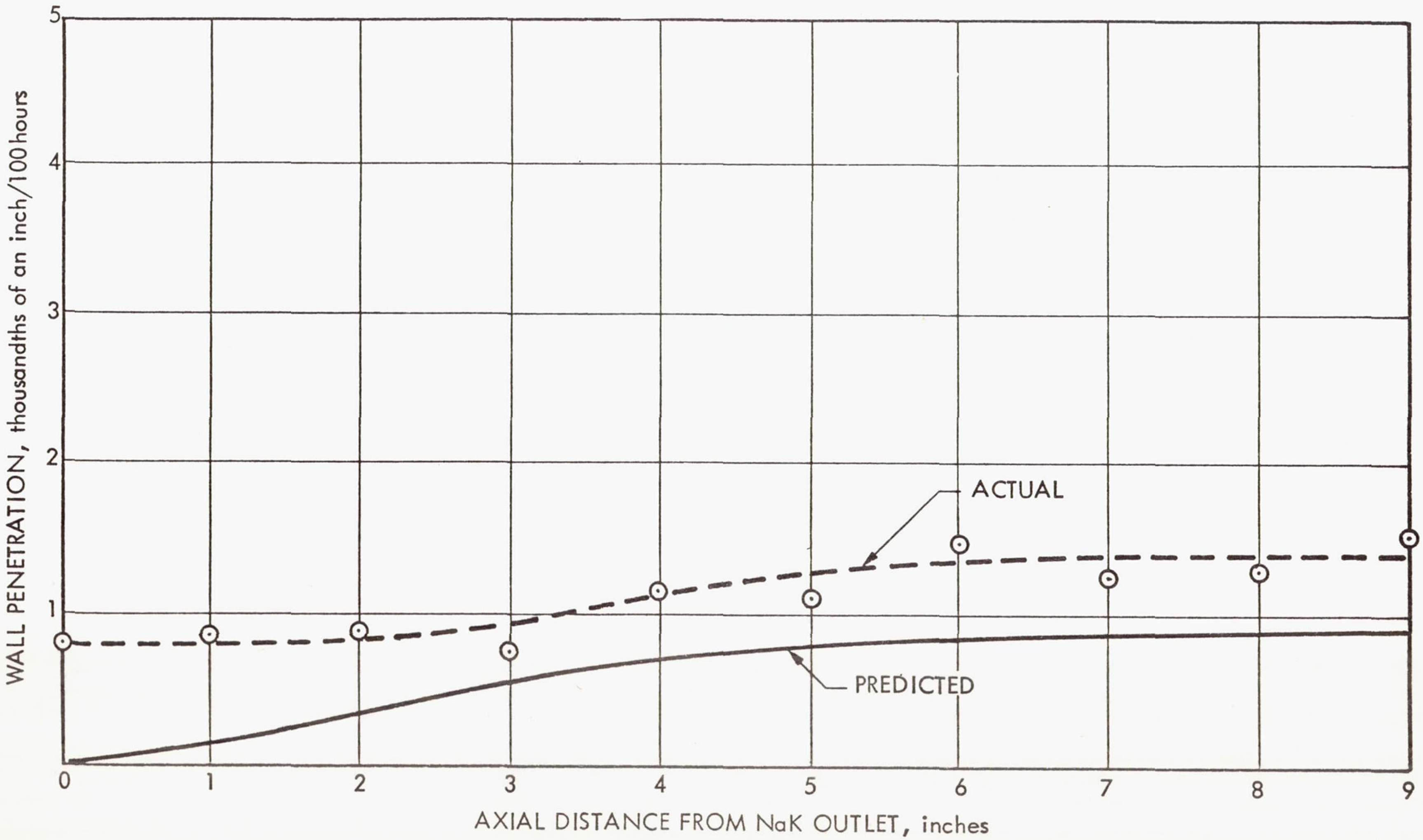

Figure 21

Predicted Preheat-Region Corrosion Rate for Test Section 4A-4

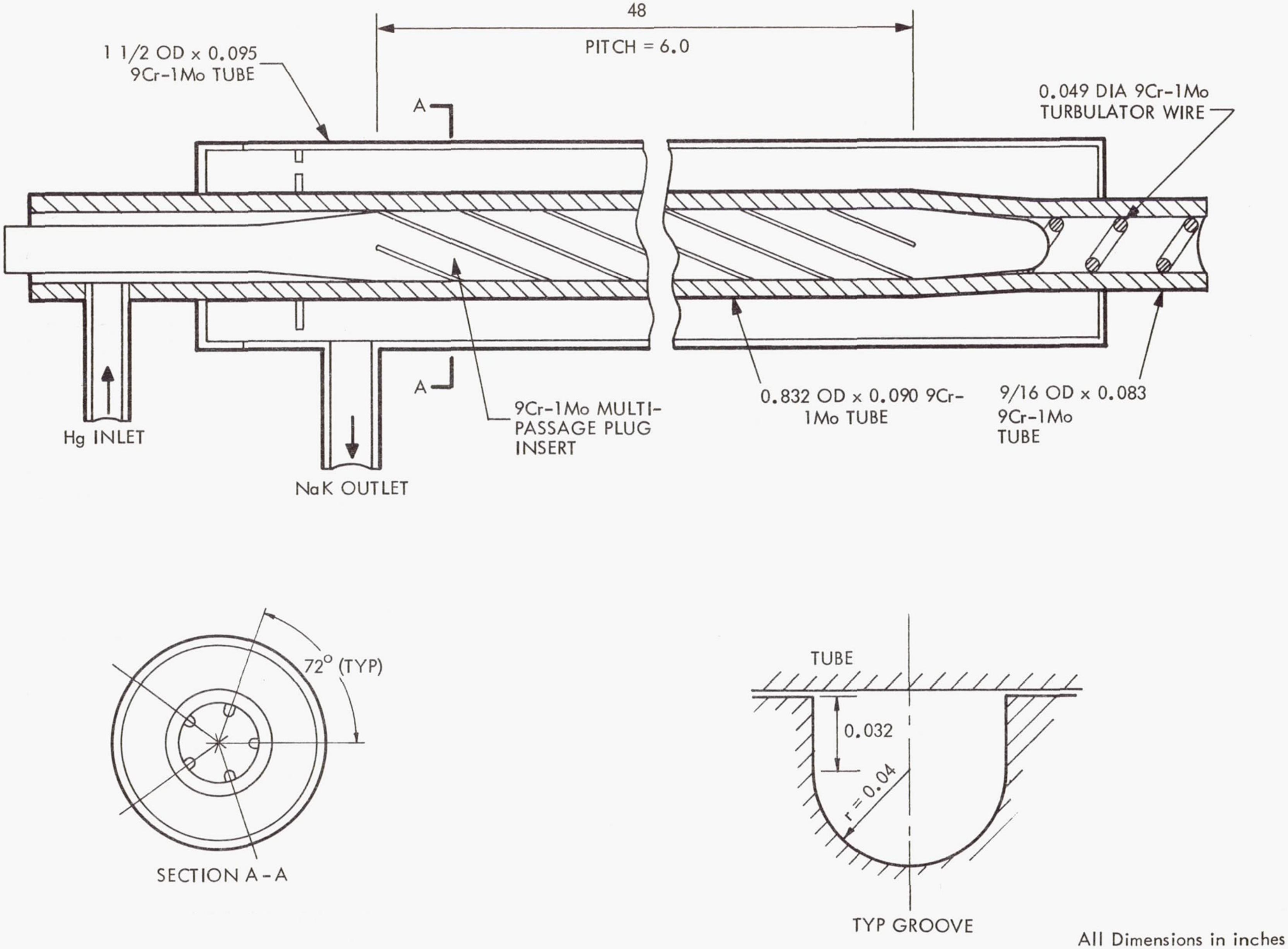

Figure 22

Test Section 4A-1 Schematic

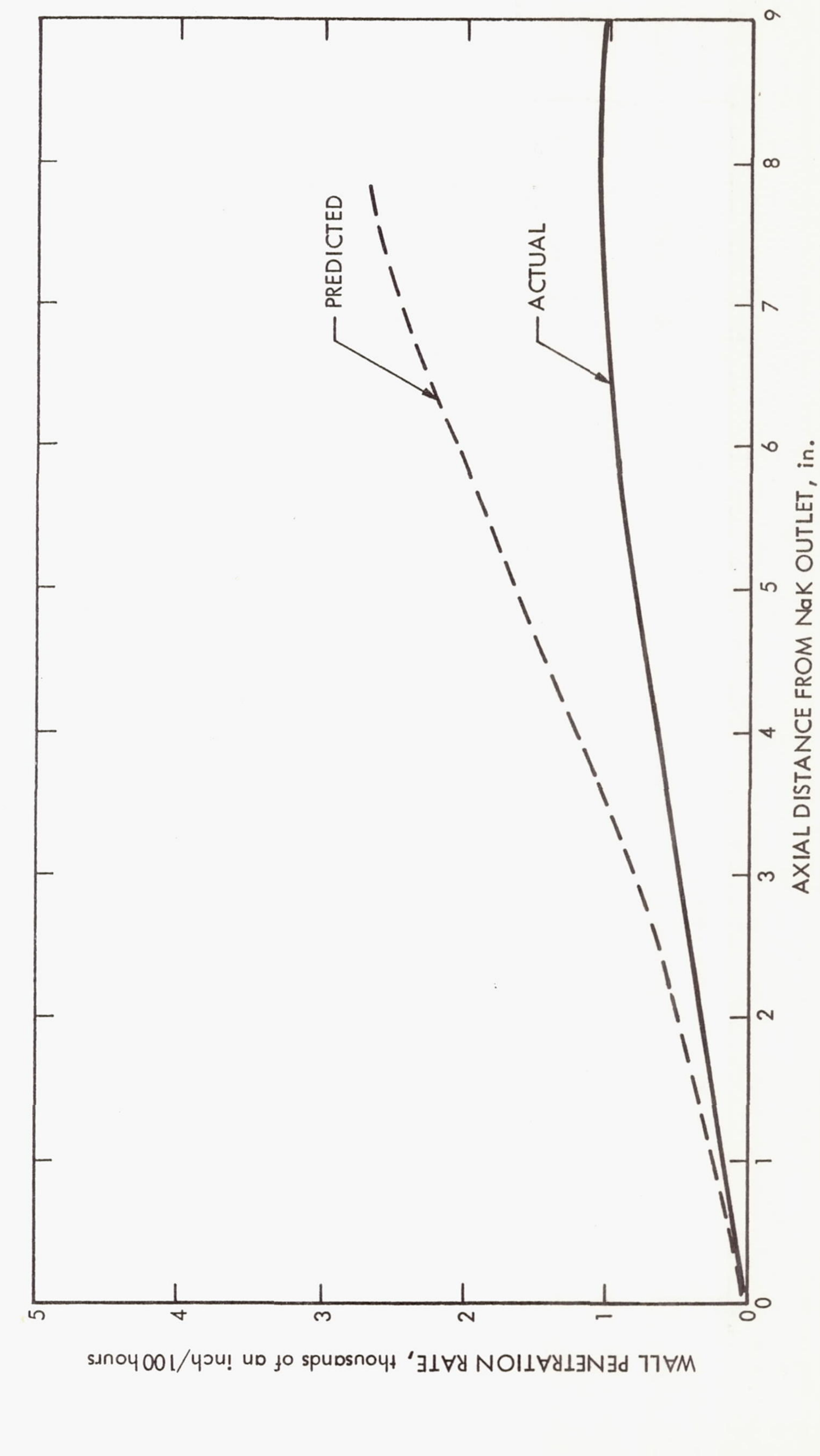

Predicted Preheat-Region Corrosion Rate for Test Section 4A-1

Figure 23

1066-NF-1147

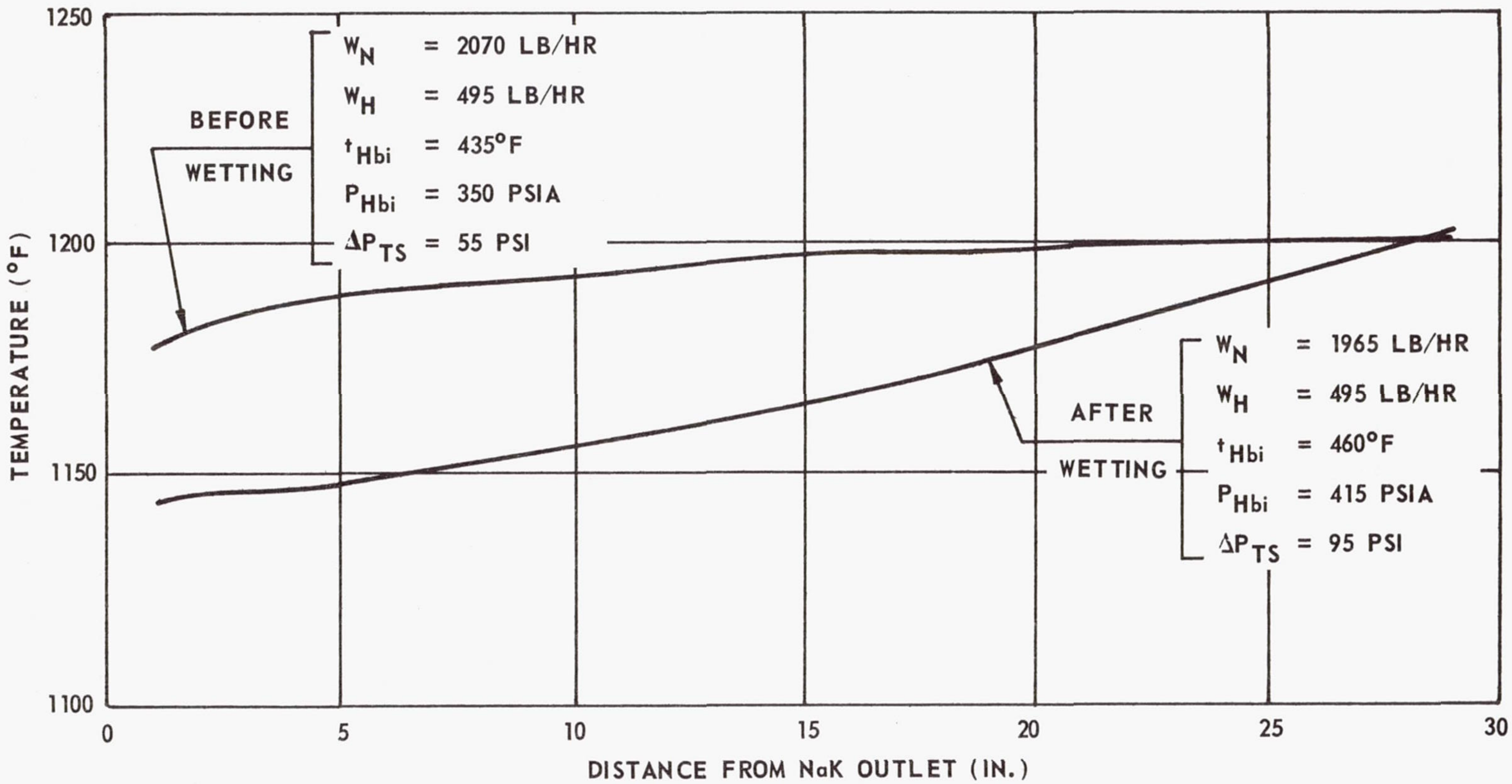

NaK Shell Temperature Profiles, Test Section 4A-3

Figure 24

4A-3 TEST SECTION

269-NF-1278

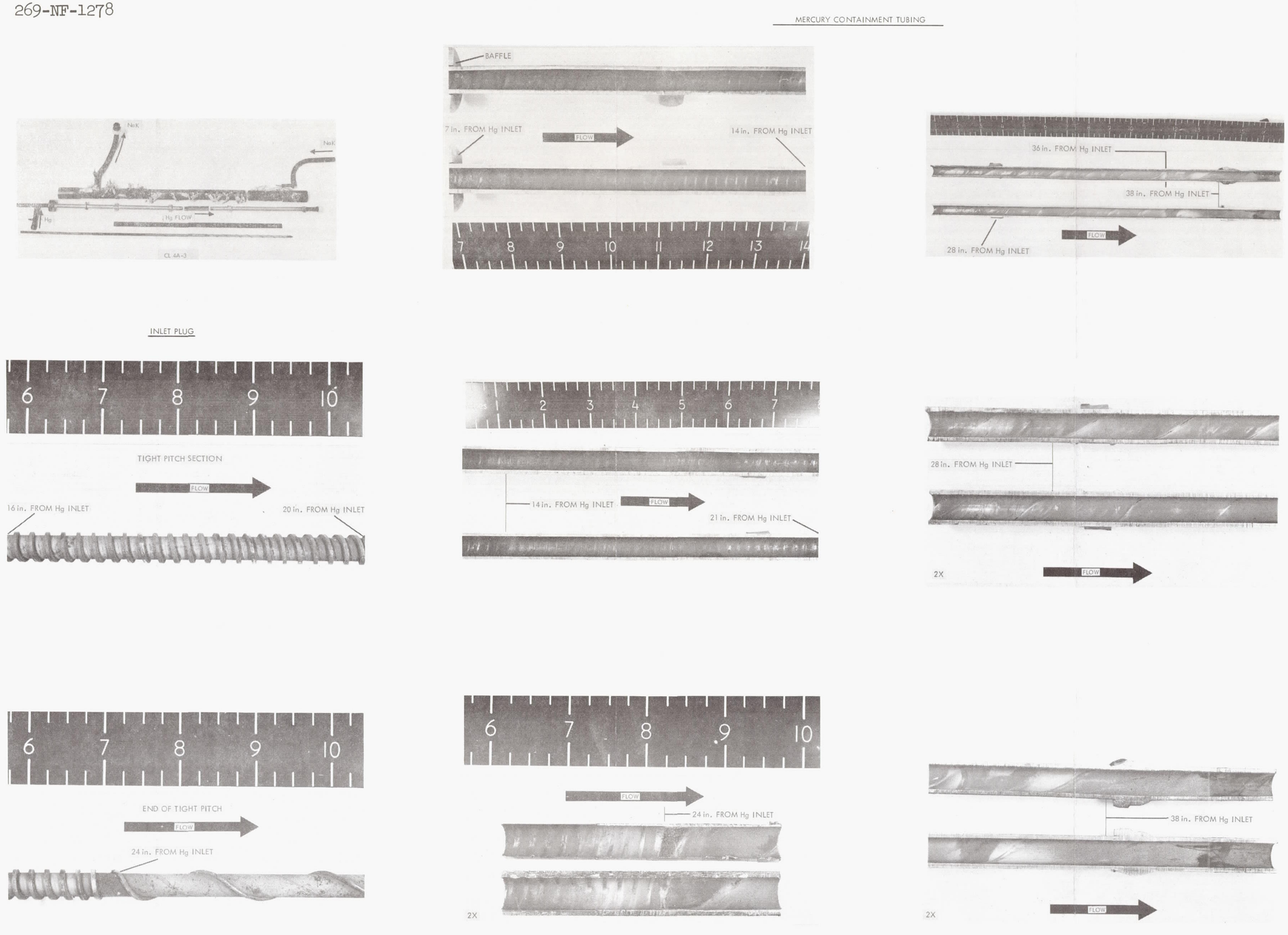

MACROPHOTOGRAPHS OF THE 4A-3 TEST SECTION

Figure 25

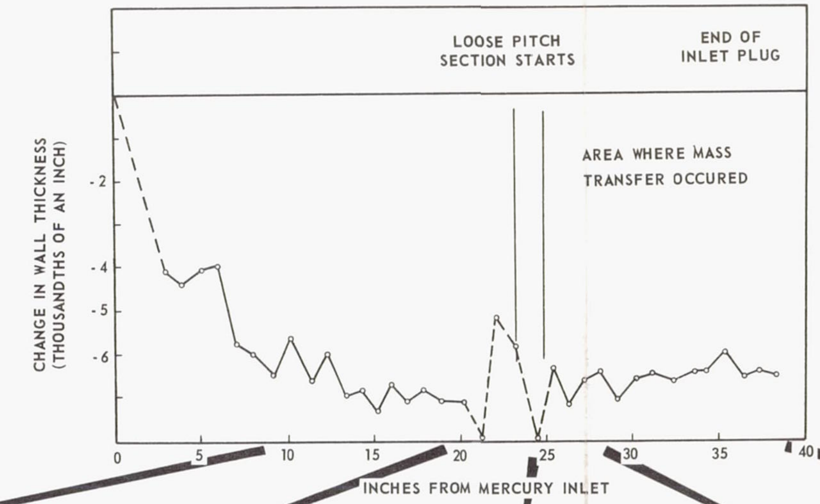

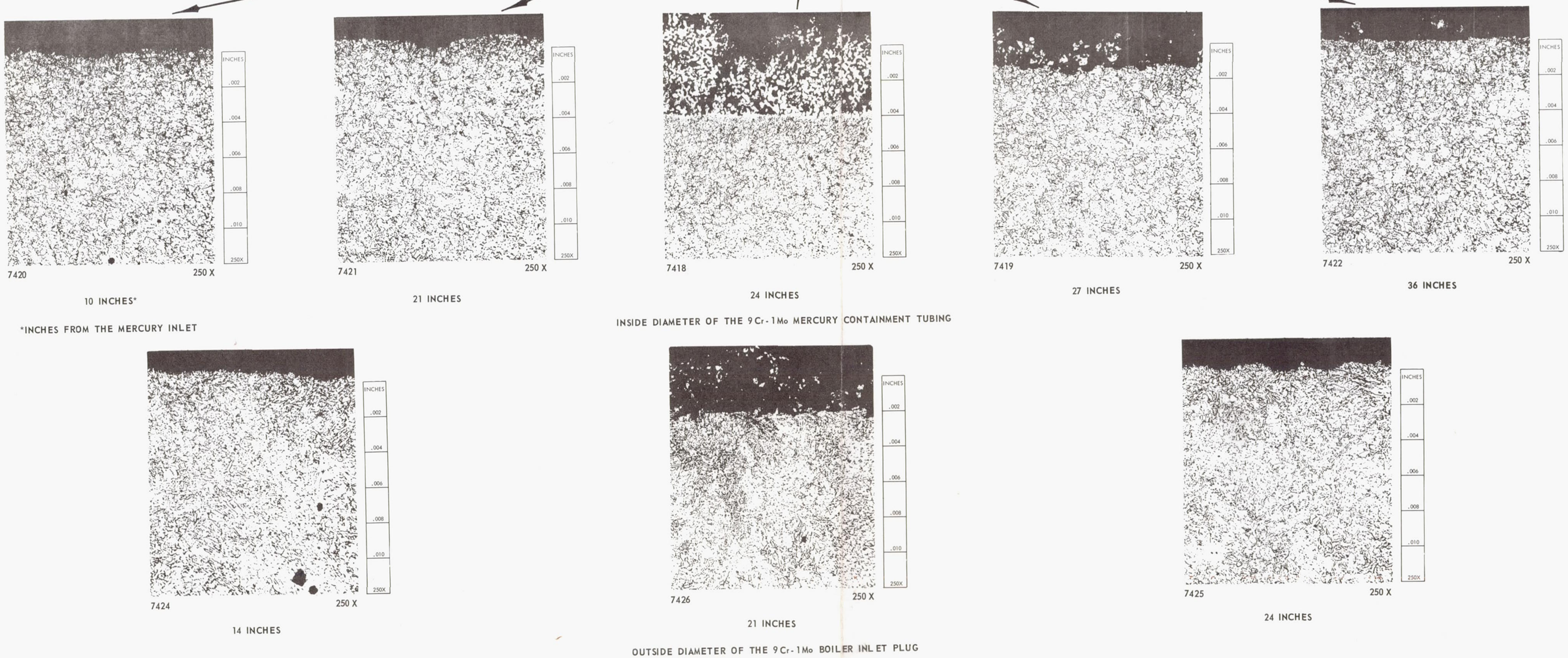

Figure 26 Microstructures of the 9Cr-1Mo Tubing and Inlet Plug of Test Section 4A-3

1066-NF-1173

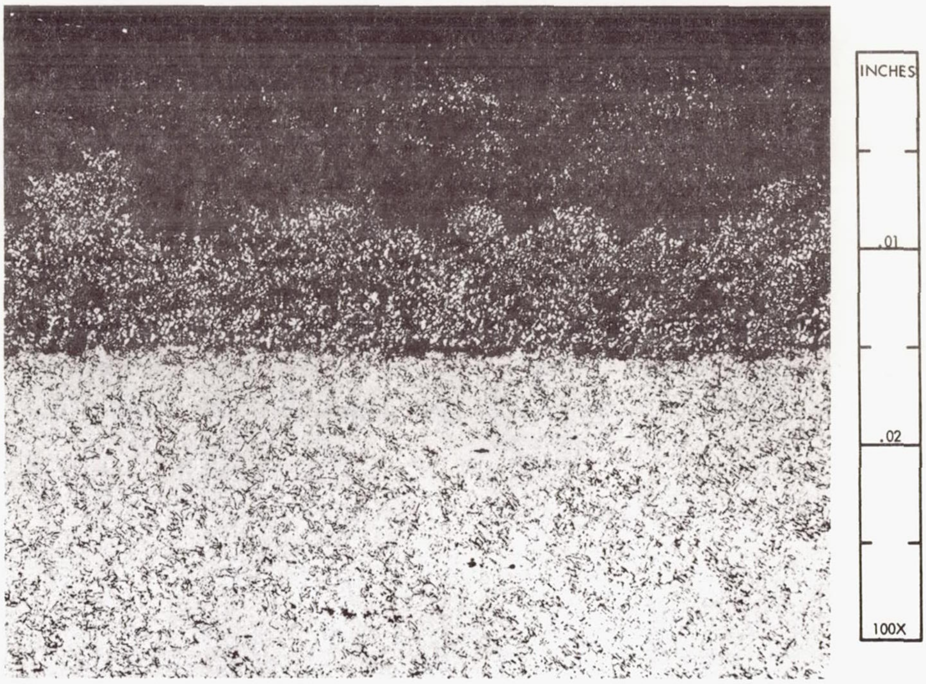

7394

TYPICAL STRUCTURE OF THE MASS TRANSFER DEPOSIT THAT CAUSED THE PRESSURE-DROP INCREASE

Microstructure of the Mass-Transfer Deposit in the 4A-3 Test Section

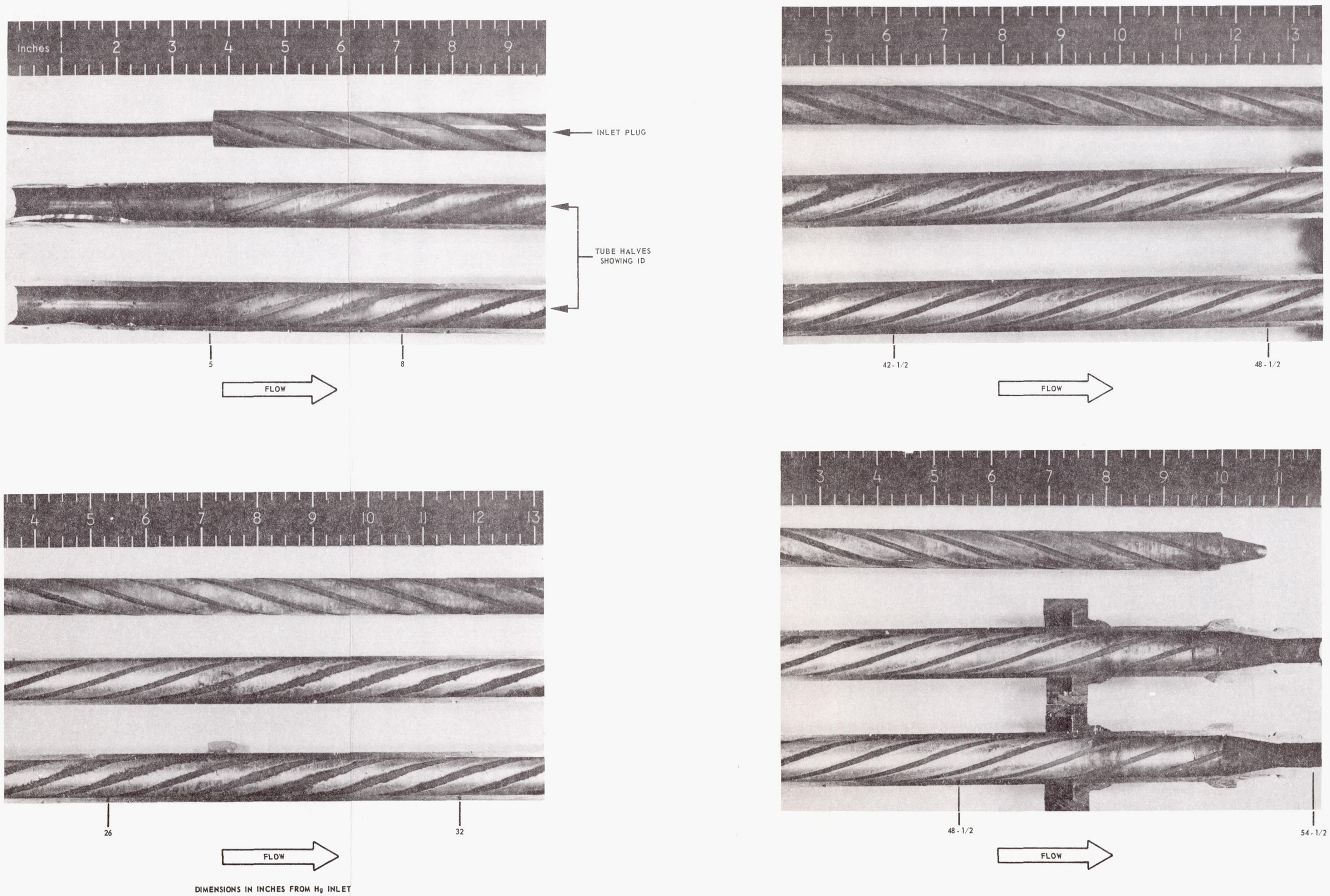

Disassembled Test Section 4A-1

Figure 28

167-NF-1244

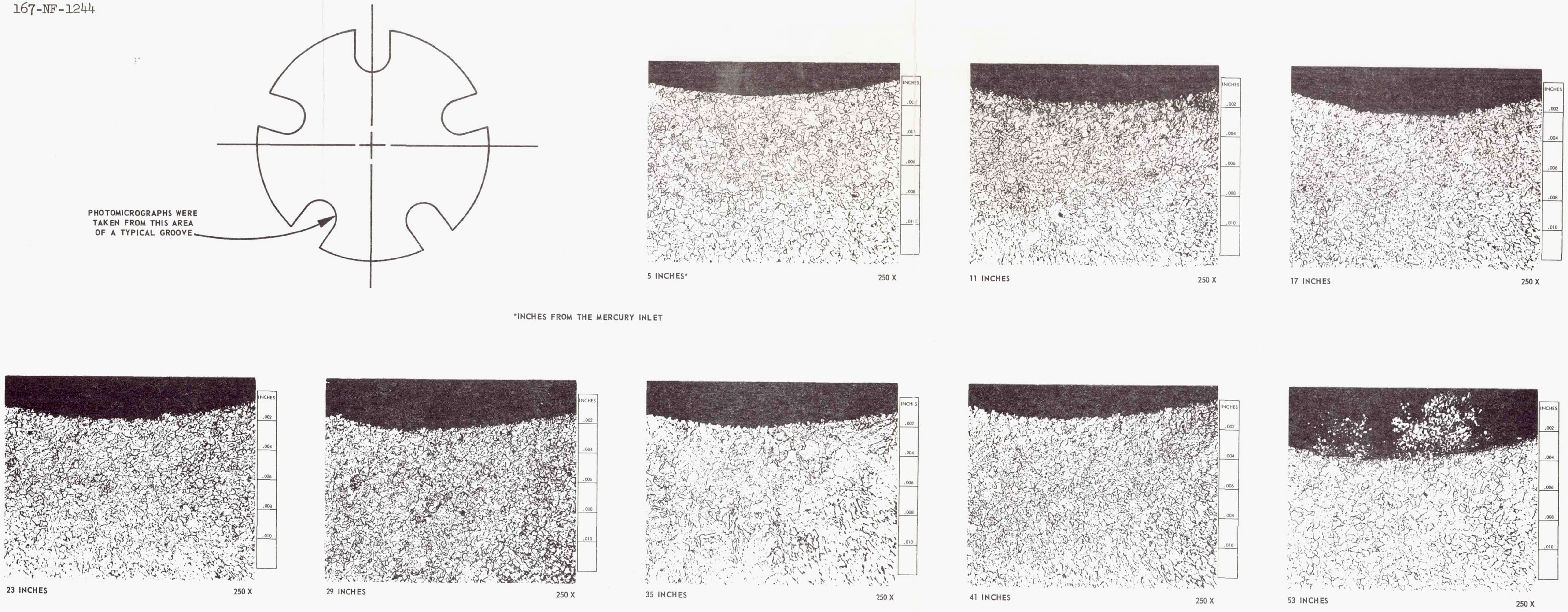

Microstructure of the Inlet Plug, Test Section 4A-1

Figure 30

167-NF-1243

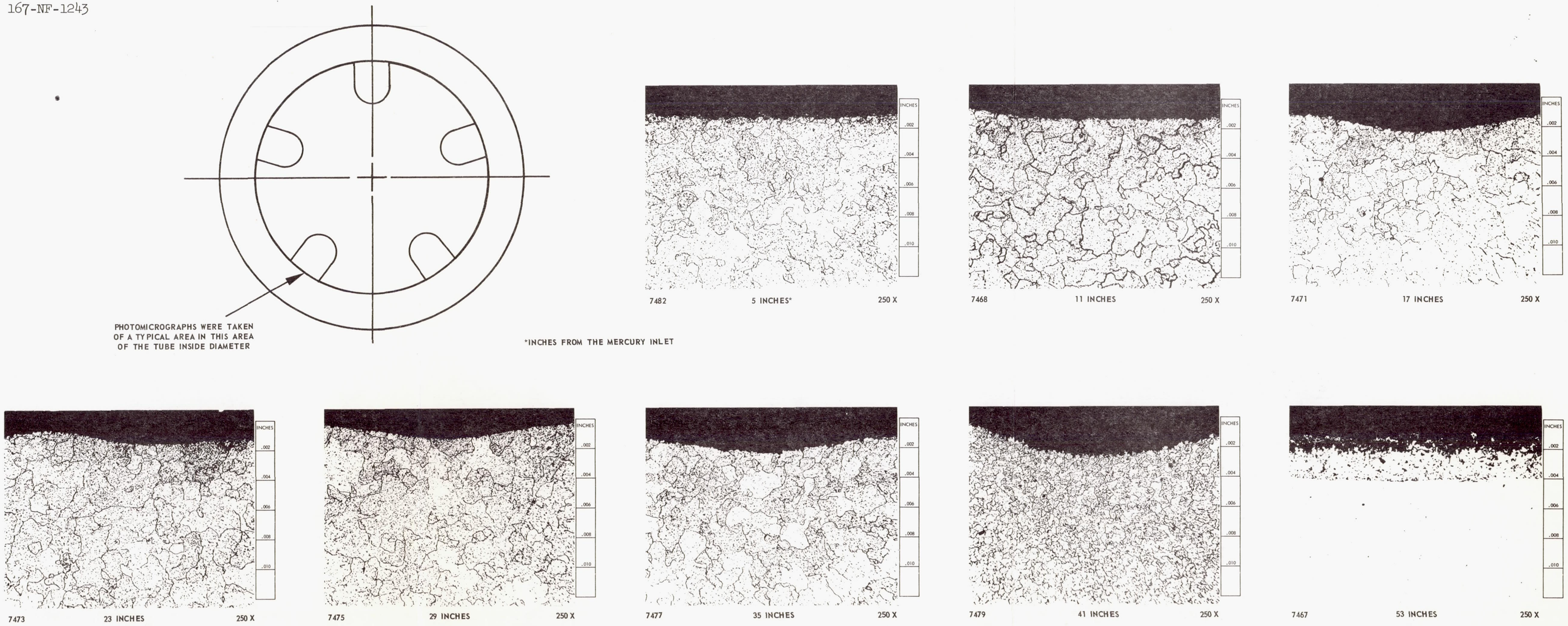

rostructure of the Mercury Containment Tube, Test Section 4.

Figure 29

Figure 31

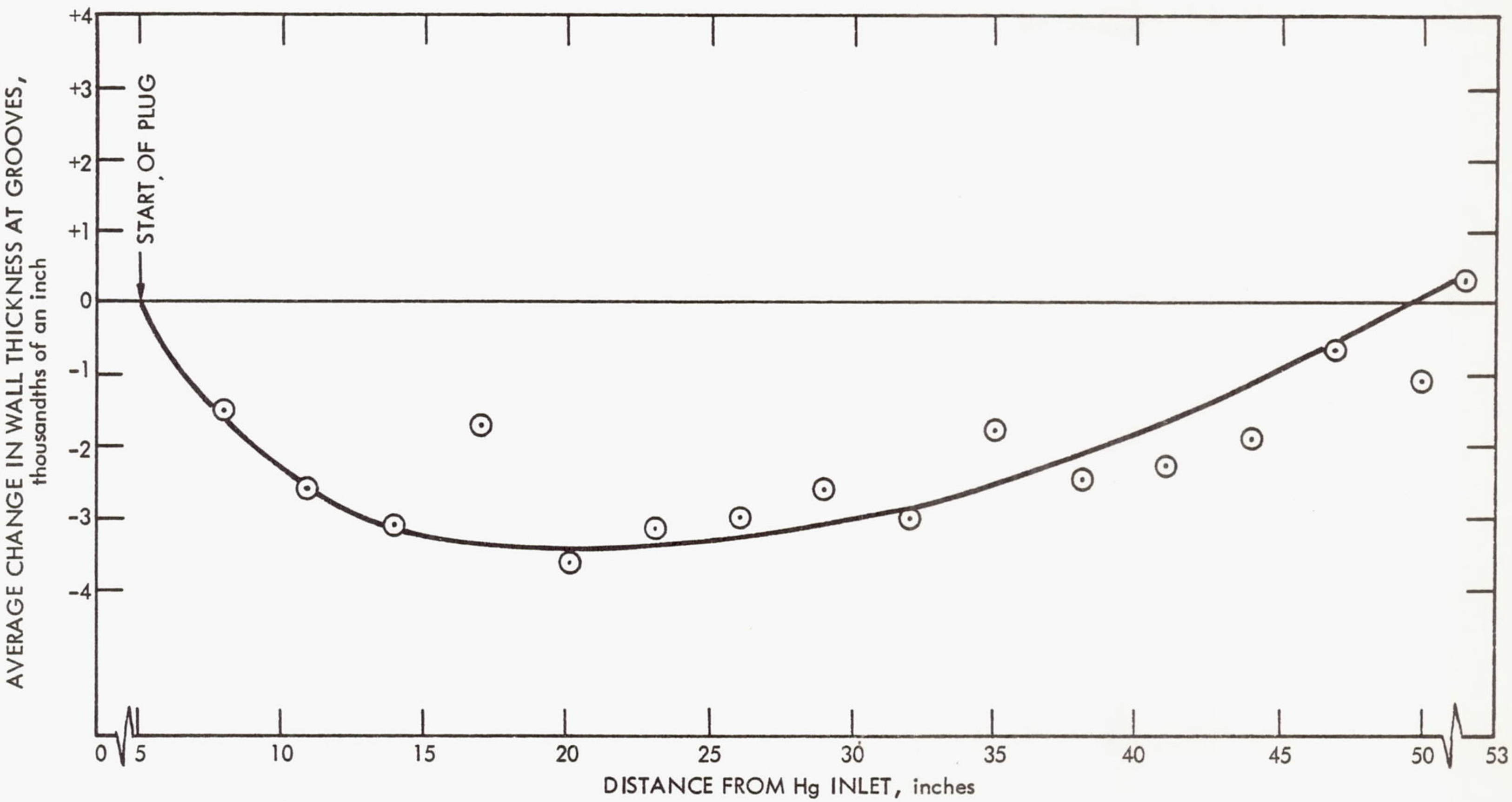

Change in Wall Thickness, Test Section 4A-1

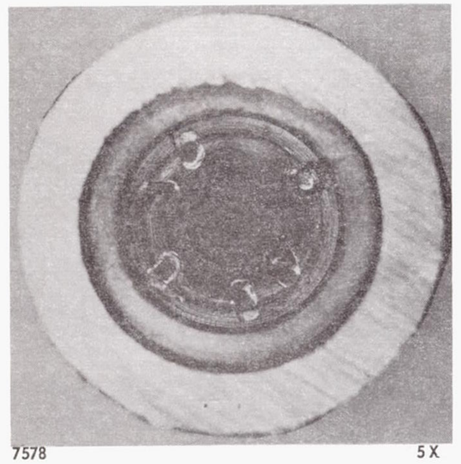
7578 5X

INLET END OF AS BUILT TUNGSTEN ORIFICE END ORIFICE CARRIER SIMILAR TO THE ONE EXPOSED IN 4A-4

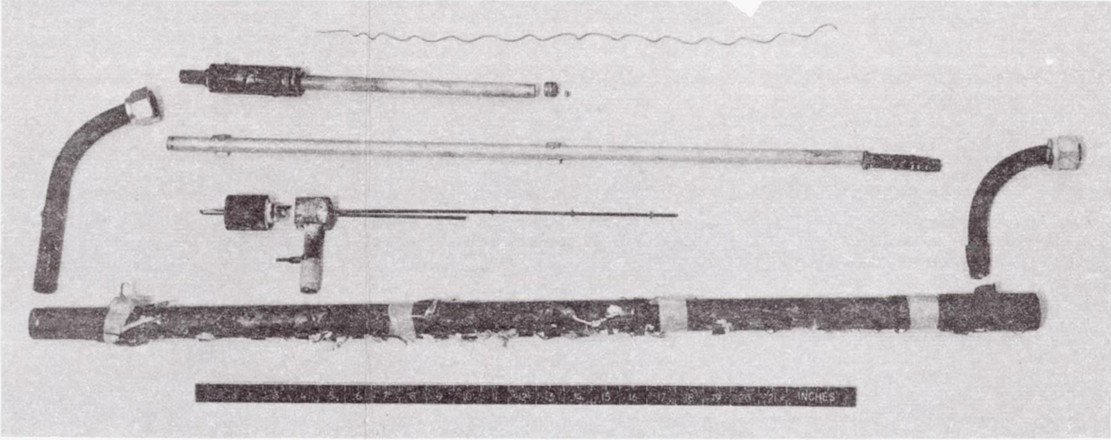
N-5 7845

4A-4 DISASSEMBLED

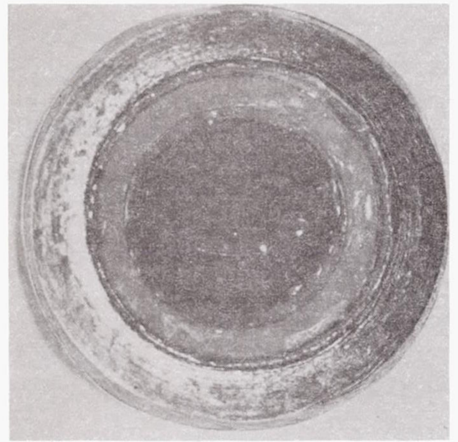
7580 5.5X

TUNGSTEN ORIFICE AND CARRIER AFTER TEST. NOTE THAT ORIFICE CARRIER HAS CORRODED AWAY LEAVING ORIFICE FREE TO MOVE

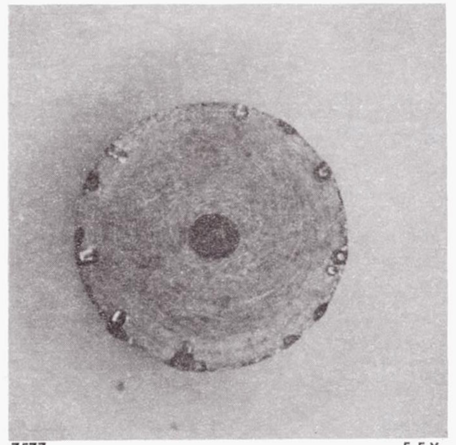
7577 5.5X

INLET END OF TUNGSTEN ORIFICE AFTER TEST

THIS POINT IS 15 IN. FROM THE MERCURY INLET

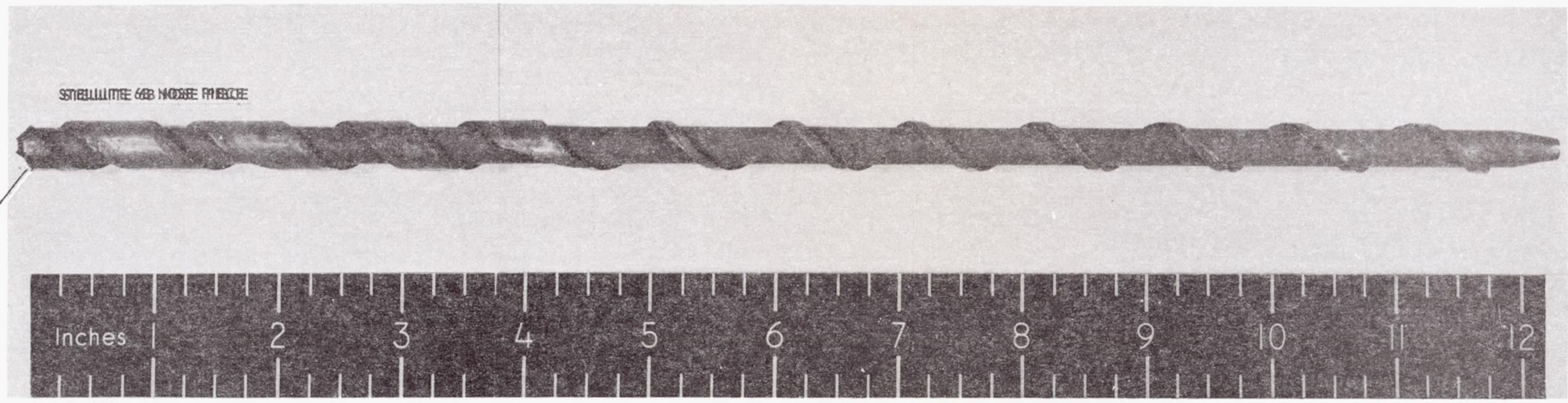

7574 & 7572

PLUG DOWNSTREAM OF THE ORIFICE

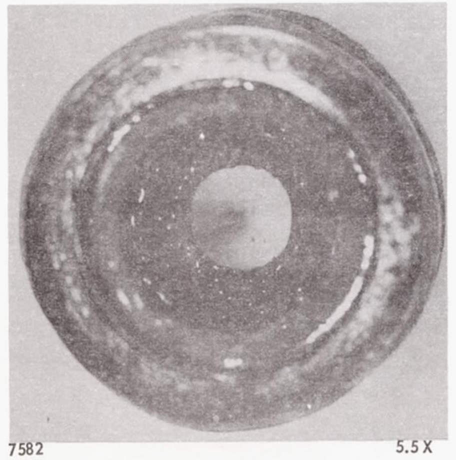
7582 5.5X

INLET SIDE OF ORIFICE CARRIER

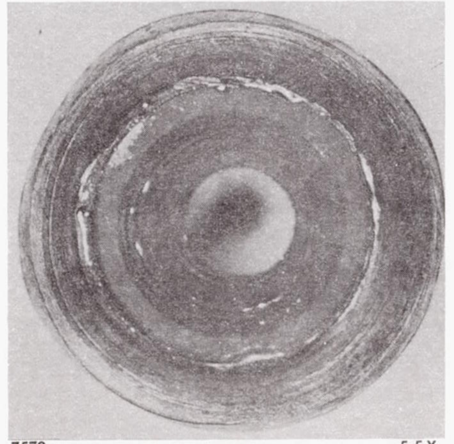
7579 5.5X

OUTLET SIDE OF ORIFICE CARRIER

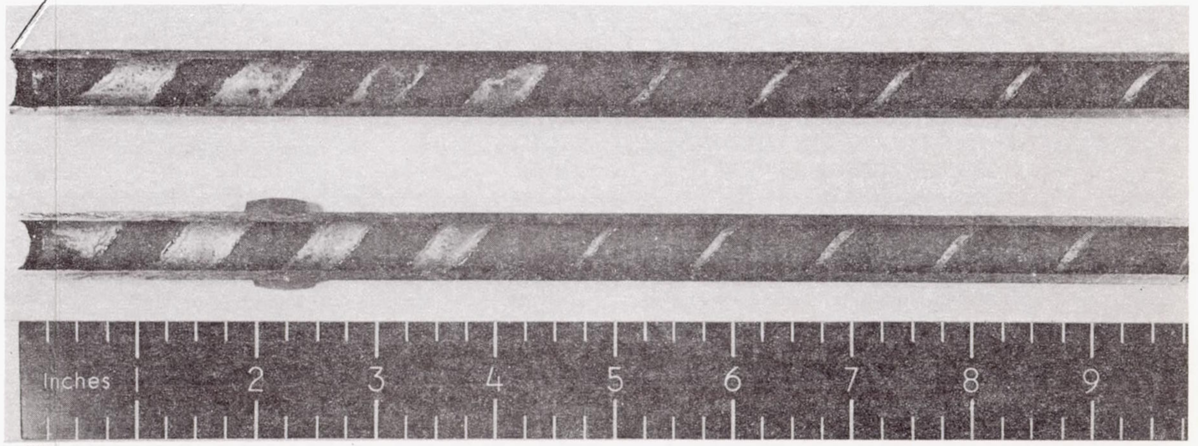

7575

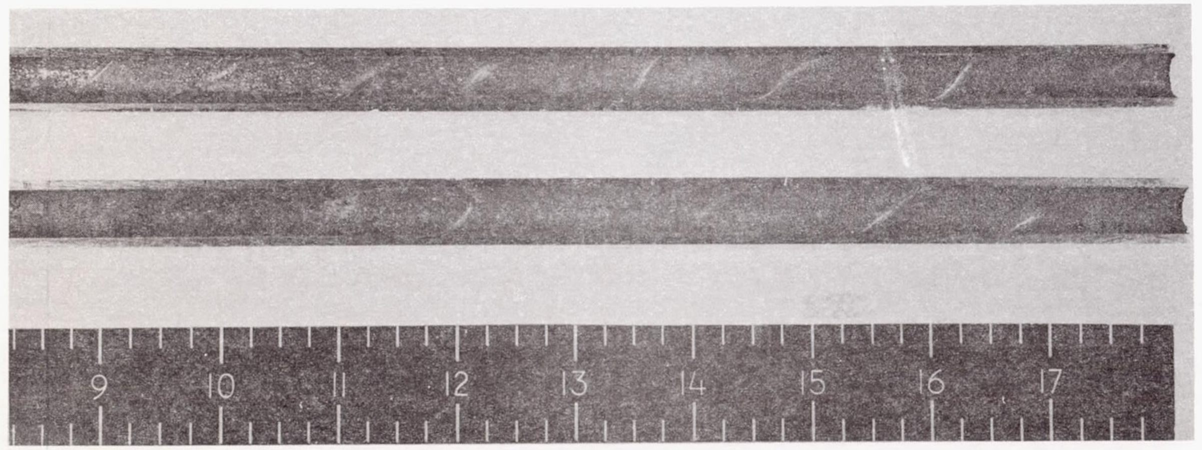

7576

MERCURY CONTAINMENT TUBING DOWN STREAM OF THE PLUG SHOWING THE INSIDE DIAMETER OF THE TUBING

Photomacrographs of the CL 4A-4 Test Section

Figure 32

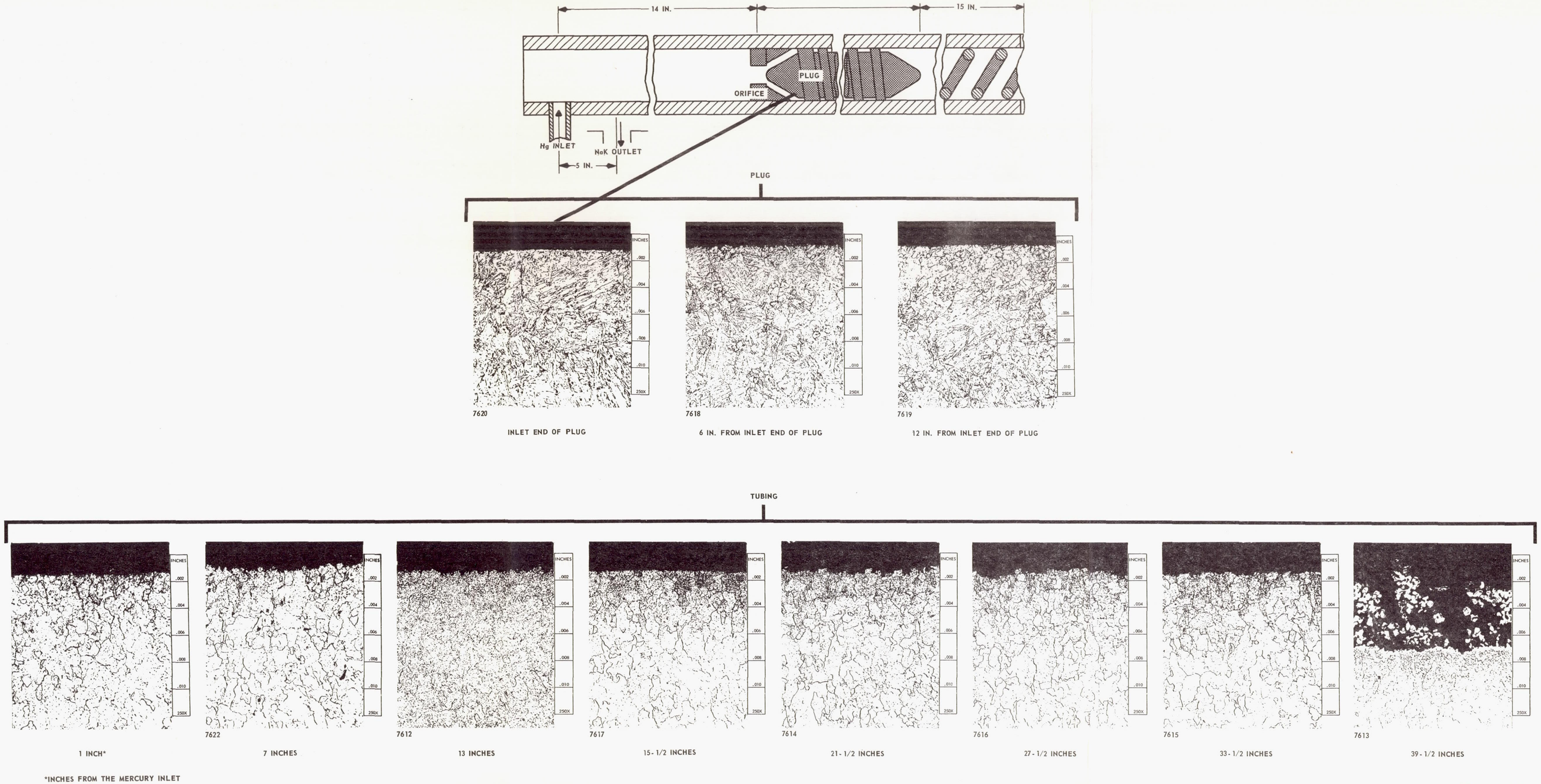

Figure 33

Photomicrographs of the 9Cr-1Mo Plug and Tubing of the Test Section 4A-4

567-NF-1243

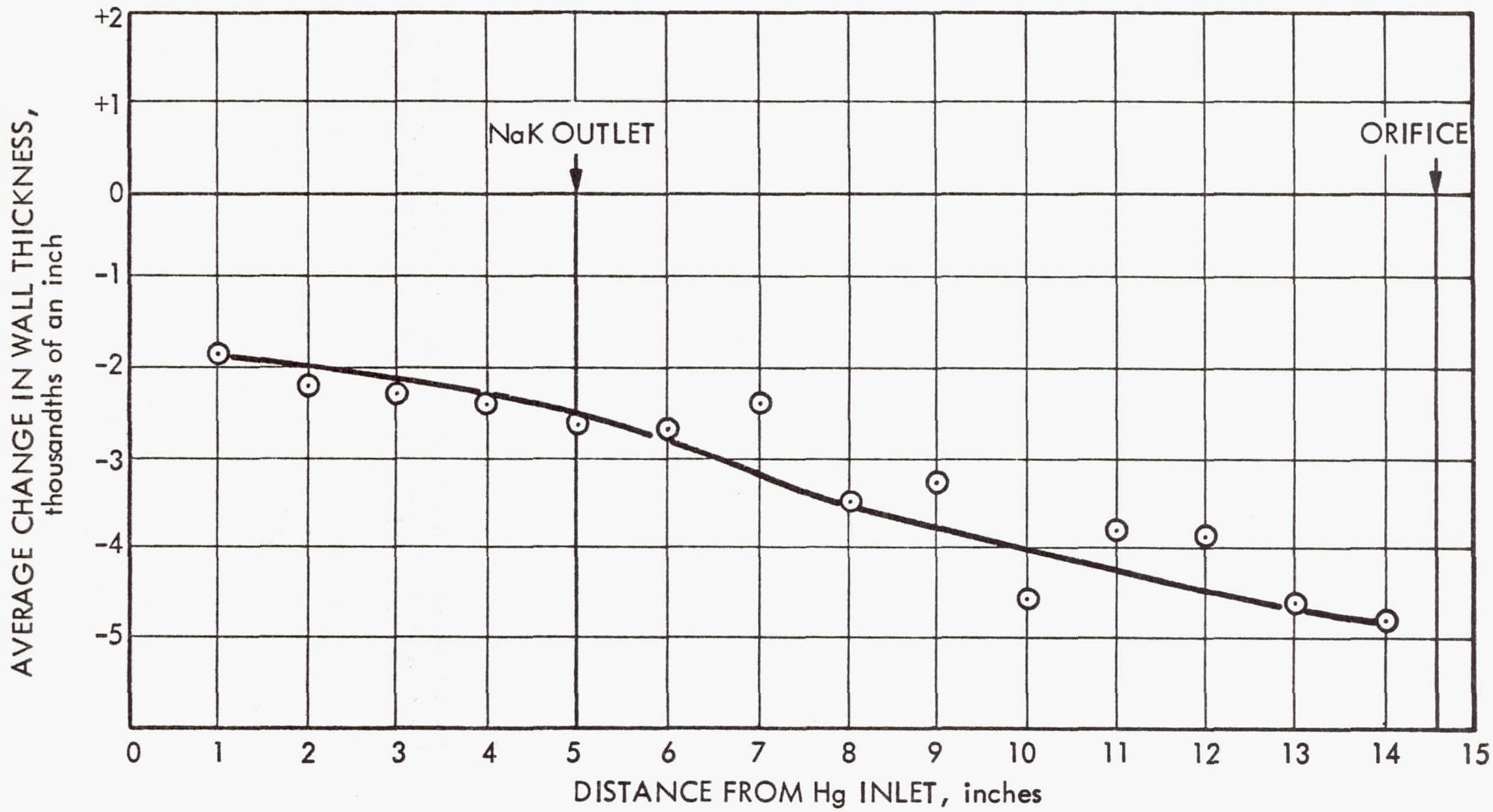

Change in Wall Thickness of the 9Cr-1Mo Tubing,
Preheat Region of Test Section 4A-4

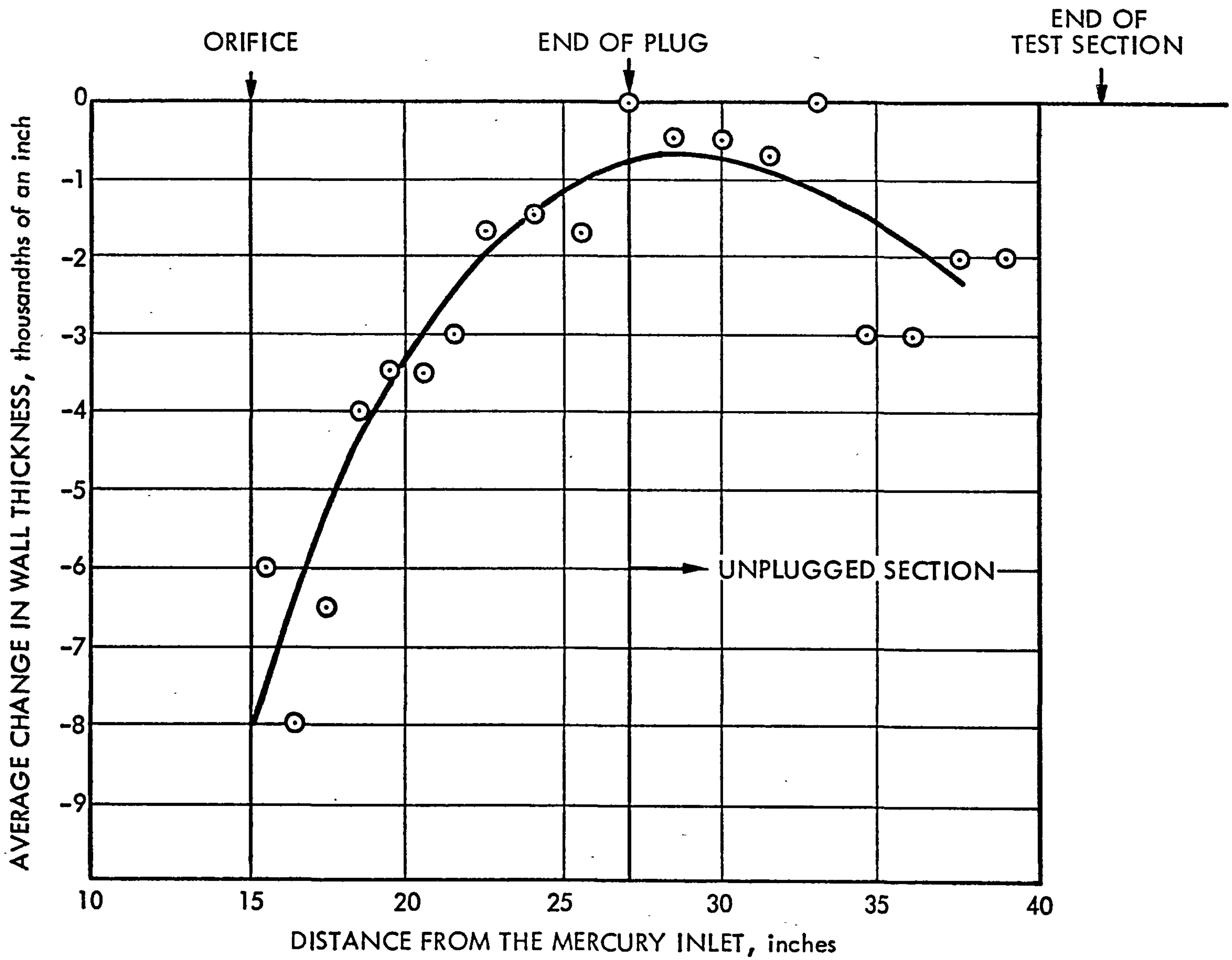

Figure 35

Change in Wall Thickness of the 9Cr-1Mo Tubing Downstream of the Orifice, Test Section 4A-4

Figure 36

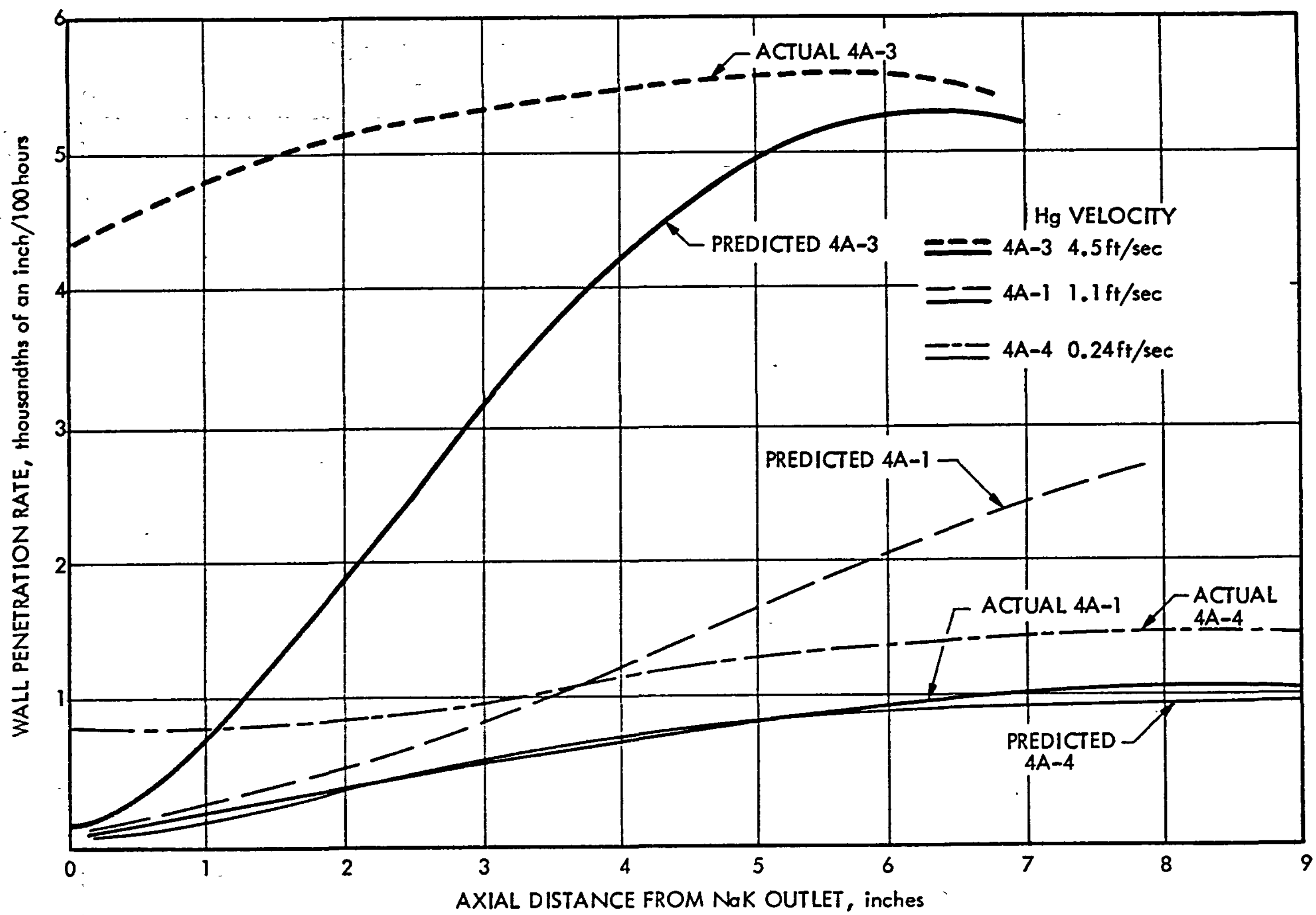

Predicted and Actual Corrosion in the Preheat Region
A Composite of Curves from the Series of Tests with the 4A Test Sections

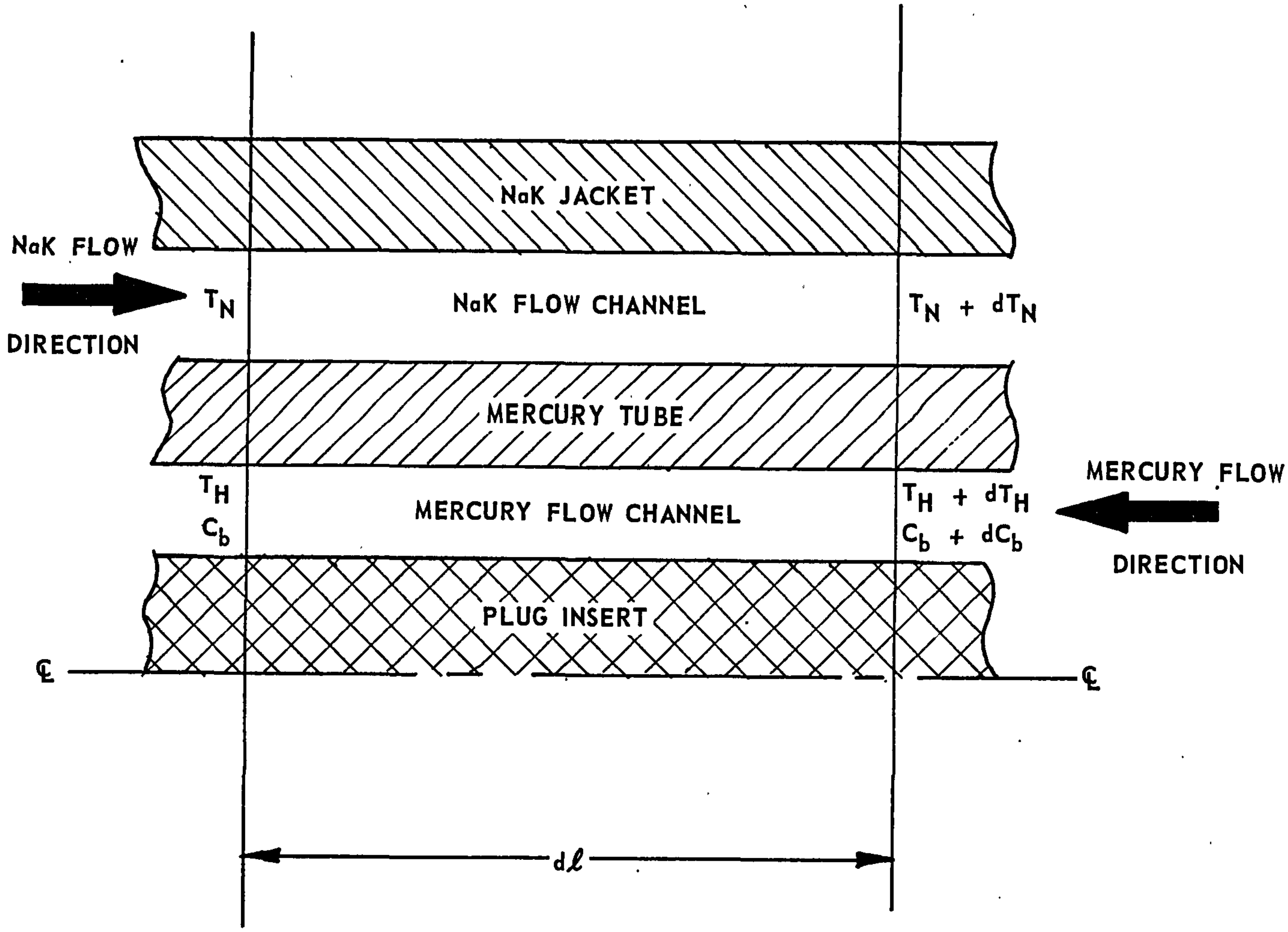

Differential Length of the SNAP-8 Boiler in the Preheat Region

Figure 37

INPUT DATA FOR PROBLEM TITLED

BASE CASE SPIRAL PLUG GEOMETRY MARCH 23,1966

BOILER GEOMETRY SPECIFICATIONS

BOILER ID(IN)	3.990	NO.OF TUBES	7.0	TUBE OD(IN)	0.832
TUBE ID(IN)	0.652	THREAD HT(IN)	0.062	THREAD PITCH(IN)	0.375
CHANNELS/TUBE	1.0	THREAD WIDTH(IN)	0.062	DELTA Z PRINT(IN)	0.200

BOILER OPERATING CONDITIONS

NAK OUT(DEG.F)	1110.0	HG IN(DEG.F)	500.0	HG OUT(DEG.F)	1097.0
NAK FLOW(LB/HR)	47500.0	HG FLOW(LB/HR)	11500.0	HG SIDE H MULT	1.000
NAK SIDE H MULT	1.000	WALL COND(BTU/FT-DEG.F)	15.67	MAX DELTA T(DEG.F)	5.000

* * * SPIRAL PLUG GEOMETRY * * *

CALCULATED RESULTS

NAK FLOW AREA(SQ.FT)	6.040E-02	NAK WETTED PER (FT)	2.569E 00	NAK EQ.DIA(FT)	9.404E-02
HG FLOW AREA(SQ.FT)	1.321E-04	HG WETTED PER (FT)	5.626E-02	HG EQ.DIA(FT)	9.391E-03
G-NAK(LB/SQ.FT-SEC)	2.184E 02	G-HG(LB/SQ.FT-SEC)	3.455E 03	HG VEL T-AV(FT/SEC)	4.411E 00

Figure 38
Sheet 1 of 5

Sample Output for Computer Code SECAT

* * * *AXIAL DISTRIBUTION OF PARAMETERS-PART 1* * * *

PROBLEM TITLE - - -BASE CASE SPIRAL PLUG GEOMETRY MARCH 23,1966

DIST FROM HG IN(IN)	NAK BULK TEMP(F)	HG BULK TEMP(F)	HG WALL TEMP(F)	* * * IRON CONCENTRATION(PPM) * * * IN HG	SAT (HOT)	SAT(COLD)	PENETRATION (MILS/YR) TUBE	PLUG
0.000	1110.0	500.0	607.5	5.464E-03	1.747E-02	5.464E-03	1.118E 01	0.000E-39
0.200	1111.1	528.5	630.4	5.572E-03	2.179E-02	7.642E-03	1.571E 01	2.005E 00
0.400	1112.1	555.7	652.4	5.728E-03	2.671E-02	1.035E-02	2.108E 01	4.648E 00
0.600	1113.1	581.7	673.5	5.941E-03	3.223E-02	1.364E-02	2.734E 01	8.001E 00
0.800	1114.0	606.6	693.8	6.222E-03	3.835E-02	1.752E-02	3.449E 01	1.213E 01
1.000	1114.9	630.4	713.2	6.582E-03	4.506E-02	2.203E-02	4.253E 01	1.708E 01
1.200	1115.7	653.2	731.8	7.034E-03	5.232E-02	2.717E-02	5.147E 01	2.288E 01
1.400	1116.5	674.9	749.7	7.589E-03	6.011E-02	3.294E-02	6.125E 01	2.956E 01
1.600	1117.3	695.7	766.7	8.258E-03	6.840E-02	3.932E-02	7.185E 01	3.711E 01
1.800	1118.1	715.5	783.1	9.052E-03	7.714E-02	4.629E-02	8.321E 01	4.551E 01
2.000	1118.8	734.4	798.7	9.982E-03	8.629E-02	5.383E-02	9.527E 01	5.474E 01
2.200	1119.4	752.5	813.6	1.106E-02	9.581E-02	6.189E-02	1.079E 02	6.474E 01
2.400	1120.1	769.7	827.9	1.229E-02	1.057E-01	7.045E-02	1.212E 02	7.548E 01
2.600	1120.7	786.2	841.6	1.368E-02	1.158E-01	7.945E-02	1.349E 02	8.689E 01
2.800	1121.3	801.9	854.7	1.524E-02	1.261E-01	8.886E-02	1.490E 02	9.887E 01
3.000	1121.9	816.9	867.1	1.698E-02	1.367E-01	9.862E-02	1.633E 02	1.114E 02
3.200	1122.4	831.2	879.1	1.890E-02	1.474E-01	1.087E-01	1.779E 02	1.243E 02
3.400	1122.9	844.9	890.5	2.101E-02	1.582E-01	1.190E-01	1.927E 02	1.376E 02
3.600	1123.4	858.0	901.4	2.330E-02	1.691E-01	1.296E-01	2.074E 02	1.512E 02
3.800	1123.9	870.4	911.8	2.579E-02	1.800E-01	1.403E-01	2.222E 02	1.650E 02
4.000	1124.3	882.3	921.7	2.846E-02	1.909E-01	1.511E-01	2.369E 02	1.738E 02
4.200	1124.8	893.7	931.2	3.132E-02	2.018E-01	1.621E-01	2.514E 02	1.929E 02
4.400	1125.2	904.5	940.3	3.437E-02	2.127E-01	1.731E-01	2.656E 02	2.066E 02
4.600	1125.6	914.9	949.0	3.761E-02	2.234E-01	1.841E-01	2.796E 02	2.204E 02
4.800	1125.9	924.7	957.3	4.103E-02	2.341E-01	1.951E-01	2.932E 02	2.340E 02
5.000	1126.3	934.2	965.2	4.463E-02	2.446E-01	2.061E-01	3.065E 02	2.474E 02
5.200	1126.6	943.1	972.7	4.840E-02	2.550E-01	2.170E-01	3.193E 02	2.605E 02
5.400	1127.0	951.7	980.0	5.235E-02	2.652E-01	2.277E-01	3.317E 02	2.733E 02
5.600	1127.3	959.9	986.8	5.646E-02	2.753E-01	2.384E-01	3.435E 02	2.856E 02
5.800	1127.6	967.8	993.4	6.073E-02	2.851E-01	2.489E-01	3.549E 02	2.976E 02
6.000	1127.8	975.2	999.7	6.515E-02	2.948E-01	2.593E-01	3.656E 02	3.092E 02
6.200	1128.1	982.4	1005.7	6.972E-02	3.042E-01	2.695E-01	3.759E 02	3.202E 02
6.400	1128.4	989.2	1011.5	7.442E-02	3.135E-01	2.795E-01	3.855E 02	3.308E 02
6.600	1128.6	995.7	1017.0	7.926E-02	3.225E-01	2.893E-01	3.945E 02	3.408E 02
6.800	1128.9	1001.9	1022.2	8.421E-02	3.313E-01	2.989E-01	4.030E 02	3.503E 02
7.000	1129.1	1007.8	1027.2	8.929E-02	3.398E-01	3.083E-01	4.108E 02	3.592E 02
7.200	1129.3	1013.5	1032.0	9.447E-02	3.481E-01	3.175E-01	4.181E 02	3.676E 02
7.400	1129.5	1018.9	1036.5	9.975E-02	3.562E-01	3.264E-01	4.247E 02	3.754E 02
7.600	1129.7	1024.1	1040.9	1.051E-01	3.640E-01	3.351E-01	4.308E 02	3.827E 02
7.800	1129.9	1029.0	1045.0	1.106E-01	3.717E-01	3.436E-01	4.363E 02	3.894E 02

Figure 38
Sheet 2 of 5

. * * * *AXIAL DISTRIBUTION OF PARAMETERS-PART 2* * * *

PROBLEM TITLE - - -BASE CASE SPIRAL PLUG GEOMETRY - MARCH 23,1966

DIST FROM HG IN(IN)	* REYNOLDS NUMBER * NAK	HG	* * PRANDTL NUMBER * * NAK	HG	SCHMIDT NO HG	HEAT TRANSFER COEF (BTU/HR-SQ.FT-F) NAK	HG	OVERALL	MASS TRANSFER COEF(FT/HR)
0.000	1.815E 05	5.223E 04	5.698E-03	9.526E-03	2.166E 01	2.241E 03	6.059E 03	1.129E 03	5.296E 00
0.200	1.816E 05	5.327E 04	5.695E-03	9.199E-03	2.023E 01	2.241E 03	6.111E 03	1.130E 03	5.526E 00
0.400	1.817E 05	5.425E 04	5.693E-03	8.908E-03	1.908E 01	2.241E 03	6.160E 03	1.132E 03	5.746E 00
0.600	1.818E 05	5.519E 04	5.690E-03	8.650E-03	1.803E 01	2.241E 03	6.205E 03	1.133E 03	5.961E 00
0.800	1.819E 05	5.607E 04	5.688E-03	8.419E-03	1.710E 01	2.240E 03	6.247E 03	1.135E 03	6.169E 00
1.000	1.819E 05	5.690E 04	5.686E-03	8.212E-03	1.628E 01	2.240E 03	6.285E 03	1.136E 03	6.369E 00
1.200	1.820E 05	5.770E 04	5.683E-03	8.025E-03	1.555E 01	2.240E 03	6.323E 03	1.137E 03	6.563E 00
1.400	1.821E 05	5.846E 04	5.681E-03	7.855E-03	1.489E 01	2.240E 03	6.357E 03	1.138E 03	6.759E 00
1.600	1.822E 05	5.917E 04	5.680E-03	7.702E-03	1.430E 01	2.240E 03	6.389E 03	1.139E 03	6.932E 00
1.800	1.822E 05	5.985E 04	5.678E-03	7.562E-03	1.377E 01	2.240E 03	6.420E 03	1.140E 03	7.104E 00
2.000	1.823E 05	6.050E 04	5.676E-03	7.434E-03	1.329E 01	2.240E 03	6.448E 03	1.141E 03	7.270E 00
2.200	1.824E 05	6.111E 04	5.674E-03	7.317E-03	1.285E 01	2.239E 03	6.475E 03	1.142E 03	7.431E 00
2.400	1.824E 05	6.170E 04	5.673E-03	7.210E-03	1.246E 01	2.239E 03	6.500E 03	1.143E 03	7.586E 00
2.600	1.825E 05	6.225E 04	5.671E-03	7.111E-03	1.210E 01	2.239E 03	6.523E 03	1.143E 03	7.734E 00
2.800	1.826E 05	6.278E 04	5.670E-03	7.020E-03	1.176E 01	2.239E 03	6.546E 03	1.144E 03	7.877E 00
3.000	1.826E 05	6.328E 04	5.668E-03	6.936E-03	1.146E 01	2.239E 03	6.567E 03	1.145E 03	8.014E 00
3.200	1.827E 05	6.376E 04	5.667E-03	6.858E-03	1.118E 01	2.239E 03	6.587E 03	1.145E 03	8.145E 00
3.400	1.827E 05	6.421E 04	5.666E-03	6.785E-03	1.092E 01	2.239E 03	6.605E 03	1.146E 03	8.271E 00
3.600	1.828E 05	6.464E 04	5.665E-03	6.718E-03	1.069E 01	2.239E 03	6.623E 03	1.146E 03	[illegible]
3.800	1.828E 05	6.505E 04	5.664E-03	6.656E-03	1.047E 01	2.239E 03	6.640E 03	1.147E 03	8.508E 00
4.000	1.829E 05	6.544E 04	5.662E-03	6.597E-03	1.026E 01	2.239E 03	6.656E 03	1.147E 03	8.619E 00
4.200	1.829E 05	6.581E 04	5.661E-03	6.543E-03	1.007E 01	2.239E 03	6.671E 03	1.148E 03	8.724E 00
4.400	1.829E 05	6.617E 04	5.660E-03	6.492E-03	9.898E 00	2.239E 03	6.685E 03	1.148E 03	8.829E 00
4.600	1.830E 05	6.650E 04	5.659E-03	6.444E-03	9.734E 00	2.238E 03	6.699E 03	1.148E 03	8.926E 00
4.800	1.830E 05	6.683E 04	5.659E-03	6.399E-03	9.582E 00	2.239E 03	6.712E 03	1.149E 03	9.020E 00
5.000	1.830E 05	6.713E 04	5.658E-03	6.357E-03	9.440E 00	2.238E 03	6.724E 03	1.149E 03	9.117E 00
5.200	1.831E 05	6.742E 04	5.657E-03	6.318E-03	9.307E 00	2.239E 03	6.735E 03	1.149E 03	9.196E 00
5.400	1.831E 05	6.770E 04	5.656E-03	6.281E-03	9.183E 00	2.238E 03	6.746E 03	1.150E 03	9.279E 00
5.600	1.831E 05	6.796E 04	5.655E-03	6.246E-03	9.067E 00	2.238E 03	6.757E 03	1.150E 03	9.358E 00
5.800	1.832E 05	6.822E 04	5.655E-03	6.213E-03	8.958E 00	2.238E 03	6.767E 03	1.150E 03	9.433E 00
6.000	1.832E 05	6.846E 04	5.654E-03	6.182E-03	8.855E 00	2.238E 03	6.776E 03	1.151E 03	9.505E 00
6.200	1.832E 05	6.868E 04	5.653E-03	6.153E-03	8.759E 00	2.238E 03	6.785E 03	1.151E 03	9.575E 00
6.400	1.833E 05	6.890E 04	5.653E-03	6.126E-03	8.669E 00	2.238E 03	6.794E 03	1.151E 03	9.641E 00
6.600	1.833E 05	6.911E 04	5.652E-03	6.100E-03	8.584E 00	2.238E 03	6.802E 03	1.151E 03	9.704E 00
6.800	1.833E 05	6.931E 04	5.652E-03	6.075E-03	8.505E 00	2.238E 03	6.810E 03	1.152E 03	9.765E 00
7.000	1.833E 05	6.950E 04	5.651E-03	6.052E-03	8.429E 00	2.238E 03	6.817E 03	1.152E 03	9.823E 00
7.200	1.833E 05	6.968E 04	5.650E-03	6.030E-03	8.358E 00	2.238E 03	6.824E 03	1.152E 03	9.879E 00
7.400	1.834E 05	6.985E 04	5.650E-03	6.009E-03	8.292E 00	2.238E 03	6.831E 03	1.152E 03	9.932E 00
7.600	1.834E 05	7.001E 04	5.650E-03	5.990E-03	8.228E 00	2.238E 03	6.840E 03	1.152E 03	9.933E 00
7.800	1.834E 05	7.017E 04	5.649E-03	5.971E-03	8.169E 00	2.238E 03	6.849E 03	1.153E 03	1.003E 01

Figure 38
Sheet 3 of 5

* * * *AXIAL DISTRIBUTION OF PARAMETERS-PART 1* * * *

PROBLEM TITLE - - -BASE CASE SPIRAL PLUG GEOMETRY MARCH 23,1966

DIST FROM HG IN(IN)	NAK BULK TEMP(F)	HG BULK TEMP(F)	HG WALL TEMP(F)	* * * IRON CONCENTRATION(PPM) * * * IN HG	SAT (HOT)	SAT(COLD)	PENETRATION (MILS/YR) TUBE	PLUG
8.000	1130.1	1033.7	1049.0	1.161E-01	3.790E-01	3.51[illegible]E-01	4.412E 02	3.956E 02
8.200	1130.2	1038.2	1052.8	1.217E-01	3.862E-01	3.59[illegible]E-01	4.455E 02	4.011E 02
8.400	1130.4	1042.5	1056.4	1.274E-01	3.931E-01	3.676E-01	4.493E 02	4.062E 02
8.600	1130.6	1046.6	1059.9	1.331E-01	3.998E-01	3.751E-01	4.525E 02	4.107E 02
8.800	1130.7	1050.5	1063.2	1.389E-01	4.063E-01	3.824E-01	4.553E 02	4.147E 02
9.000	1130.9	1054.3	1066.4	1.447E-01	4.125E-01	3.895E-01	4.575E 02	4.182E 02
9.200	1131.0	1057.8	1069.4	1.506E-01	4.185E-01	3.963E-01	4.592E 02	4.212E 02
9.400	1131.1	1061.2	1072.3	1.564E-01	4.244E-01	4.029E-01	4.605E 02	4.237E 02
9.600	1131.2	1064.5	1075.0	1.623E-01	4.300E-01	4.093E-01	4.613E 02	4.257E 02
9.800	1131.4	1067.6	1077.7	1.682E-01	4.354E-01	4.155E-01	4.617E 02	4.273E 02
10.000	1131.5	1070.6	1080.2	1.742E-01	4.406E-01	4.214E-01	4.617E 02	4.284E 02
10.200	1131.6	1073.4	1082.6	1.801E-01	4.457E-01	4.272E-01	4.613E 02	4.291E 02
10.400	1131.7	1076.1	1084.9	1.860E-01	4.505E-01	4.327E-01	4.605E 02	4.294E 02
10.600	1131.8	1078.7	1087.1	1.919E-01	4.552E-01	4.381E-01	4.593E 02	4.294E 02
10.800	1131.9	1081.2	1089.2	1.978E-01	4.597E-01	4.432E-01	4.578E 02	4.289E 02
11.000	1132.0	1083.6	1091.2	2.037E-01	4.640E-01	4.481E-01	4.559E 02	4.281E 02
11.200	1132.1	1085.8	1093.1	2.096E-01	4.682E-01	4.529E-01	4.533E 02	4.270E 02
11.400	1132.1	1088.0	1094.9	2.155E-01	4.722E-01	4.575E-01	4.514E 02	4.256E 02
11.600	1132.2	1090.0	1096.6	2.213E-01	4.760E-01	4.619E-01	4.487E 02	4.238E 02
11.800	1132.3	1092.0	1098.3	2.271E-01	4.797E-01	4.66[illegible]E-01	4.457E 02	4.219E 02
12.000	1132.4	1093.9	1099.9	2.328E-01	4.832E-01	4.702E-01	4.425E 02	4.195E 02
12.200	1132.4	1095.7	1101.4	2.385E-01	4.866E-01	4.741E-01	4.391E 02	4.170E 02
12.356	1132.5	1097.0	1102.9	2.430E-01	4.900E-01	4.771E-01	4.376E 02	4.148E 02

Figure 38
Sheet 4 of 5

* * * *AXIAL DISTRIBUTION OF PARAMETERS—PART 2* * * *

PROBLEM TITLE - - -BASE CASE SPIRAL PLUG GEOMETRY MARCH 23,1966

DIST FROM HG IN(IN)	* REYNOLDS NUMBER * NAK	HG	* * PRANDTL NUMBER * * NAK	HG	SCHMIDT NO HG	HEAT TRANSFER COFF (BTU/HR-SQ.FT-F) NAK	HG	OVERALL	MASS TRANSFER KD(FT/HR)
8.000	1.834E 05	7.032E 04	5.649E-03	5.953E-03	8.112E 00	2.238E 03	6.857E 03	1.153E 03	1.008E 01
8.200	1.834E 05	7.046E 04	5.648E-03	5.937E-03	8.059E 00	2.238E 03	6.864E 03	1.153E 03	1.012E 01
8.400	1.834E 05	7.060E 04	5.648E-03	5.921E-03	8.009E 00	2.238E 03	6.872E 03	1.153E 03	1.016E 01
8.600	1.835E 05	7.073E 04	5.647E-03	5.906E-03	7.961E 00	2.238E 03	6.879E 03	1.153E 03	1.021E 01
8.800	1.835E 05	7.085E 04	5.647E-03	5.891E-03	7.916E 00	2.238E 03	6.885E 03	1.154E 03	1.024E 01
9.000	1.835E 05	7.097E 04	5.647E-03	5.878E-03	7.873E 00	2.238E 03	6.892E 03	1.154E 03	1.028E 01
9.200	1.835E 05	7.108E 04	5.646E-03	5.865E-03	7.833E 00	2.238E 03	6.898E 03	1.154E 03	1.032E 01
9.400	1.835E 05	7.119E 04	5.646E-03	5.852E-03	7.794E 00	2.238E 03	6.903E 03	1.154E 03	1.035E 01
9.600	1.835E 05	7.129E 04	5.646E-03	5.841E-03	7.758E 00	2.237E 03	6.909E 03	1.154E 03	1.039E 01
9.800	1.835E 05	7.139E 04	5.646E-03	5.830E-03	7.723E 00	2.237E 03	6.914E 03	1.154E 03	1.041E 01
10.000	1.836E 05	7.148E 04	5.645E-03	5.819E-03	7.691E 00	2.237E 03	6.919E 03	1.155E 03	1.044E 01
10.200	1.836E 05	7.157E 04	5.645E-03	5.809E-03	7.660E 00	2.237E 03	6.924E 03	1.155E 03	[illegible]
10.400	1.836E 05	7.166E 04	5.645E-03	5.800E-03	7.630E 00	2.237E 03	6.928E 03	1.155E 03	1.050E 01
10.600	1.836E 05	7.174E 04	5.645E-03	5.791E-03	7.602E 00	2.237E 03	6.933E 03	1.155E 03	1.053E 01
10.800	1.836E 05	7.181E 04	5.644E-03	5.782E-03	7.575E 00	2.237E 03	6.937E 03	1.155E 03	1.055E 01
11.000	1.836E 05	7.189E 04	5.644E-03	5.774E-03	7.550E 00	2.237E 03	6.941E 03	1.155E 03	1.057E 01
11.200	1.836E 05	7.196E 04	5.644E-03	5.766E-03	7.526E 00	2.237E 03	6.945E 03	1.155E 03	1.060E 01
11.400	1.836E 05	7.203E 04	5.644E-03	5.758E-03	7.503E 00	2.237E 03	6.948E 03	1.155E 03	1.062E 01
11.600	1.836E 05	7.209E 04	5.643E-03	5.751E-03	7.481E 00	2.237E 03	6.952E 03	1.155E 03	[illegible]
11.800	1.836E 05	7.215E 04	5.643E-03	5.744E-03	7.461E 00	2.237E 03	6.955E 03	1.155E 03	1.066E 01
12.000	1.836E 05	7.221E 04	5.643E-03	5.738E-03	7.441E 00	2.237E 03	6.958E 03	1.156E 03	1.068E 01
12.200	1.836E 05	7.227E 04	5.643E-03	5.732E-03	7.422E 00	2.237E 03	6.961E 03	1.156E 03	1.070E 01
12.356	1.837E 05	7.231E 04	5.643E-03	5.727E-03	7.408E 00	2.237E 03	6.926E 03	1.155E 03	1.071E 01

THE NAK SIDE DELTA P 3.727E-02 PSI THE HG SIDE DELTA P 1.816E 01 PSI

Figure 38
Sheet 5 of 5

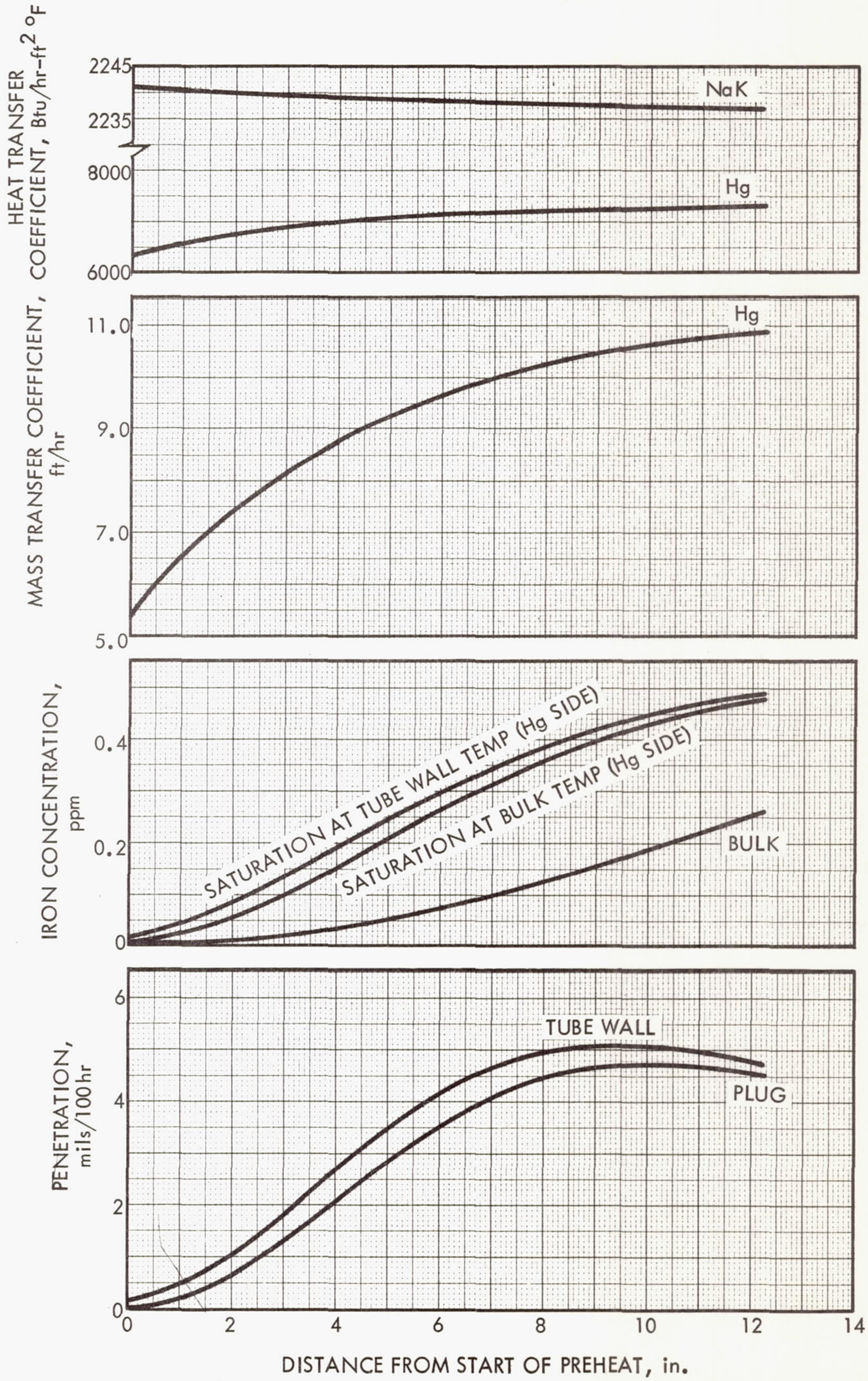

Axial Distribution of Variables, Base Case

866-NF-1126

Figure 39

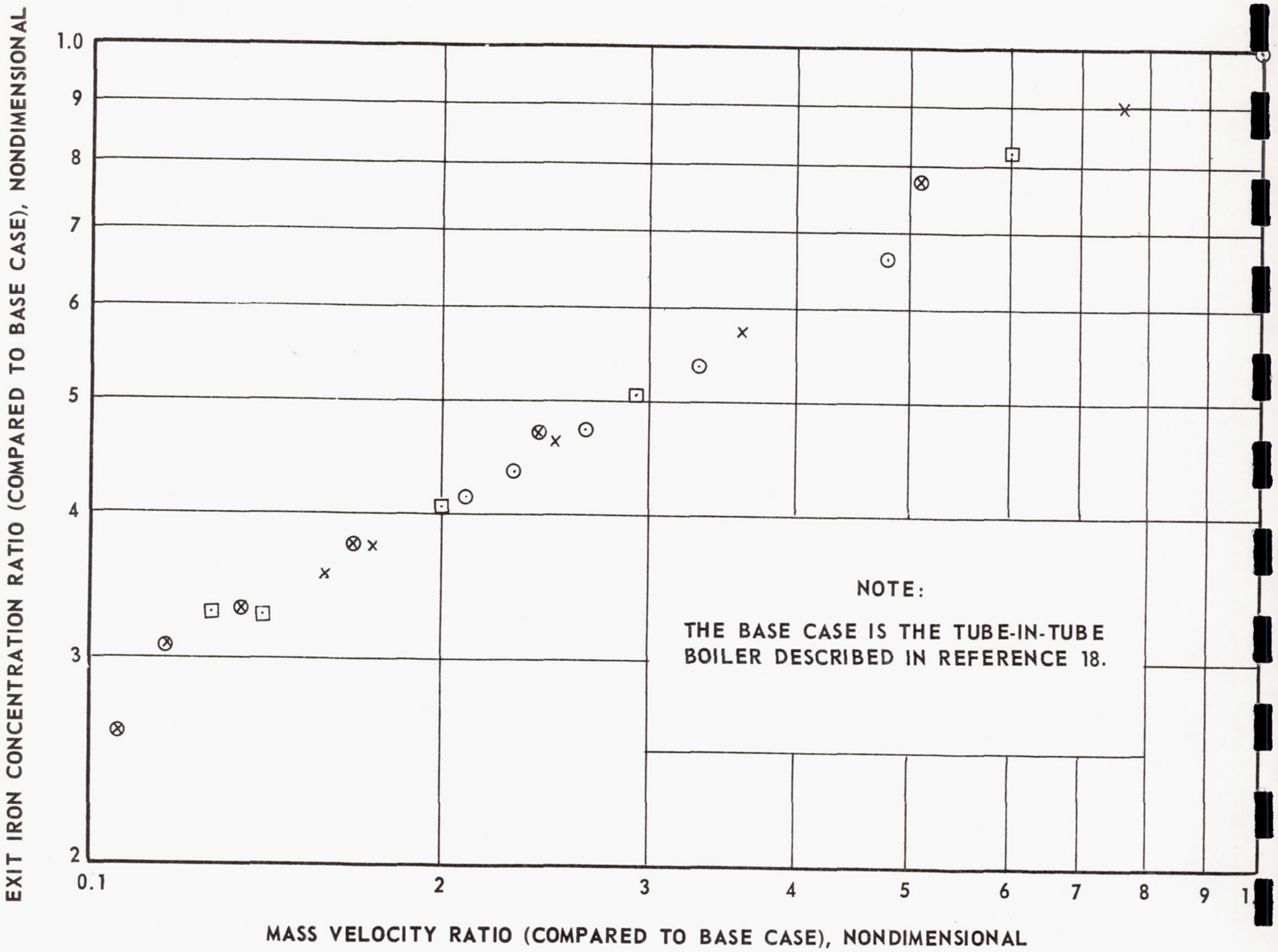

Calculated Effect of Mass Velocity on Preheat Exit Mercury Iron Concentration

Figure 40

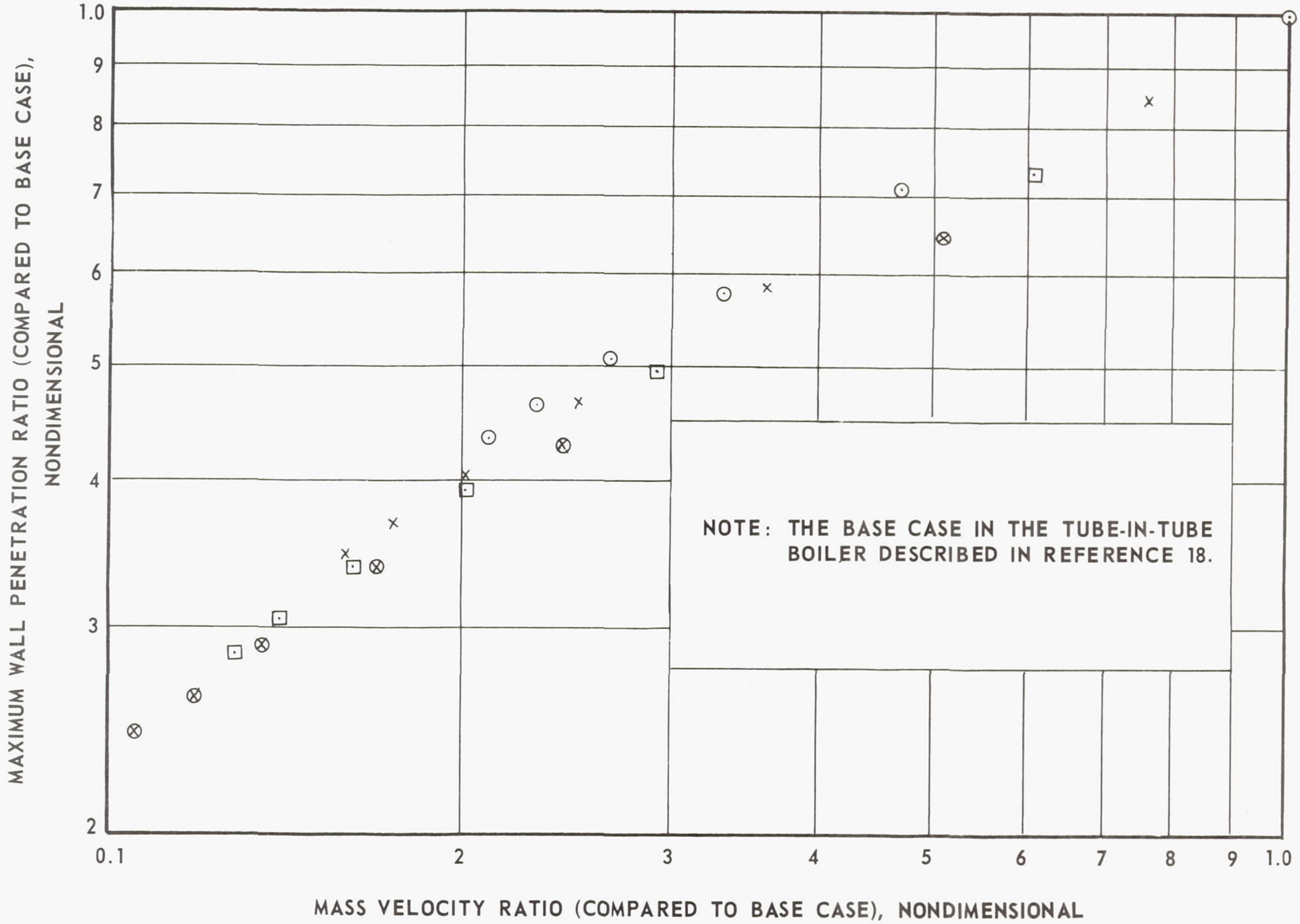

Calculated Effect of Mass Velocity on Maximum Wall Penetration Rate

Figure 41

APPENDIX

MERCURY WETTING PROCEDURE

This procedure describes the method of pre-wetting the boiler test section by a lithium and mercury solution. Test section is located in Corrosion Loop 4 and the mercury system is assumed to be fully checked out.

A schematic of the apparatus for pre-wetting the test section is shown in Figure A-1. The numbers in each step below refer to points on the schematic.

1. Close V-801, V-802, V-803, V-804, V-805, V-806, V-807, V-808, V-809, V-810, V-811, V-812, V-234, V-813.
2. Pump down on vacuum system to ≈25 microns, or less, when both systems are leak tight.
3. Open V-807 and V-810.
4. Open V-234 and evacuate Hg loop to 25 microns or less.
5. Open V-804 and V-803 and evacuate setting system to 25 microns or less.
6. Open V-801 and V-802 and equalize the systems under vacuum.
7. Close V-253 and V-802, V-803, V-804; open V-229, V-250 and V-213.
8. Pressurize Hg expansion tank to 15 psig.
9. Open V-803, then slowly open V-802 until the three level lights (A, B, and C) are lighted; then quickly close V-802.
10. Release pressure on Hg expansion tank to atmosphere.
11. Open V-801 and drain down Hg in test section.
12. Close V-810; open V-813 and bring loop pressure to 5 psig with argon.
13. Close V-801 and release loop pressure to atmospheric.
14. Close V-813, open V-810 and evacuate loop.

15. Close V-807, open V-808 and pressurize system to atmospheric; close V-808.

16. When ready for Step 15, be ready to open V-806 quickly and remove Li from container and drop small pieces into tank with tweezers, making sure that Li is inserted into tank area and not stuck to sides of tubing or fittings.

17. Close V-806 and pressurize tank with argon to 1 psig.

18. Turn on wetting tank guard heater and heat to 390/400°F. Leave on at this temperature for 12 hr.

19. After the Li/Hg solution remains 12 hr at 390/400°F reduce to 180°F.

20. Hook up argon line to V-809 and bubble to mix Hg/Li solution for 2 hr at 8 to 12 psi.

21. Purge ≈5 cc of Li/Hg mix from sampling valve V-809; then withdraw ≈1-3 cc of mix for analysis.

22. If analysis is between 300-500 ppm Li, proceed with Step 24; if not, bubble with argon for additional hr and then repeat 21 and 22.

23. Open V-808 and pressurize wetting tank to 10 psig.

24. Open V-802, then open V-808 slowly until the top (A) and middle (B) probe lights go out. Close V-808 and V-802.

25. Close V-808, open V-807 slowly and evacuate the system over Li/Hg solution.

26. Close V-810 and V-242; open V-813 slowly and pressurize loop to 100 psig.

27. Start primary NaK loop and slowly heat up to 900°F. Do not allow loop pressure to exceed 150 psia. Pressure can be reduced through V-812.

28. Slowly increase NaK temperature to 950°F while maintaining loop pressure at 135 psia.

29. Slowly reduce the Hg loop pressure until the Li/Hg solution is slowly boiling in the test section and Hg condensing takes place around the boiler outlet vertical riser.

30. Hold the conditions in Step 27 for 16 hr.

31. Shut off primary NaK heater and allow test section temperature to cool to 300 to 500°F.

32. Reduce Hg loop pressure to 50 psig.

33. Open V-802 and V-804 and drain all Li/Hg mix into dump tank and remove from dump tank with V-803 closed; Hg/Li solution will remain for next Li run.

34. Drain test section to dump tank and sample for Li.

35. Close V-802, V-813, open V-812 and bleed off loop pressure to atmospheric.

36. Open V-810 and evacuate Hg loop.

37. When Hg loop is less than 25 microns, proceed with standard loop # startup.

167-NF-1227

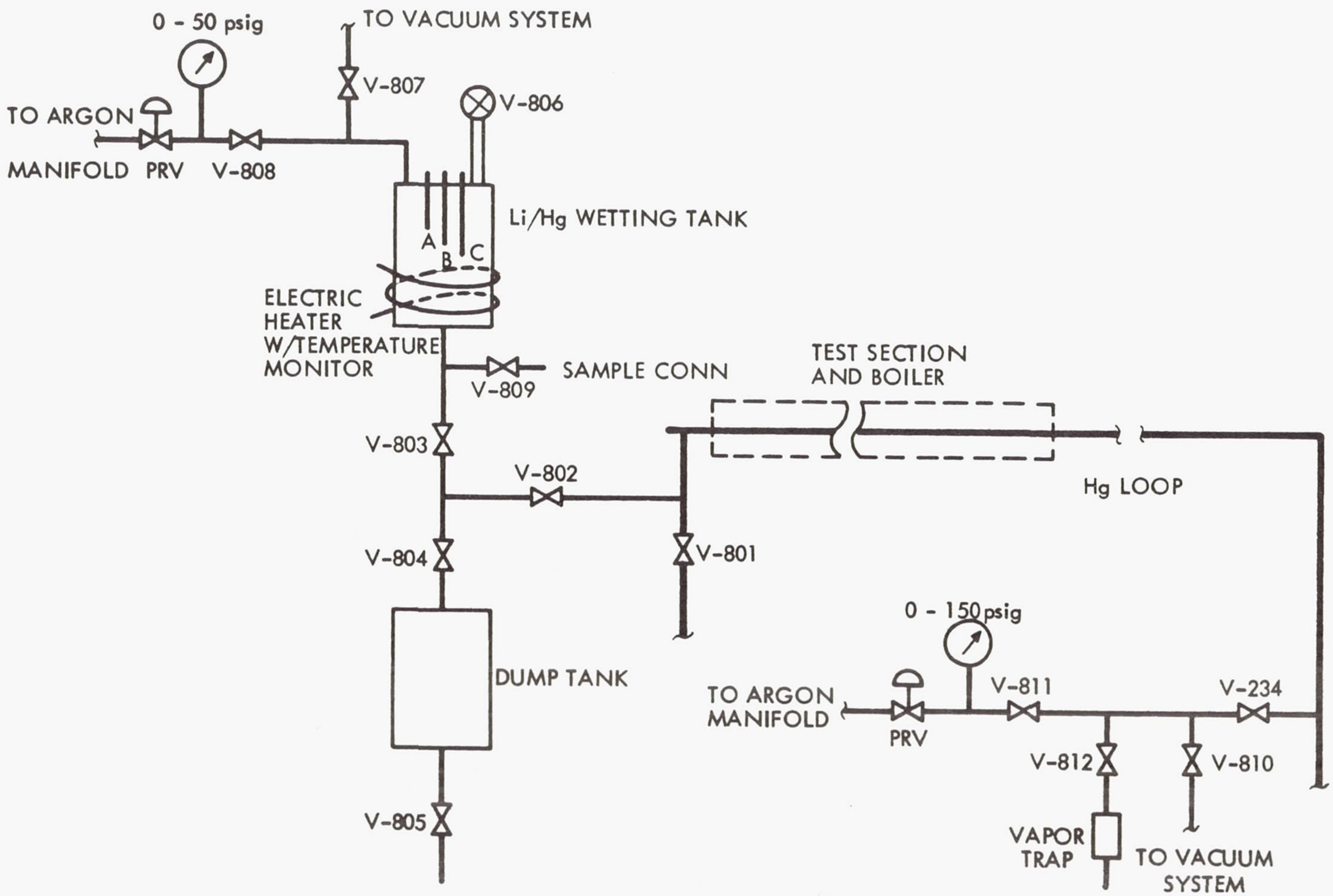

Mercury Wetting Apparatus Schematic - Corrosion Loop 4

Figure A-1

DISTRIBUTION LIST

National Aeronautics and Space Administration
Washington, D. C. 20546
Attention: P. R. Miller (RNP)
James J. Lynch (RNP)
George C. Deutsch (RR)
Dr. Fred Schulman (RNP)
H. Rochen (RNP)

National Aeronautics and Space Administration
Scientific and Technical Information Facility
P. O. Box 33
College Park, Maryland 20740
Attention: Acquisitions Branch
(SQT - 34054) 2 copies

National Aeronautics and Space Administration
Ames Research Center
Moffett Field, California 94035
Attention: Librarian

National Aeronautics and Space Administration
Goddard Space Flight Center
Greenbelt, Maryland 20771
Attention: Librarian

National Aeronautics and Space Administration
Langley Research Center
Hampton, Virginia 23365
Attention: Librarian

National Aeronautics and Space Administration
Manned Spacecraft Center
Houston, Texas 77001
Attention: Librarian

National Aeronautics and Space Administration
George C. Marshall Space Flight Center
Huntsville, Alabama 35812
Attention: Librarian

National Aeronautics and Space Administration
Jet Propulsion Laboratory
4800 Oak Grove Drive
Pasadena, California 91103
Attention: Librarian

National Aeronautics and Space Administration
Lewis Research Center
21000 Brookpark Road
Cleveland, Ohio 44135
Attention: Librarian
H. O. Slone, MS 500-201
G. M. Ault, MS 105-1
P. L. Stone, MS 500-201
G. M. Thur, MS 500-202
J. E. Dilley, MS 500-309
Maxine Sabala, MS 3-19
E. R. Furman, MS 500-202
M. J. Saari, MS 500-202
Report Control Office, MS 5-5
V. F. Hlavin, MS 3-14 (Final only)

National Bureau of Standards
Washington, D.C. 20546
Attention: Librarian

AFSC
Aeronautical Systems Division
Wright-Patterson Air Force Base, Ohio 45433
Attention: Charles Armbruster (ASRPP-10)
T. Cooper
Librarian

Army Ordnance Frankford Arsenal
Bridesburg Station
Philadelphia, Pennsylvania 19137
Attention: Librarian

U. S. Atomic Energy Commission
Technical Information Service Extension
P. O. Box 62
Oak Ridge, Tennessee 37831

U. S. Atomic Energy Commission
Washington, D. C. 20545
Attention: M. J. Whitman
J. M. Simmons

Argonne National Laboratory
9700 South Cass Avenue
Argonne, Illinois 60440
Attention: Librarian

Battelle Memorial Institute
505 King Avenue
Columbus, Ohio 43201
Attention: R. T. Niehoff, DMIC

Brookhaven National Laboratory
Upton, Long Island, New York 11973
Attention: Librarian
Dr. D. H. Gurinsky
Dr. J. R. Weeks

Oak Ridge National Laboratory
Oak Ridge, Tennessee 37831
Attention: J. Devan
R. MacPherson
Librarian

Office of Naval Research
Power Division
Washington, D. C. 20360
Attention: Librarian

Bureau of Weapons
Research and Engineering
Materials Division
Washington, D. C. 20546
Attention: Librarian

U. S. Naval Research Laboratory
Washington, D. C. 20390
Attention: Librarian

Aerojet-General Nucleonics
P. O. Box 77
San Ramon, California 94583
Attention: B. E. Farwell
E. Johnson

AiResearch Manufacturing Company
Division of the Garrett Corporation
Sky Harbor Airport
402 South 36th Street
Phoenix, Arizona 85034
Attention: Librarian

AiResearch Manufacturing Company
Division of the Garrett Corporation
9851-9951 Sepulveda Boulevard
Los Angeles, California 90009
Attention: Librarian

IIT Research Institute
10 West 35th Street
Chicago, Illinois 60616
Attention: Librarian

Babcock & Wilcox Company
Research Center
Alliance, Ohio 44601
Attention: Librarian

North American Aviation, Inc.
Atomics International Division
8900 DeSoto Avenue
Canoga Park, California 91304
Attention: Librarian

AVCO
Research & Advanced Development Department
201 Lowell Street
Wilmington, Massachusetts 01887
Attention: Librarian

Battelle Memorial Institute
505 King Avenue
Columbus, Ohio 43201
Attention Librarian

Electro-Optical Systems, Inc.
Advanced Power Systems Division
Pasadena, California 91107
Attention: Librarian

Fansteel Metallurgical Corporation
North Chicago, Illinois 18201
Attention: Librarian

Philco Corporation
Aeronutronics
Newport Beach, California 92663
Attention: Librarian

General Dynamics Corporation
General Atomic Division
John Jay Hopkins Lab.
P. O. Box 608
San Diego, California 92112
Attention: Librarian

General Electric Company
Nuclear Systems Programs
Missile 9 Space Division
Cincinnati, Ohio 45215
Attention: R. W. Harrison

General Electric Company
Missile and Space Vehicle Department
3198 Chestnut Street
Philadelphia, Pennsylvania 19104
Attention: Librarian

General Electric Company
Vallecitos Atomic Laboratory
Pleasanton, California 94566
Attention: Librarian

General Dynamics/Fort Worth
P. O. Box 748
Fort Worth, Texas 76101
Attention: Librarian

General Motors Corporation
Allison Division
Indianapolis, Indiana 46206
Attention: Librarian

Hamilton Standard
Division of United Aircraft Corporation
Windsor Locks, Connecticut 06096
Attention: Librarian

Hughes Aircraft Company
Engineering Division
Culver City, California 90230
Attention: Librarian

Lawrence Radiation Laboratory
Livermore, California 94550
Attention: Librarian

Lockheed Missiles and Space Division
Lockheed Aircraft Corporation
Sunnyvale, California 90221
Attention: Librarian

The Martin Company
Nuclear Division
P. O. Box 5042
Baltimore, Maryland 21203
Attention: Librarian

Martin Marietta Corporation
Metals Technology Laboratory
Wheeling, Illinois 60090

Materials Research Corporation
Orangeburg, New York 10962
Attention: Librarian

McDonnel Aircraft
St. Louis, Missouri 63166
Attention: Librarian

MSA Research Corporation
Callery, Pennsylvania 16024
Attention: Librarian

National Research Corporation
70 Memorial Drive
Cambridge, Massachusetts 02142
Attention: Librarian

North American Aviation
Los Angeles Division
Los Angeles, California 90009
Attention: Librarian

United Aircraft Corporation
Pratt & Whitney Aircraft Division
400 Main Street
East Hartford, Connecticut 06108
Attention: Librarian

Republic Aviation Corporation
Farmingdale, Long Island, New York 11735
Attention: Librarian

Sandia Corporation
P. O. Box 5800
Albuquerque, New Mexico 87116
Attention: Librarian

Solar
2200 Pacific Highway
San Diego, California 92112
Attention: Librarian

Southwest Research Institute
8500 Culebra Road
San Antonio, Texas 78228
Attention: Librarian

Superior Tube Company
Norristown, Pennsylvania 19404
Attention: Librarian

TRW Inc.
23555 Euclid Avenue
Cleveland, Ohio 44117
Attention: Librarian

Union Carbide Corporation
1020 W. Park Avenue
Kokomo, Indiana 46901
Attention: Librarian
Technology Department

Westinghouse Electric Corporation
Astronuclear Laboratory
P. O. Box 10864
Pittsburgh, Pennsylvania 15236
Attention: Librarian

Wah Chang Corporation
Albany, Oregon 97321
Attention: Librarian

Whittaker Corporation
Nuclear Metals Division
West Concord, Massachusetts 01781
Attention: Librarian

Wright-Patterson Air Force Base
Research and Technology Division
Dayton, Ohio 45404
Attention: M. P. Wannemacher, APIP-1

Defense Metals Information Center
Battelle Memorial Institute
Columbus Laboratories
505 King Avenue
Columbus, Ohio 43201